# Assessing the quality of molecular simulations for vapor-liquid equilibria: An analysis of the TraPPE database

Becky L. Eggimann,\*,† Yangzesheng Sun,‡ Robert F. DeJaco,‡,¶ Ramanish Singh,‡,¶ Muhammad Ahsan,‡ Tyler R. Josephson,‡ and J. Ilja Siepmann\*,‡,¶

†Department of Chemistry, Wheaton College, Wheaton, IL, 60187-5501, United States

‡Department of Chemistry and Chemical Theory Center,

University of Minnesota, Minneapolis, MN, 55455-0431, United States

¶Department of Chemical Engineering and Materials Science,

University of Minnesota, Minneapolis, MN, 55455-0431, United States

E-mail: becky.eggimann@wheaton.edu; siepmann@umn.edu

#### Abstract

As molecular modeling and simulation techniques become increasingly important sources of thermophysical property and phase equilibrium data, the ability to assess the robustness of that data becomes more critical. Recently, the use of the compressibility factor (Z) has been suggested as a metric for testing the quality of simulation data for vapor-liquid equilibria (VLE). Here, we analyze predicted VLE data from the transferable potentials for phase equilibria (TraPPE) database and show that, apart from data entry or typographical errors, Z will always be well-behaved in Gibbs ensemble Monte Carlo (GEMC) simulations even when the simulations are not sufficiently equilibrated, but the same does not hold true for grand canonical Monte Carlo simulations.

When the pressure is calculated from the internal forces, then pressure and density are strongly correlated for the vapor phase and, for GEMC simulations, it is recommended to treat Z as an instantaneous mechanical property. From analysis of the TraPPE VLE data, we propose a complementary metric based on the predicted vapor pressures at three neighboring temperatures and their deviation from a local Clausius-Clapeyron fit.

# Introduction

Molecular modeling and simulation (MMS) techniques, as tools for research and data collection, are maturing. Most obviously, computing power has increased dramatically since the first simulations were performed. Sophisticated algorithms and varying levels of abstraction in molecular models—from interactions described at the level of Kohn-Sham density functional theory to interactions of coarse-grained supra-atoms or even multi-molecule beads—have allowed MMS to reach an ever widening range of applications. MMS approaches are routinely used to calculate thermophysical properties and phase equilibrium data, and these data sources are becoming increasingly important as alternatives to experiment. Furthermore, software packages are available that provide non-experts with relatively easy access to MMS methods. In a recent review, one of the pioneers of MMS noted that, where before researchers had to think carefully about how to perform their simulations because they were expensive, they now must think carefully because they have become cheap (mostly). The barriers for the use of MMS are already low and continue to decrease. When this ease of use is combined with broad applicability, carelessness leading to low-quality data becomes a real danger. 1–4

There are a large number of factors that contribute to the quality of simulation data. These span the choices of models and algorithms, their implementation into a simulation program, the choice of experimental data for (and approach to) validation, the myriad of small details involved in correctly setting up the simulation algorithm, and the methods used

for analysis and averaging of properties. With so many critical decisions to make, expertise and experience will always be important for the proper execution of MMS techniques. As the use of MMS grows, it becomes more important than ever to complement experience with careful analysis of metrics, or "auxiliary quantities,"  $^{5,6}$  that can be monitored to assess simulation quality. A recent publication in this journal demonstrates such an approach for vapor-liquid equilibria (VLE). In that study, Nezbeda<sup>7</sup> showcases an unfortunate lack of quality in a number of published VLE data, and suggests the use of the compressibility factor (Z) as a metric for uncovering these mistakes before the data are published. We want to affirm and support this approach, and others like it,  $^{2,3}$  but here offer some necessary additions and clarifications that are particularly relevant for VLE data generated using Gibbs ensemble Monte Carlo (GEMC) simulations.  $^{8,9}$ 

Nezbeda's own interests led him to calculate the compressibility factor for the vapor phase data from several published VLE studies using common water models. The results were sufficiently poor (i.e., the vapor data revealed significant outliers and weak agreement with experiment for compressibility factors along the vapor-liquid coexistence curve, see Figures 1-3 in the original work? that further compounds were investigated, leading ultimately to a not insignificant number of poorly represented vapor phases. As Nezbeda indicates, the primary interest in VLE simulations is often the liquid phase and interfacial properties. In our own work, developing models for the transferable potentials for phase equilibria (TraPPE) force field by fitting to VLE data, we have historically allowed less relative precision/accuracy in the vapor-phase density compared to that of the liquid phase (less than 10% relative error for the vapor versus 1% for the liquid). Still, the frequency and type of errors noted by Nezbeda are perhaps unexpected and indicate more attention must be paid to the vapor phase in these important simulations. Interestingly, the first two TraPPE publications 11,12 reported numerical values of the compressibility factor, but this practice was unfortunately not continued in subsequent TraPPE publications.

The data analyzed by Nezbeda span three common simulation techniques: Monte Carlo

or molecular dynamics simulations using an elongated simulation box with two explicit interfaces, GEMC simulations, and grand canonical Monte Carlo (GCMC) simulations. All compressibility factors were calculated from the data available for the saturated vapor pressure and the vapor densities. However, utility of Z as a metric will be affected by the differing methods used to determine pressure for each simulation technique. In particular, GEMC simulations employ the virial equation (Eqn. 1) to obtain the instantaneous pressure as a mechanical property for a given configuration of a given box (usually, data are reported only for the vapor phase) that is then averaged throughout the course of the simulation where the number of molecules,  $N_{\text{box}}$ , and the volume of the box,  $V_{\text{box}}$ , of interest fluctuate:

$$P_{\text{GEMC}} = \left\langle \frac{N_{\text{box}} k_{\text{B}} T}{V_{\text{box}}} - \frac{1}{3V_{\text{box}}} \left( \sum_{i=1}^{N_{\text{box}}} \mathbf{r}_{i} \cdot \mathbf{f}_{i} \right) \right\rangle$$

$$= \left\langle \frac{N_{\text{box}} k_{\text{B}} T}{V_{\text{box}}} - \frac{1}{3V_{\text{box}}} \left( \sum_{i=1}^{N_{\text{box}}-1} \sum_{j=i+1}^{N_{\text{box}}} \mathbf{r}_{ij} \cdot \mathbf{f}_{ij} \right) \right\rangle$$
(1)

The first term represents the contribution from the ideal gas law and the second term, the virial term, depends on the total internal force,  $\mathbf{f}_i$ , acting on particle i at position  $\mathbf{r}_i$  or, for pairwise-additive potentials, on the intermolecular forces between atoms i and j in the box. As the number density decreases and the mean separation between molecules increases, the forces diminish and, consequently, the second term drops out and the instantaneous pressure becomes equal to that of an ideal gas at this density. Given this method of calculating the pressure, the compressibility factor, which is just the ratio of the molar volume of a real gas to that of an ideal gas, has to approach unity whenever the number density becomes small (assuming negligible aggregation). At low reduced temperatures ( $T_{\rm r} = T/T_{\rm crit}$ ), the vapor phase of a GEMC simulation will have weak molecule—molecule interactions due to the low density and its pressure will be that of an ideal gas, i.e., P, calculated using Equation 1, must approach  $P_{\rm ideal}$ , and Z must approach unity. This implies that when performed correctly, GEMC simulations should always produce well-behaved compressibility factors at low  $T_{\rm r}$  (the same temperature region where Nezbeda saw the largest deviations in the data he

analyzed<sup>7</sup>). Of particular concern is that this behavior for Z is always expected, even when GEMC simulations under-sample the vapor phase by a phase ratio that leads to a very small average number of particles in the vapor, or have not reached equilibrium due to insufficient accepted transfer moves between the phases. Thus, Z is not a useful metric for detecting common sampling problems in GEMC simulations. In contrast, the pressure calculation for GCMC simulations with the histogram reweighting (HR) approach is based on the partition function,  $\Xi$ :

$$P_{\text{GCMC}} = \frac{k_{\text{B}}T}{V} \ln \Xi(\mu, V, T)$$
 (2)

Thus, insufficient sampling in a GCMC simulation can lead to an erroneous pressure (and therefore an erroneous Z) even for a low-density vapor phase.

Here we calculate the compressibility factors for a large set of VLE data, that of the TraPPE database,  $^{13}$  and evaluate the use of Z as a metric for simulation quality. We also present a complementary metric based on the deviation of pressure triads (composed of three neighboring data points) from the Clausius-Clapeyron relationship, which is expected to do a better job of detecting sampling issues in GEMC simulations. For both metrics (Z-based and P-based), we develop quantitative measures of the extent of deviation from expected Z and P values and relate this to simulation quality; more deviation means less robust simulation data. The bounds of these quantitative measures are based on validation data  $^{14}$  obtained from longer simulations for larger system sizes for the seventeen compounds listed in Table 1.

Table 1: Chemical Compounds, Models, and Purity $^a$ 

chemical name	chemical or linear formula	CAS number	model
oxygen	$\mathrm{H_2O}$	7782-44-7	TraPPE-small
carbon dioxide	$\mathrm{CO}_2$	124-38-9	$TraPPE\!-\!small$
ethane	$\mathrm{C_2H_6}$	74-84-0	TraPPE-UA
n-butane	$\mathrm{CH_{3}(CH_{2})_{2}CH_{3}}$	106-97-8	TraPPE-UA
n-decane	$\mathrm{CH_{3}(CH_{2})_{8}CH_{3}}$	124 - 18 - 5	TraPPE-UA
2-methylpropane	$CH(CH_3)_3$	75-28-5	TraPPE-UA
2,2-dimethylpropane	$C(CH_3)_4$	463-82-1	TraPPE-UA
2-methylpropene	$(CH_3)_2C=CH_2$	115-11-7	TraPPE-UA
2-methyl-1,3-butadiene	$CH_2 = CHC(CH_3) = CH_2$	78-79-5	TraPPE-UA
naphthalene	$\mathrm{C}_{10}\mathrm{H}_{8}$	91-20-3	TraPPE-UA
ethanol	$\mathrm{CH_{3}CH_{2}OH}$	64 - 17 - 5	TraPPE-UA
2-butanol	$CH_3CH(OH)CH_2CH_3$	78-92-2	TraPPE-UA
ethanal	$\mathrm{CH_{3}CHO}$	75-07-0	TraPPE-UA
pentanal	$\mathrm{CH_{3}(\mathrm{CH_{2}})_{3}\mathrm{CHO}}$	110-62-3	TraPPE-UA
acetone	$\mathrm{CH_{3}COCH_{3}}$	67-64-1	TraPPE-UA
2-methoxy-2-methylpropane	$(CH_3)_3COCH_3$	1634-04-4	TraPPE-UA
methyl acetate	$\mathrm{CH_{3}COOCH_{3}}$	79-20-9	TraPPE-UA
2-butanethiol	$CH_3CH_2CH(SH)CH_3$	513-53-1	TraPPE-UA
dimethyl sulfide	$(\mathrm{CH_3})_2\mathrm{S}$	75-18-3	TraPPE-UA
<i>n</i> -perfluoropentane	$CF_3(CF_2)_3CF_3$	678-26-2	TraPPE-UA

<sup>&</sup>lt;sup>a</sup> All chemical samples are pure as specified by their respective input files.

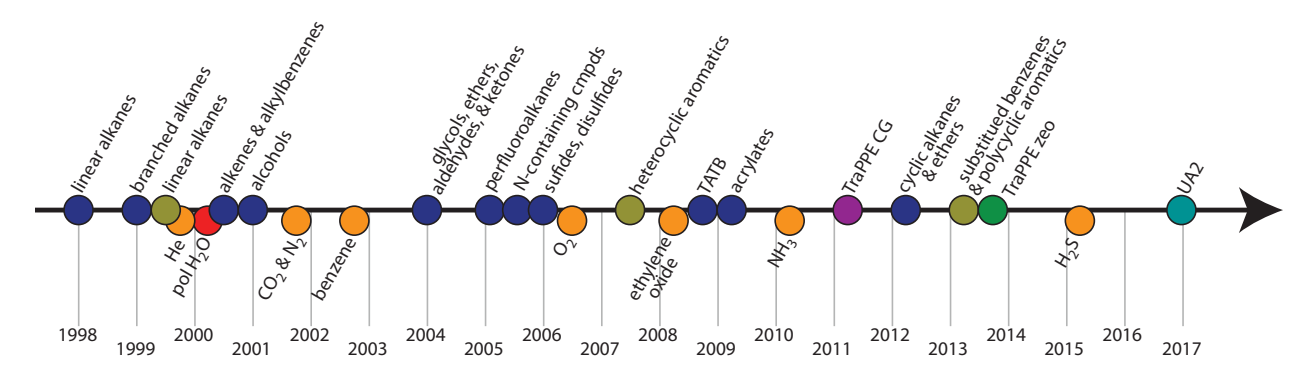


Figure 1: Timeline for the development of the TraPPE family of force fields. TraPPE families are represented as follows, in order from least to most coarse-graining: polarizable (red), <sup>31</sup> all-atom small molecules (orange), <sup>26–30</sup> explicit hydrogen (green), <sup>18,23–25</sup> zeolites (bright green), <sup>35</sup> united atom-2nd generation "UA2" (teal), <sup>34</sup> united atom (blue), <sup>11,12,15–22</sup> coarse grain (purple). <sup>33</sup>

# Computational Methods

#### The TraPPE Database

The development of the TraPPE family of force fields started with united-atom models for alkanes in 1998 and now includes (see Figure 1 for publication years and chemical functionalities): united-atom models for organic molecules containing C, H, N, and S atoms (TraPPE–UA), 11,12,15–22 explicit-hydrogen models for alkanes, some aliphatic nitrogen-containing compounds, and aromatics (TraPPE–EH), 18,23–25 all-atom models (including off-atom partial charges) for small molecules (TraPPE–small), 26–30 polarizable models for water and methane (TraPPE–pol), 31,32 coarse-grain models for hydrocarbons (TraPPE–CG), 33 second-generation united-atom models with off-atom sites (TraPPE–UA2), 34 and zeolites (TraPPE–zeo). 35 The TraPPE database, 10 which can be accessed online through a dedicated website, 13 is a collection of parameters and properties for several models and currently includes all TraPPE–UA models, some TraPPE–EH models, and all TraPPE–small models. One of the stated goals of the database and accompanying website is to provide users with supplemental information to facilitate the successful implementation and accurate use of TraPPE force fields. This necessarily includes force field parameters, simulation data, and additional documentation

Table 2: Data Availability in the TraPPE Database

Total Number of Mole	ecules	Number of Data Points	Z	P Triads
with VLCC data	163			
with $P_{\rm vap}$ data	159	development data	1072	754
with validation data	20	validation data	209	169

of TraPPE's conventions and unique features. A full description of the database and the available data has been previously published. <sup>10</sup> Briefly, the available force field description consists of all functional forms and corresponding parameters for the bonded and non-bonded interactions of a given molecule, and properties are typically vapor—liquid coexistence densities, critical properties ( $T_{\rm crit}$ ,  $\rho_{\rm crit}$ , and sometimes  $P_{\rm crit}$ ), saturated vapor pressures, and the normal boiling point. For our analysis here, we calculate the compressibility factor for all TraPPE models in the database using the previously published specific density and pressure of the vapor phase. We also use the vapor pressures to investigate the deviation of triads from the Clausius-Clapeyron relationship. Whereas the compressibility data are available at every temperature, the use of triads leads to  $n_T - 2$  data points for a given compound (where  $n_T$  is the number of temperatures investigated for this compound). The resulting total numbers of data points for each metric are listed in Table 2.

Table 2 also references a validation dataset previously available only through the website <sup>14</sup> but not yet published in the peer-reviewed literature. Data for these models (see Table 1) were determined from new simulations and confirm that previously developed parameters are still valid when used with much more rigorous simulation standards. For example, when ethane was originally parameterized in 1998, the simulation properties were calculated for a system of 400 molecules at six temperatures (from  $T_r = 0.58$  to  $T_r = 0.90$ ) by dividing a single independent run into 5 blocks, each 5000 cycles long (a cycle consists, in this case, of 400 Monte Carlo moves, or one move per particle in the simulation). <sup>11</sup> When ethane was simulated again in 2017, <sup>34</sup> the system size was increased to 1500 particles, eight temperatures were used (from  $T_r = 0.58$  extending up to  $T_r = 0.96$ ), the vapor phase was adjusted to make sure that 10-20% of the particles on average were in the vapor box for every temperature,

and rather than five blocks from a single run, system averages were calculated from eight truly independent runs, each 1,000,000 cycles in length. Numerical values of the validation data are provided in the Supporting Information.

#### Simulation Details

The work presented here includes 159 previously simulated TraPPE molecules and 20 newly simulated validation models. Complete simulation details for each previously published model can be found in the corresponding publications. 11,12,15-25,31 In general, the majority of TraPPE models were simulated using coupled-decoupled configurational-bias Monte Carlo  $^{12}$ in the Gibbs ensemble,  $^{8,9}$  though some models (especially in TraPPE- $6^{17}$  and TraPPE- $8^{19}$ ) used GCMC-HR techniques. <sup>36,37</sup> As computational resources have become more accessible, system sizes have been increased, the simulations have been run longer, and more independent runs are utilized to compute average properties with statistical uncertainties. The TraPPE potential is similar to other molecular mechanics force fields and includes explicit terms for both bonded and nonbonded interactions of UA and EH beads. Bond lengths (1-2 interactions) are kept fixed in Monte Carlo simulations for all TraPPE models, bend angles (1-3 interactions) are governed by harmonic potentials, and torsions (1-4 interactions) use one of several functional forms as described in the original publications or on the website. Note that the website provides further detail on the specific conventions for defining the minimum-energy point for the dihedral angle, which varies depending on the functional form being used. For the models available in the TraPPE database, the nonbonded interactions are modeled with Lennard-Jones and Coulomb potentials. The Lennard-Jones potential is spherically truncated at 14 Å, with analytic tail corrections beyond the cutoff. When partial charges are included, the Ewald summation technique is employed for calculating the Coulomb interactions. Over time, the Ewald convergence parameter has also been increased to reflect gains in computing power.

All of the 20 validation models are simulated in the NVT-Gibbs ensemble with coupled-

decoupled configurational-bias Monte Carlo, with at least eight independent trajectories using the MCCCS–MN software (Monte Carlo for Complex Chemical Systems–Minnesota).  $^{38}$  System sizes are determined such that the liquid phase maintains a box length of more than 32 Å. At each temperature, the system volume is adjusted so that (on average) 10-20% of the molecules are in the vapor phase throughout the simulation. Each model is simulated at a minimum of eight temperatures that range from below the normal boiling point to very near the critical point. At least three, but usually four or more, temperatures are higher than  $0.9T_{\rm crit}$  and are used for estimating the critical properties. Simulations are also run until the relative standard errors of the mean are less than 0.5% for the liquid densities, 2% for the vapor pressures, 1% for the critical temperature, and 5% for the critical pressure. To achieve these standards, the simulations use optimized protocols for efficient GEMC simulations.  $^{39,40}$ 

# Results and Discussion

The TraPPE database represents one of the largest (if not the largest) available collections of VLE data determined by Monte Carlo simulations, and includes data from both the grand canonical and Gibbs ensembles. As Figure 1 shows, the available models cover a wide-range of chemical functionalities, span a number of years, and will naturally reflect the increasing simulation standards that have come with gains in computational power over time. As such, the TraPPE database contains an ideal collection of VLE data, especially useful for evaluating various metrics that might be used to judge simulation quality.

# A Metric Based on the Compressibility Factor

The compressibility factor, Z, is a measure of the deviation shown by a real gas from ideal-gas behavior, and can be used to determine whether or not the vapor phase of a VLE simulation is well-behaved.<sup>7,41</sup> As shown in Equation 3, Z is just the ratio of the molar volume of a real gas to that of an ideal gas, and can be calculated from the pressure and specific density of

the vapor phase in a VLE simulation:

$$Z = \frac{V_{\text{m,real}}}{V_{\text{m,ideal}}} = \frac{W/\rho}{RT/P} = \frac{P}{\rho} \frac{W}{RT}$$
(3)

Here, P is the pressure of the vapor in Pa,  $\rho$  is the specific density of the vapor in kg/m<sup>3</sup>, W is the molecular weight of the molecule in kg/mol, R is the gas constant in J/(K mol), and T is the absolute temperature in K.

For the vapor-liquid coexistence region, the expected behavior is that Z should be unity for low  $T_{\rm r}$  (where both the density and pressure of the vapor are sufficiently low for the vapor to behave ideally) and decrease with increasing rapidity (as molecular interactions become increasingly important) toward some value of the critical compressibility factor. Robust VLE simulations for non-associating molecules should capture this trend, despite several published examples failing to do so, especially for low  $T_{\rm r}$ . According to this metric, the more deviation from the expected trend in Z, the more likely it is that the simulations are flawed in some manner, thus yielding untrustworthy results. The amount of deviation from the expected compressibility is then a measure of simulation quality.

However, it should also be noted that for a few molecules, such as low-molecular-weight carboxylic acids and hydrogen fluoride, Z will deviate strongly from those of non-associating fluids at these conditions. There is a significant degree of association in the vapor-phase, even at low- $T_r$ , due to the formation of hydrogen-bonded aggregates for these molecules. Their behavior differs from that of water and simple alcohols because their vapor pressures are relatively high due to their relatively low heats of vaporization resulting from similar numbers of hydrogen bonds in the liquid and vapor phases. Near the critical point, hydrogen-bond formation for water and alcohols also leads to a lowering of Z but to a lesser degree.

Even with these natural variations, the use of Z as a metric is especially appealing because it is easy to calculate and unexpected deviations should be immediately obvious. However, in simulations, the average compressibility can be calculated in two different ways and we show here that these different approaches result in Z values that are systematically different and can lead to dramatic overestimations of the statistical uncertainty. Relying on Z as a metric requires further clarity about which approach was used to determine Z.

In the first approach, Z is calculated from ensemble-average values of P and  $\rho$  as utilized by Nezbeda.<sup>7</sup> Statistical uncertainties would be calculated using error propagation from the resulting uncertainties in  $\langle P \rangle$  and  $\langle \rho \rangle$ . This is called here the ensemble average approach  $(Z_e)$ .

$$Z_{\rm e} = \frac{\langle P \rangle}{\langle \rho \rangle} \frac{W}{RT} \tag{4}$$

The second approach calculates Z as a mechanical observable at fixed intervals throughout the simulation and determines errors directly from  $\langle P/\rho \rangle$  for multiple independent runs (or block averages). This is the instantaneous average approach  $(Z_i)$ .

$$Z_{\rm i} = \left\langle \frac{P}{\rho} \right\rangle \frac{W}{RT} \tag{5}$$

To discuss the differences between these approaches, we denote the compressibility factor at each pressure calculation step as  $z = P/(\rho RT)$  and evaluate the difference between  $Z_{\rm e}$  and  $Z_{\rm i}$  as

$$Z_{e} - Z_{i} = \frac{\langle P \rangle}{\langle \rho \rangle RT} - \langle z \rangle$$

$$= \frac{\langle z \rho RT \rangle}{\langle \rho \rangle RT} - \langle z \rangle$$

$$= \frac{\langle z \rho \rangle}{\langle \rho \rangle} - \langle z \rangle$$

$$= \frac{\langle z \rho \rangle - \langle z \rangle \langle \rho \rangle}{\langle \rho \rangle}$$

$$= \frac{\text{cov}(z, \rho)}{\langle \rho \rangle}$$

where  $cov(\cdot, \cdot)$  is the covariance between two variables. The correlation between the instantaneous compressibility factor and density is directly proportional to the difference between

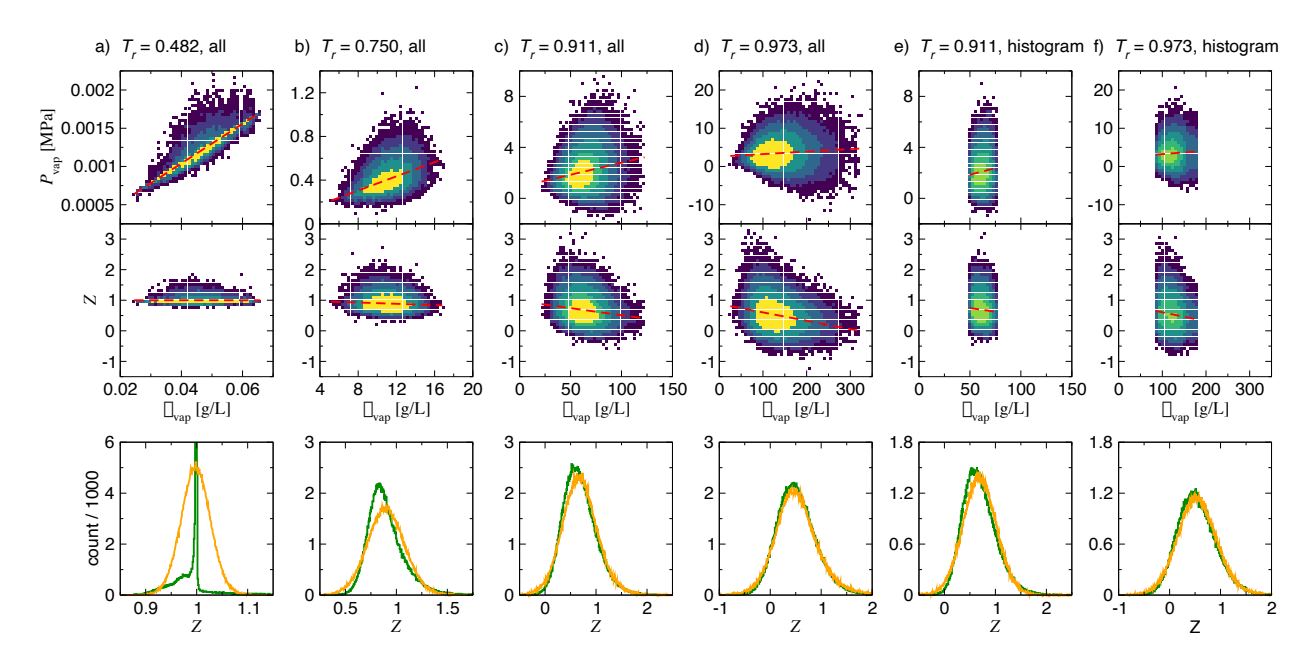


Figure 2: Distributions of P,  $\rho$  and z obtained from validation simulations for pentanal at  $T_r$  of (a) 0.482, (b) 0.750, (c) 0.911, and (d) 0.973, and columns (e) and (f) show data obtained after histogram analysis of the vapor density for  $T_r > 0.9$ . The top and middle rows show 2D distributions of  $(P, \rho)$  and  $(z, \rho)$ , respectively, with the dashed red lines showing the linear regressions. Color gradients from dark purple to yellow corresponds to the count of simulation frames N binned by  $1 \le N \le 9$ ,  $10 \le N \le 49$ ,  $50 \le N \le 249$ ,  $250 \le N \le 999$ ,  $1000 \le N \le 2499$ , and  $N \ge 2500$ . The bottom row shows histograms of compressibility factors from the simulation results (green) and from Gaussian maximum likelihood estimates that yield the same mean and covariance matrix as the simulation results (orange).

### $Z_{\rm e}$ and $Z_{\rm i}$ .

To illustrate the differences between  $Z_{\rm e}$  and  $Z_{\rm i}$ , we use validation data for pentanal as an example (see Figure 2 and Table 3). Large fluctuations near  $T_{\rm crit}$  may lead to interchange between liquid and vapor box identities, so larger system sizes (800 instead of 400 molecules) were used closed to  $T_{\rm crit}$  to prevent switching and provide a robust comparison between  $Z_{\rm e}$  and  $Z_{\rm i}$ . At low  $T_{\rm r}$ , the behavior of the vapor pressure is dominated by the ideal-gas contribution (see Eqn. 1) and, as a consequence, the compressibility factor is unity for a great majority of simulation steps. As a consequence, the vapor pressure is strongly correlated with the vapor density; the instantaneous pressure values are always positive and, at a given vapor density, the spread of the observed pressure values is smaller than a factor of two. However, the compressibility factor ( $z \approx 1$ ) is nearly independent of the vapor density. Thus, at low

Table 3: Discrepancies between Compressibility Factor Measurements Observed in Validation Simulations for Pentanal and their Gaussian Maximum Likelihood Estimates<sup>a</sup>

$T_r$	data	$Z_e$	$Z_i$	$R(P, \rho)$	$R(z, \rho)$	$(Z_e - Z_i)/Z_i$	$(Z_e - Z_i)/Z_i$
						simulation [%]	Gaussian [%]
0.482	full	$0.9981 \pm 0.0004$	$0.9981 \pm 0.0003$	$0.958 \pm 0.015$	$-0.007 \pm 0.014$	$-0.002 \pm 0.005$	$-0.003 \pm 0.006$
0.750	full	$0.898 \pm 0.002$	$0.900 \pm 0.002$	$0.479 \pm 0.017$	$-0.072 \pm 0.008$	$-0.18 \pm 0.02$	$-0.19 \pm 0.04$
0.911	full	$0.676 \pm 0.007$	$0.685 \pm 0.006$	$0.205\pm0.007$	$-0.156 \pm 0.014$	$-1.33 \pm 0.19$	$-1.50 \pm 0.28$
0.973	full	$0.502 \pm 0.022$	$0.525 \pm 0.021$	$0.084\pm0.013$	$-0.232 \pm 0.023$	$-4.3 \pm 1.0$	$-6.0 \pm 2.3$
0.911	hist	$0.692 \pm 0.009$	$0.693 \pm 0.009$	$0.104\pm0.016$	$-0.072 \pm 0.008$	$-0.28\pm0.05$	$-0.27\pm0.05$
0.973	hist	$0.541 \pm 0.029$	$0.546 \pm 0.029$	$0.052\pm0.018$	$-0.103 \pm 0.026$	$-0.82 \pm 0.41$	$-0.86\pm0.46$

<sup>&</sup>lt;sup>a</sup>  $R(\cdot,\cdot)$  denotes the Pearson correlation coefficient. All values were calculated from each of the 16 independent simulations and reported as the mean and standard deviation.

 $T_{\rm r}$ ,  ${\rm cov}(z,\rho)$  is small, and we observe  $Z_{\rm e}-Z_{\rm i}\approx 0$ . The Pearson correlation coefficient for P and  $\rho$  is greater than 0.96, whereas that for z and  $\rho$  is negative with a magnitude less than 0.02.

In contrast, at temperatures approaching the critical point, the vapor pressure is greatly influenced by mostly attractive, but also repulsive, interactions between molecules and, at a given vapor density, the pressure varies widely from positive to negative values. With interactions playing an important role, the vapor pressure is only very weakly but positively correlated with the vapor density  $(R(P, \rho) \approx 0.05 \text{ at } T_{\rm r} = 0.973)$ . In such cases, the compressibility factor is found to exhibit a moderate negative correlation with vapor density (i.e., higher densities are more likely to encounter attractive interactions, see Figure 2), so that  $Z_{\rm e} < Z_{\rm i}$ .

Since vapor density and pressure are directly sampled from microscopic properties throughout the simulation trajectory, the instantaneous values of the compressibility factor follow a ratio distribution  $^{42}$  between the distributed density and pressure values. However, it is not feasible to analytically calculate the distribution of z given simple parametric models of  $\rho$  and P, such as a bivariate Gaussian distribution. Instead, Gaussian sampling experiments were conducted to gain insights into the distributions of simulation data and their influence on calculating the compressibility factor. Figure 2 shows histograms of z obtained from simulations versus estimations from Gaussian distributions matching the mean, variance, and

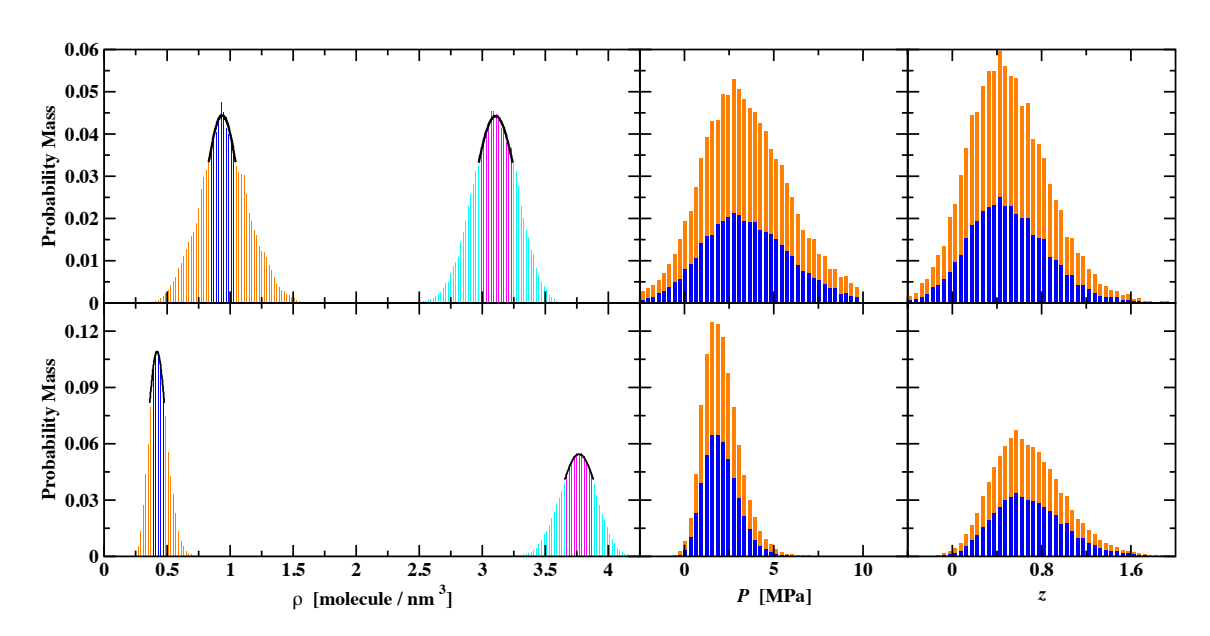


Figure 3: Probability mass histograms of the coexistence densities (left), vapor-phase pressures (middle), and compressibilities (right) obtained from the validation simulations for pentanal at  $T_{\rm r}=0.911$  (bottom row) and 0.973 (top row). Gaussian distributions (black lines) are fit to blue and magenta bars with heights of at least 0.75 of the maximum height for the vapor and liquid coexistence densities, respectively. For pressures and compressibility factors, the blue bars illustrate the distributions of the instantaneous density points selected by the Gaussian fit approach for the vapor density, whereas the orange bars show data for the entire trajectories.

covariance of the simulation distributions. With increasing  $T_{\rm r}$ , pressure and vapor density become less correlated, giving a larger difference between  $Z_{\rm e}$  and  $Z_{\rm i}$ . Although the z distributions are less similar to a Gaussian distribution at lower  $T_{\rm r}$ , using a Gaussian distribution to model the fluctuations of P and  $\rho$  is still sufficient to qualitatively estimate the discrepancy between the two types of measurements for the compressibility factor (see Table 3). The Gaussian sampling experiments also indicate that, as  $T_{\rm crit}$  is approached, the distribution of z broadens and  $Z_{\rm e}$  gives a significantly smaller value than  $Z_{\rm i}$ . The Gaussian sampling results further reveal the statistical prevalence of such discrepancies in the simulations, indicating that our analysis is also applicable to a wider range of compounds. Calculating Z as a mechanical property on-the-fly throughout GEMC simulations will avoid the error introduced through correlation of P and  $\rho$ .

For GEMC simulations close to the critical point, the distributions of the vapor and

liquid densities exhibit non-Gaussian behavior with tails toward intermediate densities. 40,43 This tailing is a consequence of the coupling of the two phases and is more pronounced for smaller system sizes. Thus, to reduce finite-size effects, the distributions near the peaks for the vapor and liquid densities can be approximated by Gaussian distributions (only bins with a height of at least 0.75 of the respective maximum peak height are included for the Gaussian fit as recommended by Dinpajooh et al. 40). The mean values obtained from these Gaussian distributions can be taken as the best estimates of the vapor and liquid coexistence densities. 40 When the vapor pressure and compressibility factor for temperatures near the critical point are calculated, then only data from configurations within the regions used for the Gaussian fits to the density distributions should be considered. At  $T_{\rm r}$  > 0.9, about 50% of the configurations meet the peak threshold. A Python script that performs this histogram analysis is described in the Supporting Information. Figure 3 shows probability mass histograms for the distributions of vapor and liquid densities, vapor-phase pressures, and compressibilities obtained from validation simulations for pentanal at  $T_{\rm r}=0.911$  and 0.973. Due to the asymmetry of the density distribution, the histogram analysis removes a slightly larger contribution from the high-density tail than from the low-density tail of the  $\rho_{\rm vap}$  distribution. These higher-density configurations are more likely to include significant attractive interactions and a lower  $P_{\text{vap}}$  and z (see Figure 2). Thus, the  $Z_{\text{i}}$  and  $Z_{\text{e}}$  values estimated from the histogram-selected configurations are slightly higher than those from the full trajectory (see Table 3). In addition, the histogram-selected data show smaller (in magnitude)  $R(P,\rho)$  and  $R(Z,\rho)$  values than the full trajectories and their  $(Z_e-Z_i)/Z_i$ differences are described better by the Gaussian sampling experiments. To reduce finite-size effects near the critical point, our recommendation is to use the histogram analysis for the calculation of  $\langle Z_i \rangle$ .

## Analysis of Compressibility Factors from the TraPPE Database

For our analysis of Z values in the TraPPE database, we, like Nezbeda, are relying on previously simulated data and must therefore calculate  $Z_{\rm e}$ . When trajectories are available for some of the most recent validation data, then we utilize the preferred  $Z_i$  values. Figure 4 shows all of the the compressibility factors, calculated as  $Z_{\rm e}$ , from the original development of UA, EH and small molecules in the development models available in the TraPPE database. We can immediately see outliers in some plots and unexpectedly large error bars in others, but before considering these deviations in greater detail, we first highlight a positive trend that can be easily overlooked. The individual plots on the left side of Figure 4 represent the passage of time, from the first TraPPE publication in panel A (linear alkanes, <sup>11</sup> 1998) to one of the more recent publications in panel I (cyclic alkanes and ethers,  $^{22}$  2012). Over time, as the standards that can be achieved for VLE simulations have increased, the TraPPE data show a corresponding narrowing and smoothing of the Z curve, with decreasing error bars noted for individual data points. The TraPPE simulation data is improving in both accuracy (more consistent curves with fewer outliers) and precision (smaller error bars) as time progresses. This trend, which assures us that trustworthy data for VLE simulations can be achieved, stands in contrast to the examples highlighted by Nezbeda, and is worth emphasizing. While it is certainly becoming easier and easier to generate low-quality data given the rapid growth of computational methods and increasing access to simulation software for non-experts, the TraPPE compressibility factors demonstrate that this need not be the case. With appropriate expertise and careful attention to the (many) details of each simulation, excellent results can be achieved. For any metric to be useful it must be able to demonstrate both the praise-worthy and the cringe-worthy in our data, and inspire all simulators to strive for increasingly more robust simulation quality.

Returning, then, to a discussion of the outliers in Figure 4, we have identified four different types of errors that emerge when applying this metric—simple typos and data entry errors (examples highlighted with magenta arrows), molecular weight mistakes (the blue arrow next

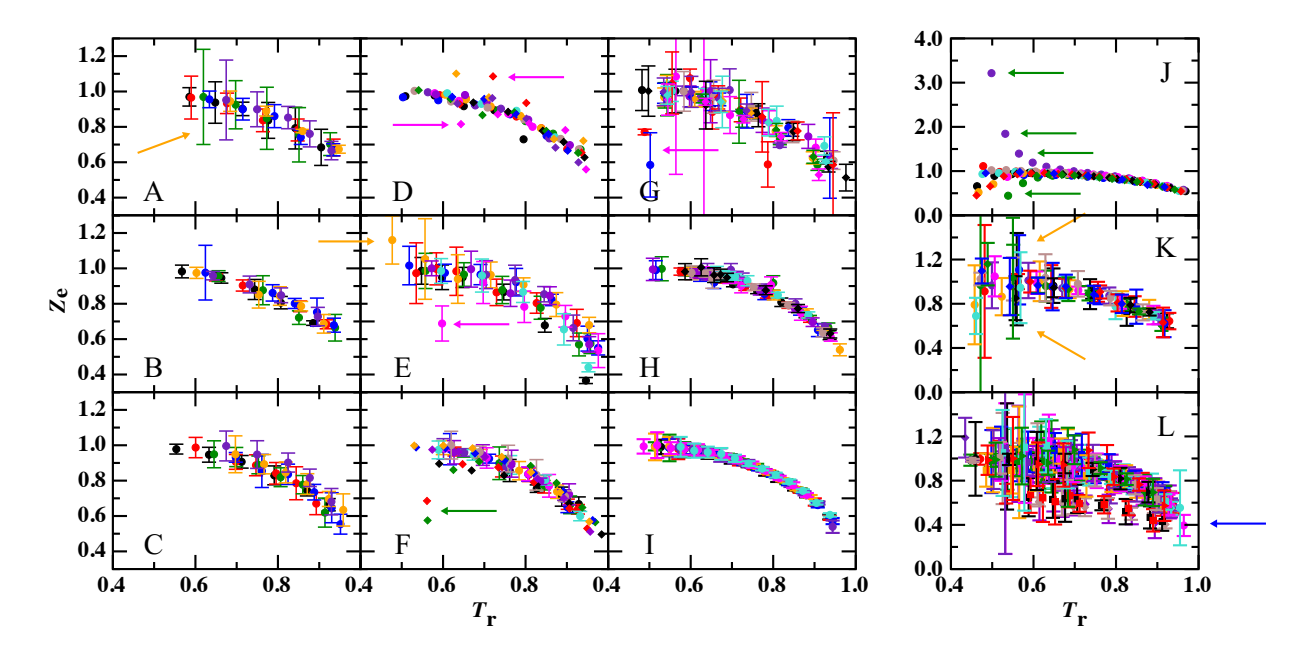


Figure 4: Compressibility factors from the TraPPE database. (A) linear alkanes, UA, <sup>11</sup> (B) branched alkanes, UA, <sup>12</sup> (C) linear alkanes, EH, <sup>23</sup> (D) alkenes and alkylbenzenes, UA, <sup>15</sup> (E) alcohols, UA, <sup>16</sup> (F) ethers, glycols, ketones, aldehydes, UA, <sup>17</sup> (G) N-containing compounds, UA and EH, <sup>18</sup> (H) acrylates, UA, <sup>21</sup> (I) cyclic alkanes and ethers, UA, <sup>22</sup> (J) sulfides, disulfides, thiophene, UA, <sup>19</sup> (K) heterocyclic aromatics, EH, <sup>24</sup> (L) substituted benzenes, polycyclic aromatics, EH. <sup>25</sup> Different colored symbols represent different compounds. Colored arrows point to identified outliers, as described in the text.

to Panel L points to a set of data points that are systematically offset from the expected Z trend), insufficient sampling for GCMC-HR (green arrows in Panels F and J indicate data points that are rapidly curving away from the expected trend, either upwards towards higher and higher Z or downwards toward 0), and potential poor sampling in GEMC (orange arrows point to several examples of large error bars). The three panels offset to the right of Figure 4 contain outliers that require a larger scale than the other TraPPE data; panels K and L, representing data for EH models of aromatic compounds, also show the majority of the simulations with large error bars.

Typos and data entry errors show up as single points that deviate significantly from the observed trend for the rest of the data set. We were able to identify and correct a small number of data entry mistakes that appear in TraPPE publications as a result of this analysis. Corrected data are available at the TraPPE website. <sup>13</sup> Some suspected errors—

those indicated with magenta arrows—could not be corroborated due to the inability to locate the original data (i.e., data collected before the era of data management plans).

Molecular weight mistakes lead to Z values that have the expected curve shape but are offset by a constant factor (even though the saturated vapor pressure may be correct; the vapor density is usually reported as specific density and not as number density or molar volume, see Eqn. 3). There are four molecules from TraPPE-10 with known molecular weight errors (Panel L, blue arrow)—anthracene, phenanthrene, naphthalene-2-carbonitrile, and naphthalen-2-ol. They have Z values that approach 0.7 (rather than unity) at low  $T_r$ . The TraPPE-EH models for aromatics use compound-specific partial charges on all ring atoms and substituent beads directly bonded to the ring, which are obtained from electronic structure calculations. These require separate entries in the parameter tables for our software and, throughout this work, we found numerous entries where the mass of a hydrogen atom was set to 0.012 kg/mol. These mistakes in correctly specifying the atomic weights also lead to specific liquid densities that are too high by a factor of about 1.4 (=  $Z^{-1}$  at low  $T_r$ ).

GCMC-HR simulations have characteristic errors that result from the particularities of that method. At low  $T_r$ , equilibration is especially challenging and the histogram-reweighting technique compounds any errors by including mistakes from insufficiently sampled low- $T_r$  simulations in the histograms for the next higher temperatures, thereby creating the curved tails observed for these simulations (Panels F and J). Likely, it is only the simulation at the lowest  $T_r$  that is problematic, and some of the errors are indeed very large. GCMC-HR related deviations account for 20% of the outlying molecules (21% of the outlying data points), which is slightly larger than the total proportion of GCMC-HR simulations represented in the database (11% of molecules; 19% of data points).

Large error bars, such as in Figure 4, panels A, B, E, G, K, and L, are an indication of potential sampling problems in GEMC simulations. However, caution should be used when interpreting error bars for  $Z_e$ . The two values needed to calculate  $Z_e$  are P and  $\rho$  (see Eqn. 4), but we have already seen that these measures can be highly correlated in the

Table 4: Error Estimates in  $Z_{\rm e}$  and  $Z_{\rm i}$  <sup>a</sup>

Molecule	$T_{ m r}$	$Z_{ m e}$	$Z_{ m i}$	Error Ratio
pentanethiol	0.4983	$0.99 \pm 0.09$	$0.9970 \pm 0.0004$	230
	0.5316	$1.00 \pm 0.07$	$0.9945 \pm 0.0005$	140
	0.5648	$0.99 \pm 0.06$	$0.9890 \pm 0.0010$	60
	0.5980	$0.99 \pm 0.03$	$0.9830 \pm 0.0010$	30
dimethyl disulfide	0.4620	$1.01 \pm 0.16$	$0.9986 \pm 0.0005$	320
	0.4950	$0.99 \pm 0.09$	$0.9968 \pm 0.0007$	130
2-butanethiol	0.4668	$1.01 \pm 0.13$	$0.9983 \pm 0.0006$	220
	0.5027	$0.99 \pm 0.09$	$0.9961 \pm 0.0005$	180

<sup>&</sup>lt;sup>a</sup> Statistical uncertainties are reported as the standard error of the mean.

vapor phase at low  $T_{\rm r}$  (see Figure 2). When using propagation of errors, applied at the end of a simulation, this correlation will lead to significant overestimations of the error in  $Z_{\rm e}$ , as much as two orders of magnitude. To illustrate this point, new GEMC simulations were carried out at  $T_{\rm r} < 0.6$  for some sulfur-containing compounds. Table 4 shows examples of  $Z_{\rm e}$  and  $Z_{\rm i}$  values and their respective statistical uncertainties obtained from the same sets of independent simulations. Treating Z as a mechanical observable  $(Z_i)$  leads to very small uncertainties and masks any sampling issues that might have emerged as large uncertainties in P or  $\rho$  from the independent GEMC simulations. Thus, for GEMC simulations that calculate  $Z_i$  (as is our recommendation), the value of Z as a metric is mostly limited to detecting molecular weight issues and typos/scripting errors when data are prepared for publication or transferred to databases. It should also be noted here that use of  $Z_i$  requires that the total volume is sufficiently large that the vapor phase always contains at least one particle. On balance, our recommendation for GEMC simulations is still to calculate Z as a mechanical observable (because of the shortcomings in  $Z_{\rm e}$  due to the correlation between P and  $\rho$  and and the issues with incorrect error propagation) and to rely on an alternative metric to look for poor sampling. That being said, calculation of  $Z_e$  is still a very good metric for GCMC-HR and liquid-slab molecular dynamics simulations because Eqn. 2 for the former and the usually small vapor region (occupied frequently by no particles at low  $T_{\rm r}$ ) for the latter make calculation of  $Z_{\rm i}$  impractical.

As a metric, Z will only be useful to the extent that deviations can be quantified. To quantify how much deviation might be allowed in high-quality VLE simulations, we use the ratio of the observed compressibility factor at a given  $T_{\rm r}$  ( $Z_{\rm sim}$ ) and the expected compressibility factor based on the average behavior of a representative group of compounds ( $Z_{\rm exd}$ ). Ratios closer to unity will signify more robust simulations.  $Z_{\rm exd}$  is first determined by fitting a logarithmic function to a reliable data set—here we use the validation data from the TraPPE database—and then using the resulting equation to calculate Z at a given  $T_{\rm r}$ . For this fit, we also include  $Z_{\rm crit}$  obtained from the ratio of the extrapolated  $P_{\rm crit}$  and  $\rho_{\rm crit}$ .

As shown in Figure 5, the data from the TraPPE validation set can be well described by the following empirical equation that strikes a balance between closeness of the fit and number of adjustable parameters, while also yielding physically meaningful Z values at  $T_{\rm r}=1$  and low  $T_{\rm r}$ :

$$Z_{\text{exd}}(T_{\text{r}}) = \begin{cases} Z^* + (1 - Z^*) \left[ 1 - \left( (1 + \alpha)T_{\text{r}} - \alpha \right)^{\beta} \right]^{\gamma} & \text{for } T_{\text{r}} \ge T_{\text{r}}^* \\ 1 & \text{for } T_{\text{r}} < \alpha/(1 + \alpha) \end{cases}$$
(7)

where the two powers with values of  $\beta=1.8$  and  $\gamma=0.46$  and  $\alpha=0.9$ , that controls the reduced temperature  $(T_{\rm r}^*=\alpha/(1+\alpha)=0.4737)$  below which Z is always set equal to unity, are three fitting parameters. The value  $Z^*$  is the average critical compressibility for the validation compounds, and its value of 0.277 is determined before the three-parameter fit. The use of a single function for  $Z_{\rm exd}$  ignores the fact that different molecule types will have different compressibilities as the vapor density increases and the critical point is approached. For example,  $Z_{\rm crit}=0.2295$  and  $0.307\pm0.005$  for water 44 and Lennard-Jonesium, 40 respectively, spanning the range observed for the TraPPE validation models. For a more specific data set of molecules with the same functional group or molecular shape, the coefficients could be modified to yield a tighter fit. For a mixed data set such as the TraPPE database, this best-fit function (Eqn. 7), with an  $R^2$  coefficient of 0.993, provides a robust empirical relationship between  $T_{\rm r}$  and  $Z_{\rm exd}$  for most models.

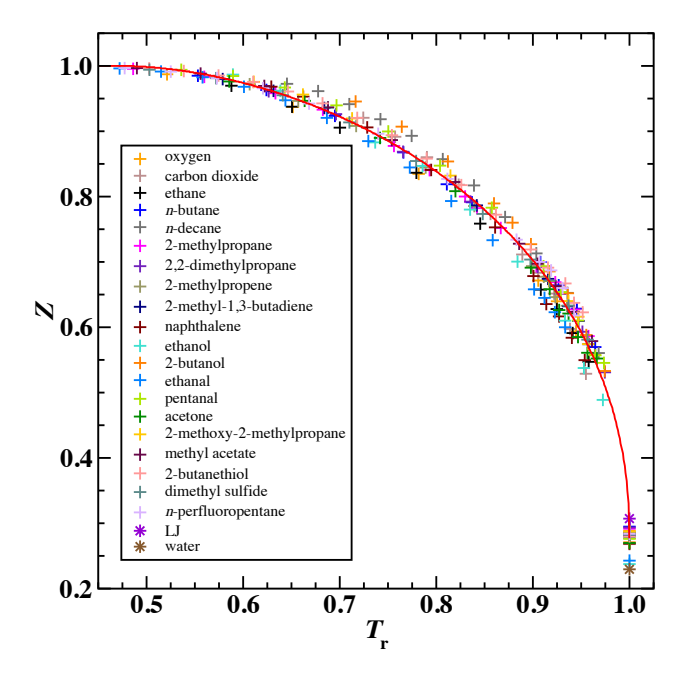


Figure 5: Compressibility factors for the TraPPE validation data. Symbols and colors for the 20 validation models are as described in the legend. Two additional critical compressibilities are shown for reference: experimental data for water <sup>44</sup> and the Lennard-Jones (LJ) model. <sup>40</sup> The red line indicates the best-fit empirical function (Eqn. 7,  $R^2 = 0.993$ ).

Next, we calculate the ratio of  $Z_{\rm sim}$  to  $Z_{\rm exd}$  for all distinct Z values in the TraPPE database and plot the distribution of the natural logarithm of this ratio for the entire data set (see Figure 6). Recognizing that simulations near the critical point and those at low  $T_{\rm r}$  have different challenges than those that are at intermediate  $T_{\rm r}$ , the distributions of  $\ln{(Z_{\rm sim}/Z_{\rm exd})}$  are plotted for three temperature ranges:  $T_{\rm r} \leq 0.70$ ,  $0.70 < T_{\rm r} \leq 0.85$ , and  $T_{\rm r} > 0.85$ . Finally, a Gaussian function is fit to each distribution to provide a numerical estimate of the mean and standard deviation, from which we can quantitatively distinguish expected values from outliers. The results of these fits are shown in Table 5.

For both development and validation data, the spread of the distribution increases with increasing  $T_{\rm r}$ . A wider distribution of  $\ln{(Z_{\rm sim}/Z_{\rm exd})}$  is expected near the critical point as we are using a general empirical value in place of a group-specific  $Z_{\rm crit}$ . The range of models in the TraPPE database will therefore lead to more variation in  $\ln{(Z_{\rm sim}/Z_{\rm exd})}$  as  $T_{\rm r}$  approaches unity. As Figure 6 shows, the validation data all have narrower distributions in each of the three  $T_{\rm r}$  ranges when compared to the development data. For both development and

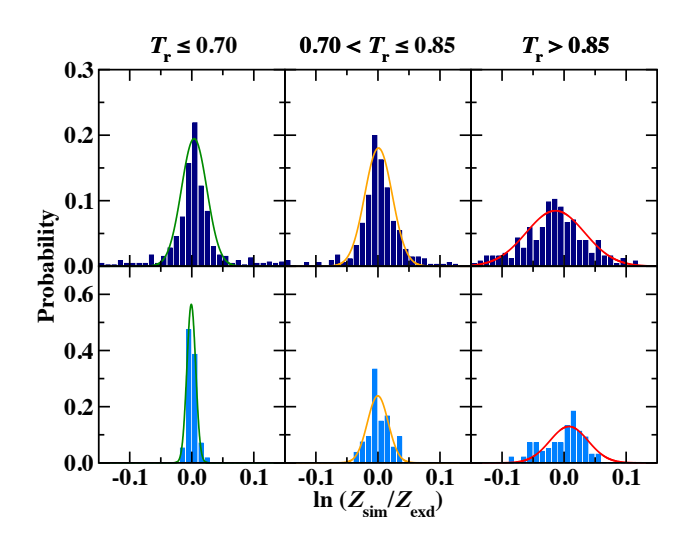


Figure 6: Gaussian fits to the distribution of  $\ln(Z_{\text{sim}}/Z_{\text{exd}})$  for the TraPPE database. Development data are shown in the top row (black); validation data in the bottom row (blue).

Table 5: Numbers of Data Points and Outliers, Mean and Standard Deviation for  $\ln (Z_{\text{sim}}/Z_{\text{exd}})$  Distributions of Development<sup>a</sup> and Validation Data

Range	Dataset	$N_{ m data}$	$N_{ m out}$	$\overline{x}$	$\sigma$
$T_{\rm r} < 0.70$	dev	466	139	0.004	0.020
	val	57	_	-0.001	0.007
$0.70 < T_{\rm r} < 0.85$	$\operatorname{dev}$	351	52	0.001	0.022
	val	54	_	-0.001	0.017
$T_{\rm r} > 0.85$	$\operatorname{dev}$	255	38	-0.014	0.047
	val	98	_	0.008	0.031

<sup>&</sup>lt;sup>a</sup>For the determination of  $\overline{x}$  and  $\sigma$  for the development set, the four molecules with known incorrect molecular weight were excluded; i.e., 14, 12, and 6 data points were removed for the low, intermediate, and high  $T_{\rm r}$  ranges, respectively. However, these points are included in the count of outliers.

validation data, the mean is near zero illustrating that Eqn. 7 yields a good fit. Though the validation dataset is small, given the higher standards used for these simulations and the overarching goal of producing a metric that sets a very high bar for success, we use the narrower validation distributions to determine the acceptable range for our Z metric. For each  $T_{\rm r}$  region, the acceptable range is taken as  $\overline{x} \pm 3\sigma$ , which should contain 99.7% of well-behaved compressibility factors. When  $T_{\rm r} \leq 0.70$ ,  $\ln{(Z_{\rm sim}/Z_{\rm exd})}$  should fall between -0.03 and 0.03, for  $0.70 < T_{\rm r} \leq 0.85$ , the acceptable range is -0.06 and 0.05, and at  $T_{\rm r} > 0.85$ ,  $\ln{(Z_{\rm sim}/Z_{\rm exd})}$  should be between -0.09 and 0.11.

Table 6: Selected  $\ln (Z_{\text{sim}}/Z_{\text{exd}})$  Outliers<sup>a</sup>

Molecule	$T_{ m r}$	$\ln\left(Z_{\mathrm{sim}}/Z_{\mathrm{exd}}\right)$	NB
ethene	0.80	$-0.15_{4}$	-0.06
ethylbenzene	0.72	0.18	0.05
	0.80	0.11	0.05
p-xylene	0.64	-0.16	-0.03
o-xylene	0.63	0.14	0.03
	0.94	0.15	0.11
ethanal	0.56	-0.36	-0.03
propan-2-ol	0.60	-0.35	-0.03
octan-1-ol	0.48	0.15	0.03
nitrobenzene	0.50	-0.53	-0.03
pentanethiol	0.50	1.17	0.03
	0.53	0.62	0.03
	0.56	0.35	0.03
anthracene	0.62	$-0.5_{3}$	-0.03
	0.70	$-0.4_{2}$	-0.03
	0.78	$-0.5_{2}$	-0.06
	0.89	$-0.5_{3}$	-0.09

<sup>&</sup>lt;sup>a</sup> When statistical uncertainties are reported in the original publication for  $P_{\text{vap}}$  and  $\rho_{\text{vap}}$ , propagated errors for  $\ln{(Z_{\text{sim}}/Z_{\text{exd}})}$  have been included as subscripts. The nearest boundary (NB) that each outlier exceeds is also shown for easy reference.

Applying the metric, we find that there are many data points that emerge as Z outliers in the TraPPE database. For the 159 TraPPE models with both VLCC and  $P_{\rm vap}$  data, 95 (60%) have at least one Z outlier. This corresponds to 229 individual data points (21% of the total data available). A complete listing of Z outliers is provided in the Supporting Information (Table S3). As illustrative examples of the types of outliers observed here, Table 6 provides numerical data for several compounds. Data for ethene, ethylbenzene, p-xylene, p-xylene, propan-2-ol, and nitrobenzene (Figure 4, Panel D: black circles, red diamonds, magenta diamonds, and orange diamonds, respectively; Panel E: magenta circle; Panel G: blue circle) are all suspected typos or data entry errors from TraPPE-4, TraPPE-5, and TraPPE-7.  $^{15,16,18}$  In each case, there are one or two Z values that are obviously outside the curve created by the other data points. Ethanal  $^{17}$  (Figure 4, Panel F, red diamonds) and pentanethiol  $^{19}$  (Figure 4, Panel J, purple circles) are both examples of data from GCMC-

HR simulations. Here, the lowest  $T_{\rm r}$  is a very significant outlier for both:  $\ln{(Z_{\rm sim}/Z_{\rm exd})}$ for ethanal's lowest  $T_{\rm r}$  exceeds  $50\sigma$  and pentanethiol's low- $T_{\rm r}$  ln  $(Z_{\rm sim}/Z_{\rm exd})$  exceeds  $150\sigma$ . Pentanethiol also shows a rapid, exponential-like decrease in Z as the temperature increases, until eventually the data becomes well-behaved nearer to the critical point. As discussed above, the histogram-reweighting technique distributes errors associated with the lowest temperatures into the nearby higher temperatures creating this distinctive curvature, seen most characteristically for pentanethiol. There are, of course, also sampling problems in the development data obtained from GEMC simulations, but these are not as apparent and usually also involve large uncertainties for  $Z_e$ . One example is octan-1-ol (Figure 4, Panel E: orange circle) with  $Z_e \approx 1.2$ . Under-sampling of the vapor phase at lower  $T_r$  can also be seen in the deviations from linearity in the Clausius-Clapeyron plots for both GCMC-HR and many GEMC examples (see next section). The last of the selected outliers in Table 6 is anthracene (Figure 4, Panel L, red squares), 25 which is one of four molecules that used the wrong molecular weight to compute the VLCC during transferability tests of models that were parameterized to (usually) compounds of lower molecular weight or fewer substituent groups. Discerning the actual shape of the anthracene curve is difficult due to the large error bars, but the Z values appear to have the right curvature, just offset by a consistent factor of about 1.6 (equivalent to the molecular weight ratio of  $C_{28}$  and  $C_{14}H_{10}$ ). This leads to  $\ln (Z_{\rm sim}/Z_{\rm exd})$  values for anthracene close to -0.5 at each temperature.

# A Metric Based on Clausius-Clapeyron Triads

As discussed in the previous section, the Z metric (particularly, when  $Z_i$  is used) can fail to detect inadequate sampling in GEMC simulations. Here, we propose a complementary metric that evaluates the deviation of the vapor pressure from expected behavior. The Clausius-Clapeyron (CC) equation can be used to predict the vapor pressure at  $T_i$  when the enthalpy of vaporization,  $\Delta H_{\text{vap}}$ , and vapor pressure at  $T_j$  are known:

$$\ln\left(\frac{P(T_i)}{P(T_j)}\right) = -\frac{\Delta H_{\text{vap}}}{R} \left(\frac{1}{T_i} - \frac{1}{T_j}\right)$$
(8)

Thus, data for  $\ln P$  plotted against inverse temperature should fall onto a straight line with a slope of  $-\Delta H_{\rm vap}/R$ :

$$\ln P = \left(-\frac{\Delta H_{\text{vap}}}{R}\right) \frac{1}{T} + C \tag{9}$$

Such CC plots are shown in numerous TraPPE publications and other studies of VLE. However, the CC equation is derived from the Clapeyron equation which equates the local slope of the coexistence line to the entropy or enthalpy and the volume change of the transition:

$$\left(\frac{dP}{dT}\right)_{\text{VLCC}} = \frac{\Delta S_{\text{vap}}(T)}{(\bar{V}_{\text{vap}}(T) - \bar{V}_{\text{liq}}(T))} = \frac{\Delta H_{\text{vap}}(T)}{T(\bar{V}_{\text{vap}}(T) - \bar{V}_{\text{liq}}(T))} \tag{10}$$

The derivation of the CC equation is based on a set of assumptions that are not valid for the entire vapor-liquid coexistence region. Specifically, it is assumed that  $\bar{V}_{\text{vap}} \gg \bar{V}_{\text{liq}}$  and  $\bar{V}_{\text{vap}} = RT/P_{\text{vap}}$  (or  $Z_{\text{liq}} = 0$  and  $Z_{\text{vap}} = 1$ , respectively) and that  $\Delta H_{\text{vap}}$  is constant.

At higher  $T_{\rm r}$ ,  $\Delta H_{\rm vap}$  changes rapidly and approaches zero while the volume difference deviates strongly from the ideal gas law and also approaches zero. The approximate linearity of the CC plot is only due to cancellation of these errors. Interestingly, the deviation from CC behavior can be larger at low  $T_{\rm r}$ , despite the fact that the first two approximations hold, because  $\Delta H_{\rm vap}$  decreases with increasing temperature and there is no error cancellation, i.e.,  $(dP/dT)_{\rm VLCC}$  increases with decreasing T and there is downward curvature in the CC plot.

In principle,  $\Delta H_{\rm vap}$  is available from GEMC simulations for vapor-liquid equilibria, but it is less often reported. In addition,  $\Delta H_{\rm vap}$  is difficult to evaluate from molecular dynamics simulations of an interfacial system. Thus, to ensure wider applicability, the complementary pressure metric should not rely on knowledge of  $\Delta H_{\rm vap}$ , meaning the Clapeyron equation cannot be used. Although one could use Eqn. 9 to fit data over the entire temperature range,

this would not lead to accurate values of the expected vapor pressure,  $P_{\rm exd}$ , for most of the temperatures because of the downward curvature in the CC plot. Linearity for the entire coexistence dataset, as measured by  $R^2$ , would be too coarse a metric. Instead, we utilize triads of neighboring temperatures for our P-based metric, where two of these temperatures are used to determine the local slope,  $-\Delta H_{\rm vap}/R$ , via Eqn. 8, and  $P_{\rm CC}$  for the third point is determined by also applying the CC equation.

The P-based metric is then developed in a manner similar to the Z-based metric, but with the added understanding that the expected  $P_{\text{exd}}$  can deviate somewhat from  $P_{\text{CC}}$ . That is, we create distributions of  $\ln (P_{\rm sim}/P_{\rm CC})$ , then use the mean to determine expected values,  $\ln (P_{\rm CC}/P_{\rm exd})$ , and let the standard deviation establish numeric boundaries, all based on high-quality simulations (i.e., the validation data). Since  $\ln (P_{\rm CC}/P_{\rm exd})$  can deviate from zero, this approach includes an expectation of curvature in the CC plot, i.e.,  $\ln (P_{\text{sim}}/P_{\text{exd}}) =$  $\ln (P_{\rm sim}/P_{\rm CC}) + \ln (P_{\rm CC}/P_{\rm exd})$ . To find  $P_{\rm CC}$ , we use two of the points in each triad to predict the P of the third. Predictions are done in three ways:  $CC_{LOW}$ , where the two higher  $T_r$ points of the triad are used to predict  $P_{\rm CC}$  at the lowest  $T_{\rm r}$  of the triad;  $CC_{\rm HIGH}$ , where the two lower  $T_{\rm r}$  points are used to predict  $P_{\rm CC}$  at the highest  $T_{\rm r}$ ; and  ${\rm CC_{MID}}$ , where the highest and lowest  $T_r$  points are used to predict  $P_{\rm CC}$  at the middle  $T_r$ . If data at  $N_T$  temperatures are available, then there are  $N_T-2$  CC<sub>LOW</sub>,  $N_T-2$  CC<sub>MID</sub>, and  $N_T-2$  CC<sub>HIGH</sub> triads. As an example, the CC plot for propan-1-ol<sup>16</sup> is shown in Figure 7. For CC<sub>LOW</sub> and CC<sub>HIGH</sub>, the predicted point is extrapolated outside of the two points used in the linear fit. The range of this extrapolation can be determined by taking the ratio of two differences, the difference between the inverse temperatures of the predicted point and its nearest neighbor divided by the difference between the two inverse temperatures used to make the prediction. Ideally, this ratio should be close to 1.0 (i.e., equally spaced inverse temperatures). Larger extrapolation ranges are more likely to lead to inaccurate values of  $P_{\text{exd}}$ . As an aside, when the Gibbs-Duhem integration approach 46 is used to trace the coexistence line, then analysis of  $\Delta H_{\rm vap}$  triads would likely be more useful than of the CC triads.

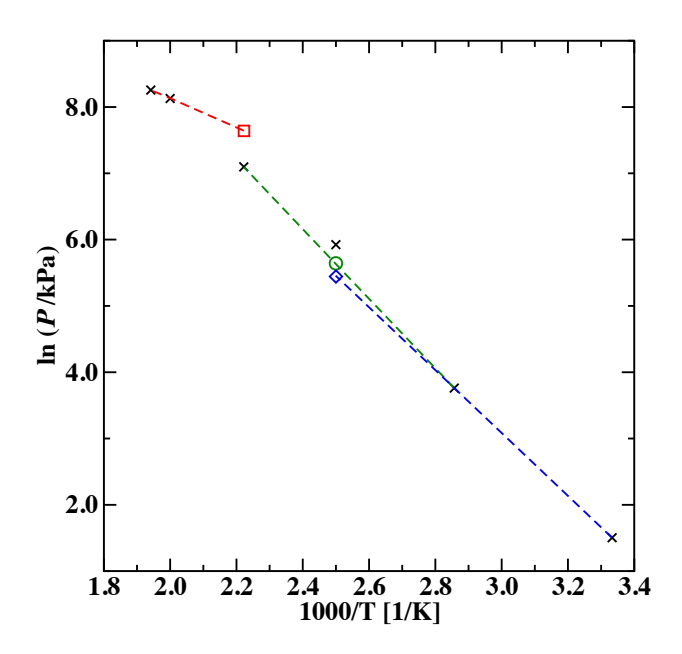


Figure 7: Clausius-Clapeyron triads obtained from simulations of the TraPPE-UA model for propan-1-ol. <sup>16</sup> Original simulation data are shown as black crosses. Linear CC fits for  $CC_{LOW}$ ,  $CC_{HIGH}$ , and  $CC_{MID}$  are shown as red, blue, and green dashed lines, and the corresponding  $P_{exd}$  values are depicted as red square, blue diamond, and green circle, respectively.

## Analysis of CC Triads from the TraPPE Database

The use of triads reduces the size of our overall TraPPE dataset compared to the Z metric, from 1072 total points to 754 (see Table 2), and leads to three distinct sets of  $P_{\text{exd}}$  values, where a  $P_{\text{sim}}$  data point at a specific  $T_{\text{r}}$  is compared to a  $P_{\text{exd}}$  value one to three times. The  $P_{\text{sim}}$  at the highest  $T_{\text{sim}}$  will only be utilized once as the highest T in a triad (similarly just once for the lowest  $T_{\text{sim}}$  as the lowest T in a triad), the next points inward can be predicted twice (CC<sub>HIGH</sub> or CC<sub>LOW</sub> and CC<sub>MID</sub>), while interior points will be involved in three triads. Of course, an erroneous  $P_{\text{sim}}$  at a single  $T_{\text{r}}$  can lead to outliers for all three triads involving this single  $T_{\text{r}}$ ; i.e., the total number of  $\ln (P_{\text{sim}}/P_{\text{exd}})$  outliers is larger than the number of erroneous pressure values.

As with the Z-based metric, provided with a reliable value for  $P_{\text{exd}}$ , the amount of tolerable deviation in  $P_{\text{sim}}$  can be determined from our validation data. We again consider three  $T_{\text{r}}$  ranges, differing in their relative nearness to the critical point, and fit Gaussian

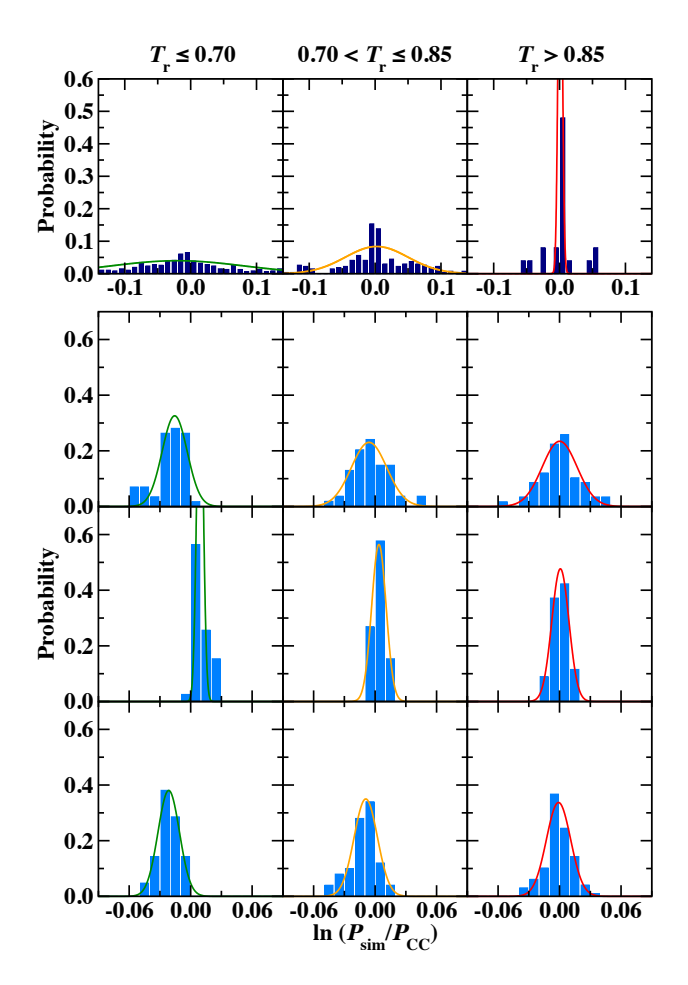


Figure 8: Gaussian fits to the distributions of  $\ln{(P_{\rm sim}/P_{\rm CC})}$  for the TraPPE database. Development data are shown in the top row (dark blue) for the CC<sub>LOW</sub> predictions. The following three rows show validation data (light blue) for the CC<sub>LOW</sub>, CC<sub>MID</sub>, and CC<sub>HIGH</sub> predictions, respectively.

functions separately for each. The results of these fits are shown in Figure 8 and Table 7. For the development data, the standard deviation is on average ten times larger in magnitude than the value of  $\overline{x} = \ln{(P_{\rm CC}/P_{\rm exd})}$ , suggesting there is no statistically significant deviation from linearity in the CC plot. The distributions for the validation set are much narrower than those for the development set (by factors of 11, 4, and 2 for  $T_{\rm r} \leq 0.70$ ,  $0.70 < T_{\rm r} \leq 0.85$ , and  $T_{\rm r} > 0.85$ , respectively), with the exception of the high- $T_{\rm r}$  range for CC<sub>LOW</sub>. We attribute this to the validation effort emphasizing precise and accurate estimation of the critical point and including a much larger number of data points with  $T_{\rm r} > 0.9$ . The average value of the third highest  $T_{\rm r}$  (highest  $T_{\rm r}$  considered for CC<sub>LOW</sub>) for the 159 development compounds is

Table 7: Numbers of Data Points and Outliers, Mean ( $\bar{x} = \ln{(P_{\rm CC}/P_{\rm exd})}$ ), and Standard Deviation for the  $\ln{(P_{\rm sim}/P_{\rm CC})}$  Distributions of the Development and Validation Data<sup>a</sup>

			$T_{\rm r}$ :	$\leq 0.70$		0.	70 <	$T_{\rm r} \leq 0.3$	85		$T_{\rm r}$ :	> 0.85	
Triad	Dataset	$N_{\mathrm{data}}$	$N_{\rm out}$	$\overline{x}$	$\sigma$	$N_{\mathrm{data}}$	$N_{\rm out}$	$\overline{x}$	$\sigma$	$N_{\rm data}$	$N_{\rm out}$	$\overline{x}$	$\sigma$
$\overline{\text{CC}_{\text{LOW}}}$	dev	462	236	-0.020	0.100	267	107	0.002	0.048	25	3	0.001	0.003
	val	57	_	-0.016	0.012	54	_	-0.006	0.017	58	_	0.001	0.017
$CC_{MID}$	$\operatorname{dev}$	309	206	0.006	0.050	341	165	0.003	0.032	104	29	-0.003	0.018
	val	39	_	0.009	0.003	52	_	0.004	0.007	78	_	-0.001	0.008
$CC_{HIGH}$	$\operatorname{dev}$	175	85	-0.008	0.086	324	170	-0.013	0.063	255	124	0.004	0.053
	val	21	_	-0.021	0.010	50	_	-0.009	0.011	98	_	-0.001	0.012

<sup>&</sup>lt;sup>a</sup> The  $T_{\rm r}$  of the predicted point determines the assignment to a specific  $T_{\rm r}$  range, i.e., the two other points in the triad may not fall into this range.

0.88, whereas it is 0.93 for the validation data. Furthermore, the shape of the  $\ln{(P_{\rm sim}/P_{\rm CC})}$  distribution for the development data at  $T_{\rm r} > 0.85$  is also not well described by the Gaussian curve, and the width may be somewhat underestimated. Considering the three CC triads, the number of data points used in the  $\ln{(P_{\rm sim}/P_{\rm CC})}$  fitting is largest near the critical point for the validation data, but the opposite holds for the development set.

With the smaller widths of the distributions, the validation data show distinct deviations from linearity in the CC plot as indicated by  $\ln{(P_{\rm CC}/P_{\rm exd})}$  that differ significantly from zero. As expected from the increase in  $(dP/dT)_{\rm VLCC}$  with decreasing T (i.e., downward curvature in the CC plot),  $\ln{(P_{\rm CC}/P_{\rm exd})}$  values are negative, positive, and negative for  ${\rm CC}_{\rm HIGH}$ ,  ${\rm CC}_{\rm MID}$ , and  ${\rm CC}_{\rm LOW}$ , respectively. The average deviation from linearity is largest for  $T_{\rm r} \leq 0.70$ , where it is on average 2.1 times larger than the standard deviation. However, for the validation data, the distributions for all three CC metrics at  $T_{\rm r} \leq 0.70$  are not well described by the Gaussian fits with clear tails on the side further away from zero. There are two potential reasons for the skew: (i) some of the data fall below  $T_{\rm r} \leq 0.55$ , and it could be that data at these lower  $T_{\rm r}$  require a larger magnitude of  $\overline{x}$ , but we do not have enough data to establish separate distributions for  $T_{\rm r} \leq 0.55$ ; (ii) the simulations for most of the validation compounds use constant temperature steps that lead to increasing step sizes in the inverse temperature used for the CC metric and, as a result, the extrapolation range increases with decreasing

temperature.

Shifts in the distribution are still visible for  $0.70 < T_{\rm r} \le 0.85$ , but here the standard deviation is on average 1.9 times larger than the shift. For  $T_{\rm r} > 0.85$ , we do not find any significant shift presumably due to the cancellation of errors resulting from the assumptions made in the derivation of the CC equation. Whereas different values of  $Z_{\rm crit}$  (due to hydrogen bonding and molecular shape) lead to a significant increase (by a factor of 4) of the width of the  $\ln{(Z_{\rm sim}/Z_{\rm exd})}$  distribution for  $T_{\rm r} > 0.85$ , the increase in the width of the  $\ln{(P_{\rm sim}/P_{\rm exd})}$  distributions is only a factor of 1.7; that is, the P metric holds well for different molecule types. Finally, the  $\ln{(P_{\rm sim}/P_{\rm CC})}$  distribution (see Figure 7) is very broad for the development data at  $T_{\rm r} \le 0.70$ , this indicates that there are indeed sampling challenges that lead to problems for the low- $T_{\rm r}$  simulations.

Identification of  $\ln{(P_{\rm sim}/P_{\rm exd})}$  outliers for the  $\rm{CC_{LOW}}$ ,  $\rm{CC_{MID}}$ , and  $\rm{CC_{HIGH}}$  tests results in high redundancy though there are differences in the specific points designated as outliers. However, problematic simulations will produce outliers for each test. For simplicity and because we expect the lower  $T_{\rm r}$  to be most informative for our metric (i.e., they are most likely to suffer from sampling problems due to low acceptance rates for molecule transfers and low numbers of molecules in the vapor phase), we focus primarily on the  $\rm{CC_{LOW}}$  test in further analysis here, but all of the data for each  $\rm{CC_{triad}}$  test are available in the Supporting Information (see Table S4).

As was done for the Z metric, the acceptable range for  $\ln{(P_{\rm sim}/P_{\rm CC})}$  is given as  $\overline{x} \pm 3\sigma$  (i.e., equivalent to the acceptable range for  $\ln{(P_{\rm sim}/P_{\rm exd})}$  being  $0 \pm 3\sigma$ ) for the two higher  $T_{\rm r}$  regions, but  $\overline{x} \pm 6\sigma$  is used for  $T_{\rm r} \leq 0.7$  to account for the skew in the data. Specifically for the  ${\rm CC_{LOW}}$  test, when  $T_{\rm r} \leq 0.70$ ,  $\ln{(P_{\rm sim}/P_{\rm CC})}$  should be between -0.09 and 0.06, for  $0.70 < T_{\rm r} \leq 0.85$ , the acceptable range is -0.06 and 0.05, and at  $T_{\rm r} > 0.85$ ,  $\ln{(P_{\rm sim}/P_{\rm CC})}$  should be between -0.06 and 0.06. The boundaries of the acceptable ranges for  ${\rm CC_{MID}}$  and  ${\rm CC_{HIGH}}$  are provided in the caption of Table S5.

Applying the  $CC_{LOW}$  test to the TraPPE database for the development molecules results

in 140 (88%) of the molecules having at least one  $P_{\rm sim}$  that falls outside of the acceptable range. The outliers comprise 346 individual data points, or 46% of the  $CC_{\rm LOW}$  triads. For comparison, the  $CC_{\rm MID}$  and  $CC_{\rm HIGH}$  tests lead to 400 and 379 outliers. Thus, extrapolation to low and high temperatures and interpolation to an intermediate temperature yield rather similar number of outliers but, again, the validation data lead to a narrower distribution for interpolation ( $CC_{\rm MID}$ ) and, in turn, narrow bounds.

Most of the CC<sub>LOW</sub> outliers come from the lowest three temperatures simulated for a given model. The numbers of  $CC_{triad}$  outliers are about a factor of 1.5 to 1.7 higher than the 229 outliers found with the Z metric. At first glance, the boundaries used for the  $CC_{triad}$  tests appear to be more restrictive than those for the Z metric. However, as discussed previously, calculation of P using the virial equation (see Eqn. 1) in GEMC simulations leads to strong correlation between P and  $\rho_{\text{vap}}$  at low  $T_{\text{r}}$  and, as a result, masks problematic simulations in the Z metric. A second reason is that more temperatures are used for the validation set (slightly above 10 on average per compound versus less than 7 for the development set), such that the  $T_{\rm r}$  intervals are on average larger for the development set. This increases the extrapolation range and the expected deviation from CC behavior. Thus, the larger inverse temperature intervals or sometimes also uneven intervals in absolute temperature may cause some false positives in the development data. In principle, it would be advantageous to make the boundaries of the CC<sub>triad</sub> tests also a function of the extrapolation range, but we do not have sufficient validation data to do this in a statistically meaningful manner, and it would introduce further complexity. Thirdly, differences in hydrogen bonding ability and molecular shape result in a larger spread for the Z metric (leading to a more permissive Z metric), whereas the curvature of the CC plots may be more universal.<sup>41</sup>

A set of selected  $CC_{LOW}$  outliers is depicted as CC plots in Figure 9 and some numerical values are provided in Table 8. The lowest- $T_r$  vapor pressures of quinoline and pyridazine are the most extreme outliers in the  $CC_{LOW}$  test, and the "hockey-stick" shape of their CC curves leads to deviations of about 250 and 200 $\sigma$  away from  $\overline{x}$ . These data correspond to  $T_r = 0.37$ 

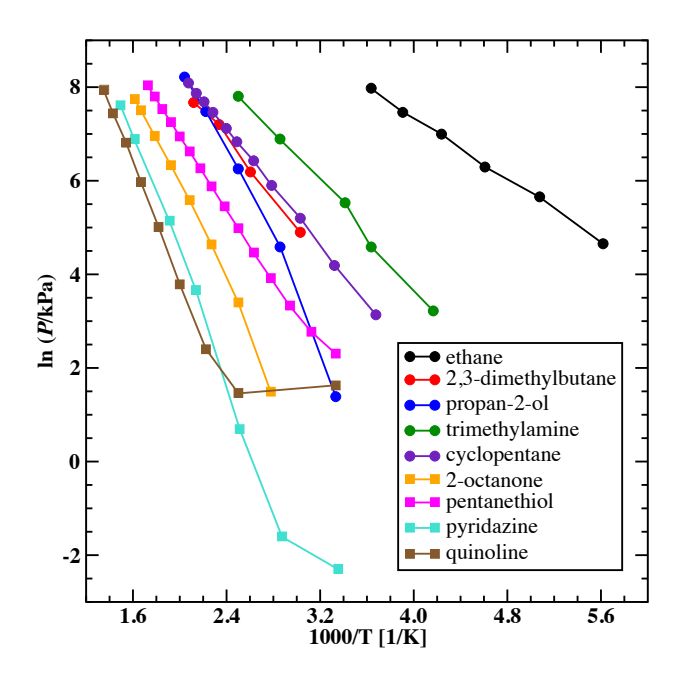


Figure 9: Clausius-Clapeyron plots for selected TraPPE models. Colors and symbols are as described in the legends. Connecting lines are provided only as an aid to visualization.

and 0.39, that are some of the lowest  $T_r$  attempted in the TraPPE database. These were used to compare to experimental liquid densities at near-ambient conditions, and the P data at these temperatures are not shown in the CC plots included in the respective publications but only appear in the respective Supporting Information. <sup>24,25</sup> Given the significant deviation from the remainders of the CC curves, the GEMC simulations at these temperature were likely not successful, and the data made it into the supporting information only due to scripting errors.

Ethane, <sup>11</sup> 2,3-dimethylbutane, <sup>12</sup> and propan-1-ol, <sup>16</sup> (see Figure 7) are examples of early TraPPE development efforts when properties were calculated from block averages in a single simulation trajectory rather than truly independent simulations. At the time, priority was given to fitting  $\rho_{\text{liq}}$  and  $T_{\text{crit}}$  with high accuracy (less than 1% error), while lower targets were accepted for the vapor phase. The CC plots show small but clear deviations from linearity for these models, often over the entire  $T_{\text{r}}$  range, and the sensitive CC<sub>triad</sub> metric flags them as outliers. Trimethylamine <sup>18</sup> and cyclopentane <sup>22</sup> are more recent examples, but involve CBMC sampling challenges as a highly branched EH model or as a ring polymer, respectively. Of

Table 8: Selected CC<sub>LOW</sub> Outliers with Their Nearest Boundary (NB<sub>CC</sub>), Extrapolation range (ER), and corresponding  $\ln (Z_{\rm sim}/Z_{\rm exd})$  and NB<sub>Z</sub> Values

Molecule	$T_{\rm r}$	$\ln\left(P_{\mathrm{sim}}/P_{\mathrm{CC}}\right)$	$NB_{CC}$	ER	$\ln\left(Z_{\rm sim}/Z_{\rm exd}\right)$	$\overline{\mathrm{NB_{Z}}}$
ethane	0.59	-0.26	-0.09	1.16	$0.01_{5}$	0.03
2,3-dimethylbutane	0.76	-0.43	-0.06	1.23	$0.00_{9}$	0.05
propan-1-ol	0.84	-0.55	-0.06	3.82	$-0.03_{8}$	-0.06
propan-2-ol	0.60	-0.97	-0.09	1.33	$-0.35_{14}$	-0.03
cyclopentane	0.64	0.136	0.06	1.59	$0.00_{3}$	0.03
trimethylamine	0.55	0.88	0.06	2.37	$0.01_{6}$	0.03
2-octanone	0.56	-0.38	-0.09	1.22	-0.54	-0.03
pentanethiol	0.50	0.16	0.06	1.13	1.17	0.03
pyridazine	0.39	2.38	0.06	1.34	$0.5_{6}$	0.03
quinoline	0.37	2.99	0.06	3.00	$0.04_{2}$	-0.03

particular interest in the pursuit of metrics for simulation quality is the fact that none of these five compounds shows an outlier in the Z metric (see Table 8). Furthermore, quinoline at  $T_{\rm r}=0.37$  yields  $Z=0.964\pm0.022$ , a much less alarming value than the huge deviation found by the CC<sub>triad</sub> metric. Conversely, an error with assigning molecular weights would be entirely invisible for the CC<sub>triad</sub> test because the pressure is calculated from the forces and is molecular-weight independent. This clearly shows that the two metrics are complementary, and together give a fuller picture of simulation quality.

A smaller number of TraPPE models did result in both Z and  $CC_{triad}$  outliers and, generally, the failures are large in these cases for both metrics. Propan-2-ol <sup>16</sup> suffers from sampling challenges due to hydrogen-bonding at the lowest  $T_r$  (and also a large temperature step down to this  $T_r$ ), but may also have a data entry mistake. This data point for propan-2-ol is the outlying magenta circle in Panel E of Figure 4. Pentanethiol <sup>19</sup> and 2-octanone <sup>17</sup> are among the examples from GCMC-HR simulations that are insufficiently sampled at low  $T_r$ . This is reflected as large upward or downward curvature (instead of scatter) in the CC plots (see Figure 9), as well as the corresponding curvatures in the Z versus  $T_r$  plots (purple circles in Panel J for pentanethiol and green circles in Panel F for 2-octanone in Figure 4). Many of the EH models for aromatics <sup>24,25</sup> also include significant outliers in the  $CC_{triad}$  metric, but not as severe as quinoline and pyridazine; transfer moves for these large, rigid molecules are

particularly challenging at low  $T_{\rm r}$ .

# Conclusions

To summarize, the analysis of the TraPPE database with the highlighted examples provided here helps to demonstrate the importance and power of the Z and  $CC_{triad}$  based metrics for simulation quality. While Z is a good metric for detecting many types of simulation errors (insufficient sampling in MD with interfacial boxes and GCMC-HR simulations, molecular weight discrepancies, and typos), it routinely fails to account for insufficient sampling in GEMC simulations. This is simply a consequence of the way that P is calculated in GEMC and signifies the need for a complementary metric, such as the  $CC_{triad}$  metric, for these types of simulations. A more powerful metric emerges when both Z and  $CC_{triad}$  can be evaluated together as part of the same set of simulations. Most of the pronounced errors (with deviations larger than  $10\sigma$ ) found in previous simulations of TraPPE models, if not all, could have been corrected with more careful attention to the simulation data; attention that in the future can be helpfully directed by the Z and  $CC_{triad}$  metrics. To this extent, a Python script for performing the Z and  $CC_{triad}$  tests is provided as Supporting Information.

For GEMC, Z should not be calculated using separate ensemble averages of P and  $\rho_{\text{vap}}$  (i.e.,  $Z_{\text{e}} = (\langle P \rangle / \langle \rho_{\text{vap}} \rangle)(W/RT)$ ) together with error propagation at the end of the simulation because, at low  $T_{\text{r}}$ , P is highly correlated with  $\rho_{\text{vap}}$  and the statistical error can be overestimated by as much as two orders of magnitude. At high  $T_{\text{r}}$ ,  $Z_{\text{e}}$  underestimates the true  $\langle Z \rangle$  value as instantaneous values of z and  $\rho_{\text{vap}}$  become more correlated; a histogram analysis of the instantaneous z value distributions leads to more accurate  $Z_{\text{i}} = \langle P/\rho_{\text{vap}} \rangle (W/RT)$  (and also  $\rho_{\text{liq}}$ ,  $\rho_{\text{vap}}$ , and P) ensemble averages. In other words, Z should be calculated as  $Z_{\text{i}}$  using histogram analysis. A Python script for carrying out the histogram analysis is provided as Supporting Information.

More persistent simulation challenges, particularly for GEMC, where Z should always

be well-behaved for properly executed simulations, require a second, complementary metric. The Clausius-Clapeyron curve (or, when available, directly calculated values of the  $\Delta H_{\rm vap}$  for sufficiently small temperature steps) can be used to detect sampling problems in GEMC simulations. Due to the inverse-temperature relation of the Clausius-Clapeyron curve, the  $CC_{\rm triad}$  metric will be most informative for simulation quality when simulation data are available at equally spaced  $T^{-1}$  values. Satisfying both the Z and  $CC_{\rm triad}$  metrics will require longer trajectories, larger system sizes, and/or better simulation protocols (and, certainly, more computer time). Most of the less significant outliers (with deviations falling into the range from 4 to  $9\sigma$ ) found for the TraPPE development data are a consequence of the more limited computer resources available at the time when the development was done, i.e., data from these earlier simulations have larger statistical uncertainties.

Taken as a whole, the analysis performed here indicates that high-quality simulation data, while certainly achievable, are by no means easy to achieve. The fact that MMS methods are increasingly accessible (and cheap) must be balanced by the much harder task of properly applying these methods to generate robust and reliable data. Still, when simulators pay careful attention to the details of the method and resist the temptation to underestimate the difficulty of performing a simulation correctly, high-quality data can be produced. The Z and CC<sub>triad</sub> metrics developed here can help guard against that temptation and set the standard for high-quality VLE data for moderately complex organic molecules described by molecular mechanics force fields. When the complexity of the compounds (e.g., number of atoms, degree of branching, or hydrogen-bonding capability) increases or when more expensive descriptions of the interactions (e.g., Kohn-Sham density functional theory) are used, then lower precision and more scatter of the VLE data is to be expected.

## Acknowledgement

This research is primarily supported through the National Science Foundation (CBET-1835067) and Wheaton College. The work on correlations between properties and histogram analysis is supported by the Department of Energy, Office of Basic Energy Sciences, Division of Chemical Sciences, Geosciences and Biosciences under Award DE-FG02-17ER16362. The development of the TraPPE database and website were supported by the National Science Foundation (RUI-1159731). Computational resources from the Minnesota Supercomputing Institute are also gratefully acknowledged. Several validation simulations were performed by Siepmann group members not included as authors (and not previously published): C. Bunner (ethanal, dimethyl sulfide, and n-perfluoropentane), J. Chen (2-butanethiol), E. Fetisov (2-methylpropene), D. Harwood (oxygen and 2,2-dimethylpropane), B. Liang (2-butanol), M. Shah (carbon dioxide), K. Struksheats (acetone, 2-methoxy-2-methylpropane, naphthalene, and 2-methyl-1,3-butadiene), and B. Xue (data for Table 4).

## Supporting Information Available

Additional simulation details and numerical VLCC data for the validation models. Description of GitHub repositories containing the version of the MCCCS–MN software together with input and output files used for validation simulations of pentanal, the Python script for the Z and  $CC_{triad}$  tests, and the Python script for the histogram analysis of coexistence properties from GEMC simulations. Tables listing all the  $\ln (Z_{sim}/Z_{exd})$  and  $\ln (P_{sim}/P_{CC})$  outliers for the TraPPE database.

#### References

- (1) Kofke, D. A.; Siepmann, J. I.; Chirico, R. D.; Kroon, M.; Mathias, P. M.; Sadowski, G.; Wu, J.; Brennecke, J. F. Editorial: Molecular Modeling and Simulation in JCED. J. Chem. Eng. Data 2016, 61, 1–2.
- (2) Frenkel, D. Simulations: The Dark Side. Eur. Phys. J. Plus 2013, 128, 1–21.
- (3) van Gunsteren, W. F.; Daura, X.; Hansen, N.; Mark, A. E.; Oostenbrink, C.; Riniker, S.; Smith, L. J. Validation of Molecular Simulation: An Overview of Issues. Angew. Chem. Int. Ed. 2018, 57, 884–902.
- (4) Schappals, M.; Mecklenfeld, A.; Kröger, L.; Botan, V.; Köster, A.; Stephan, S.; Garcia, E.; Rutkai, G.; Raabe, G.; Klein, P.; Leonhard, K.; Glass, C. W.; Lenhard, J.; Vrabec, J.; Hasse, H. Round Robin Study: Molecular Simulation of Thermodynamic Properties from Models with Internal Degrees of Freedom. J. Chem. Theo. Comput. 2017, 13, 4270–4280.
- (5) Nezbeda, I.; Kolafa, J. The Use of Control Quantities in Computer Simulation Experiments: Application to the Exp-6 Potential Fluid. *Mol. Simul.* **1995**, *14*, 153–163.
- (6) Schultz, A. J.; Kofke, D. A. Quantifying Computational Effort Required for Stochastic Averages. J. Chem. Theor. Comput. 2014, 10, 5229–5234.
- (7) Nezbeda, I. Simulations of Vapor–Liquid Equilibria: Routine versus Thoroughness. *J. Chem. Eng. Data* **2016**, *61*, 3964–3969.
- (8) Panagiotopoulos, A. Z. Direct Determination of Phase Coexistence Properties of Fluids by Monte Carlo Simulation in a New Ensemble. *Mol. Phys.* **1987**, *61*, 813–826.
- (9) Panagiotopoulos, A. Z.; Quirke, N.; Stapleton, M.; Tildesley, D. J. Phase Equilibria by Simulation in the Gibbs Ensemble: Alternative Derivation, Generalization and Application to Mixture and Membrane Equilibria. *Mol. Phys.* **1988**, *63*, 527–545.

- (10) Eggimann, B. L.; Sunnarborg, A. J.; Stern, H. D.; Bliss, A. P.; Siepmann, J. I. An Online Parameter and Property Database for the TraPPE Force Field. *Mol. Simul.* **2014**, 40, 101–105.
- (11) Martin, M. G.; Siepmann, J. I. Transferable Potentials for Phase Equilibria. 1. Unitedatom Description of n-Alkanes. J. Phys. Chem. B 1998, 102, 2569–2577.
- (12) Martin, M. G.; Siepmann, J. I. Novel Configurational-bias Monte Carlo Method for Branched Molecules. Transferable Potentials for Phase Equilibria. 2. United-atom Description of Branched Alkanes. J. Phys. Chem. B 1999, 103, 4508–4517.
- (13) TraPPE Website and Database Landing Page.

  http://chem-siepmann.oit.umn.edu/siepmann/trappe (accessed September 9, 2018).
- (14) TraPPE Validation Parameters and Properties. http://chem-siepmann.oit.umn.edu/siepmann/trappe/validation.html (accessed June 28, 2019).
- (15) Wick, C. D.; Martin, M. G.; Siepmann, J. I. Transferable Potentials for Phase Equilibria. 4. United-atom Description of Linear and Branched Alkenes and Alkylbenzenes. J. Phys. Chem. B 2000, 104, 8008–8016.
- (16) Chen, B.; Potoff, J. J.; Siepmann, J. I. Monte Carlo Calculations for Alcohols and Their Mixtures with Alkanes. Transferable Potentials for Phase Equilibria. 5. Unitedatom Description of Primary, Secondary, and Tertiary Alcohols. J. Phys. Chem. B 2001, 105, 3093–3104.
- (17) Stubbs, J. M.; Potoff, J. J.; Siepmann, J. I. Transferable Potentials for Phase Equilibria. 6. United-atom Description for Ethers, Glycols, Ketones, and Aldehydes. J. Phys. Chem. B 2004, 108, 17596–17605.

- (18) Wick, C. D.; Stubbs, J. M.; Rai, N.; Siepmann, J. I. Transferable Potentials for Phase Equilibria. 7. Primary, Secondary, and Tertiary Amines, Nitroalkanes and Nitrobenzene, Nitriles, Amides, Pyridine, and Pyrimidine. J. Phys. Chem. B 2005, 109, 18794– 18982.
- (19) Lubna, N.; Kamath, G.; Potoff, J. J.; Rai, N.; Siepmann, J. I. Transferable Potentials for Phase Equilibria. 8. United-atom Description for Thiols, Sulfides, Disulfides, and Thiophene. J. Phys. Chem. B 2005, 109, 24100–24107.
- (20) Lee, J.-S.; Wick, C.D.; Stubbs, J.M.; Siepmann, J.I. Simulating the Vapour–Liquid Equilibria of Large Cyclic Alkanes. *Mol. Phys.* **2005**, *103*, 99–104.
- (21) Maerzke, K.A.; Schultz, N.E.; Ross, R.B.; Siepmann, J.I. TraPPE–UA Force Field for Acrylates and Monte Carlo Simulations for Their Mixtures with Alkanes and Alcohols. J. Phys. Chem. B 2009, 113, 6415–6425.
- (22) Keasler, S. J.; Charan, S. M.; Wick, C. D.; Economou, I. G.; Siepmann, J. I. Transferable Potentials for Phase Equilibria. United-atom Description of Five- and Sixmembered Cyclic Alkanes and Ethers. J. Phys. Chem. B 2012, 116, 11234–11246.
- (23) Chen, B.; Siepmann, J. I. Transferable Potentials for Phase Equilibria. 3. Explicit-hydrogen Description of Normal Alkanes. *J. Phys. Chem. B* **1999**, *103*, 5370–5379.
- (24) Rai, N.; Siepmann, J. I. Transferable Potentials for Phase Equilibria. 9. Explicit-hydrogen Description of Benzene and Five-membered and Six-membered Heterocyclic Aromatic Compounds. J. Phys. Chem. B 2007, 111, 10790–10799.
- (25) Rai, N.; Siepmann, J. I. Transferable Potentials for Phase Equilibria. 10. Explicit-hydrogen Description of Substituted Benzenes and Polycyclic Aromatic Compounds. J. Phys. Chem. B 2013, 117, 273–288.

- (26) Potoff, J. J.; Siepmann, J. I. Vapor–Liquid Equilibria of Mixtures Containing Alkanes, Carbon Dioxide, and Nitrogen. *AIChE J.* **2001**, *47*, 1676–1682.
- (27) Zhang, L.; Siepmann, J. I. Direct Calculation of Henry's Law Constants from Gibbs Ensemble Monte Carlo Simulations: Nitrogen, Oxygen, Carbon Dioxide, and Methane in Ethanol. Theor. Chem. Acc. 2006, 115, 391–397.
- (28) Ketko, M.-B. H.; Rafferty, J. L.; Siepmann, J. I.; Potoff, J. J. Development of the TraPPE-UA force Field for Ethylene Oxide. *Fluid Phase Equil.* **2008**, *274*, 44–49.
- (29) Zhang, L.; Siepmann, J. I. Development of the TraPPE Force Field for Ammonia.

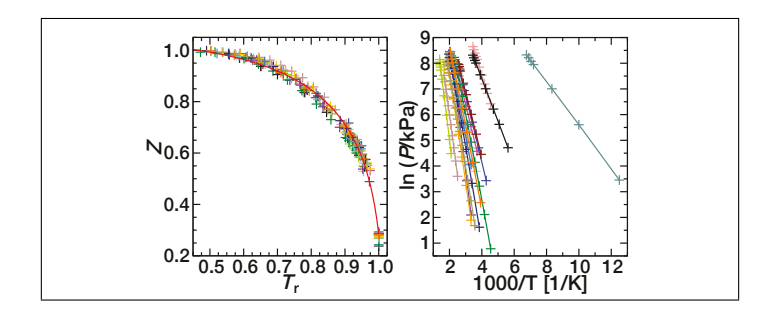
  Collect. Czech. Chem. Commun. 2010, 75, 577–591.
- (30) Shah, M. S.; Tsapatsis, M.; Siepmann, J. I. Development of the Transferable Potentials for Phase Equilibria Model for Hydrogen Sulfide. *J. Phys. Chem. B* **2015**, *119*, 7041–7052.
- (31) Chen, B.; Xing, J.; Siepmann, J. I. Development of Polarizable Water Force Fields for Phase Equilibrium Calculations. *J. Phys. Chem. B* **2000**, *104*, 2391–2401.
- (32) Chen, B. *Phase Equilibria of Hydrocarbons, Alcohols, Water, and Their Mixtures.* Ph.D. Thesis (University of Minnesota, Minneapolis, 2001).
- (33) Maerzke, K. A.; Siepmann, J. I. Transferable Potentials for Phase Equilibria. Coarse-grain Description for Linear Alkanes. *J. Phys. Chem. B* **2011**, *115*, 3452–3465.
- (34) Shah, M. S.; Tsapatsis, M.; Siepmann, J. I. Transferable Potentials for Phase Equilibria. Improved United-atom Description of Ethane and Ethylene. AIChE J. 2017, 63, 5098–5110.
- (35) Bai, P.; Tsapatsis, M.; Siepmann, J. I. TraPPE–zeo: Transferable Potentials for Phase Equilibria Force Field for All-silica Zeolites. *J. Phys. Chem.* **2013**, *117*, 24375–24387.

- (36) Potoff, J. J.; Panagiotopoulos, A. Z. Critical Point and Phase Behavior of the Pure Fluid and a Lennard-Jones Mixture. *J. Chem. Phys.* **1998**, *109*, 10914–10920.
- (37) Potoff, J. J.; Errington, J. R.; Panagiotopoulos, A. Z. Molecular Simulation of Phase Equilibria for Mixtures of Polar and Non-polar Components. *Mol. Phys.* **1999**, *97*, 1073–1083.
- (38) Siepmann, J. I.; Martin, M. G.; Chen, B.; Wick, C. D.; Stubbs, J. M.; Potoff, J. J.; Eggimann, B. L.; McGrath, M. J.; Zhao, X. S.; Anderson, K. E.; Rafferty, J. L.; Rai, N.; Maerzke, K. A.; Keasler, S. J.; Bai, P.; Fetisov, E. O.; Shah, M. S.; Chen, Q. P.; DeJaco, R. F.; Chen, J. L.; Bai, X. Monte Carlo for Complex Chemical Systems—Minnesota, version 17.1; University of Minnesota: Minneapolis, MN, 2017.
- (39) Cortes-Morales, A. D.; Economou, I. G.; Peters, C. J.; Siepmann, J. I. Influence of Simulation Protocols on the Efficiency of Gibbs Ensemble Monte Carlo Simulations.

  Mol. Simul. 2013, 39, 1135–1142.
- (40) Dinpajooh, M.; Bai, P.; Allan, D. A.; Siepmann, J. I. Accurate and Precise Determination of Critical Properties from Gibbs Ensemble Monte Carlo Simulations. J. Chem. Phys. 2015, 143, 114113.
- (41) O'Connell, J. P. Vapor-phase Nonideality: When to Worry. Chem. Eng. Prog. 2019, 115(5), 63–71.
- (42) Hinkley, D. V.; On the Ratio of Two Correlated Normal Random Variables. *Biometrika* **1969**, *56*, 635–639.
- (43) Smit, B.; De Smedt, Ph.; Frenkel, D. Computer Simulation in Gibbs Ensemble. *Mol. Phys.* **1989**, *68*, 931–950.
- (44) NIST Webbook Entry for Water.

- $https://webbook.nist.gov/cgi/inchi/InChI\%3D1S/H2O/h1H2 \quad (accessed \quad June \quad 28, \\ 2019).$
- (45) Panagiotopoulos, A. Z. Essential Thermodynamics; Drios Press: Princeton, 2011.
- (46) Kofke, D. A. Gibbs–Duhem Integration: A New Method for Direct Evaluation of Phase Coexistence by Molecular Simulation. *Mol. Phys.* **1993**, *78*, 1331–1336.

# Graphical TOC Entry



# **Supporting Information:**

# Assessing the quality of simulations for vapor-liquid equilibria: An analysis of the TraPPE database

Becky L. Eggimann,\*,† Yangzesheng Sun,‡ Robert F. DeJaco,‡,¶ Ramanish Singh,‡,¶ Muhammad Ahsan,‡ Tyler R. Josephson,‡ and J. Ilja Siepmann\*,‡,¶

†Department of Chemistry, Wheaton College, Wheaton, IL, 60187-5501, United States

‡Department of Chemistry and Chemical Theory Center,

University of Minnesota, Minneapolis, MN, 55455-0431, United States

¶Department of Chemical Engineering and Materials Science,

University of Minnesota, Minneapolis, MN, 55455-0431, United States

E-mail: becky.eggimann@wheaton.edu; siepmann@umn.edu

## Contents

Glossary of compressibility and pressure variables

[page 3]

Additional simulation details and numerical VLCC data for the validation models

[pages 4–13]

Description of GitHub repositories containing the version of the MCCCS–MN software together with input and output files used for validation simulations of pentanal, the Python script for the Z and  $CC_{triad}$  tests, and the Python script for the histogram analysis of coexistence properties from GEMC simulations near  $T_{crit}$  [page 14]

Tables listing all of the  $\ln{(Z_{\rm sim}/Z_{\rm exd})}$  and  $\ln{(P_{\rm sim}/P_{\rm CC})}$  outliers for the TraPPE database [pages 15–65]

# Glossary of Compressibility and Pressure Variables

Z	generic compressibility factor measured or calculated through various means
$Z_{ m crit}$	compressibility factor at the critical point
$Z^*$	average critical compressibility factor of 20 validation compounds
$Z_{ m e}$	compressibility factor calculated from ensemble averages of vapor pressure and
	vapor density (see eq. 4)
$Z_{ m i}$	compressibility factor calculated from ensemble average of instantaneous vapor
	pressure over vapor density ratios (see eq. 5)
z	instantaneous compressibility factor for a given configuration
$Z_{ m sim}$	average compressibility factor (either $Z_{\rm e}$ or $Z_{\rm i}$ ) obtained from simulation
$Z_{\mathrm{exd}}$	expected compressibility factor determined from eq. 7
P	generic vapor pressure measured or calculated through various means
$P_{\rm crit}$	pressure at the critical point
$P_{\mathrm{ideal}}$	ideal gas pressure
$P_{\mathrm{GEMC}}$	average vapor pressure calculated from the virial equation for the vapor box in a
	GEMC simulation (see eq. 1)
$P_{\text{GCMC}}$	vapor pressure calculated from the partition function in GCMC-HW simulations
$P_{\mathrm{sim}}$	average vapor pressure obtained from a simulation
$P_{\rm CC}$	vapor pressure of the third point in a triad determined by applying the Clausius–
	Clapeyron equation (eq. 8) using the enthalpy of vaporization and vapor pressure
	obtained from the other two points
$P_{\mathrm{exd}}$	expected vapor pressure determined from $\overline{x} = \ln(P_{\rm CC}/P_{\rm exd})$

#### Validation Simulations

#### Additional Simulation Details

As described in the main text, all validation simulations are done in the NVT-Gibbs ensemble with coupled-decoupled configurational-bias Monte Carlo. Lennard-Jones interactions are treated with a spherical potential cutoff  $(r_{\rm cut})$  and analytic tail corrections. When charges are present, Coulomb interactions are calculated using the Ewald summation technique with the same  $r_{\rm cut}$  values for the direct space part and  $\kappa = 2\pi/{\rm boxlength}$ . For the liquid phase, the standard TraPPE value  $r_{\rm cut} = 14$  Å is used for all simulations with linear dimensions typically falling into the 30 to 50 Å range. To yield predicted saturated vapor pressure and density with the desired precision requires vapor phases containing on average 10-20% of the molecules and, due to the exponential dependence of vapor pressure on temperature, a much larger spread of volumes. In particular at low reduced temperatures with very large vapor volumes, the  $r_{\rm cut}$  value is adjusted to be approximately 40% of the boxlength to yield a good balance for the computational cost of the direct and reciprocal space parts of the Ewald summation.

At high reduced temperatures near the critical point, Gaussian fits to property histograms are used to determine  $\rho_{\text{liq}}$ ,  $\rho_{\text{vap}}$ ,  $P_{\text{vap}}$ , and  $Z_{\text{vap}}$ . Critical properties are obtained using VLCC data from temperatures that exceed  $0.9T_{\text{crit}}$ . For these temperatures, coexistence densities are determined by Gaussian fits to density probability histograms, which are then used in fits to the scaling law (with a critical exponent of 0.326) and law of rectilinear diameters to obtain the critical temperature and density. An Antoine fit over this same temperature range is used for the estimation of the critical pressure. The normal boiling point is determined from a Clausius-Clapeyron fit to the vapor pressure data for those temperatures closest to the normal boiling point. Specific information is provided for each validation molecule in Table S1.

Table S1: Simulation Details for TraPPE Validation Compounds

Information is provided for the year the validation was performed, the system size (N), the number of independent simulations  $(N_{\text{IND}})$ , the total number of production cycles  $(N_{\text{cyc}})$ , the number of temperatures above  $0.9T_{\text{crit}}$  that are used to determine the critical properties  $(N_{T_{\text{crit}}})$ , and the number of temperatures near  $T_{\text{b}}$  that are used to determine the normal boiling point  $(N_{T_{\text{b}}})$ . When a range of values is given, the larger/longer simulations are those closest to the critical point.

Molecule	Year	N	$N_{ m IND}$	$N_{ m cyc}/10^3$	$N_{T_{ m crit}}$	$N_{T_{ m b}}$
oxygen	2015	1200	8	200	5	2
carbon dioxide	2015	1000	8	50	4	2
${ m ethane}^a$	2017	1500	8	1000	4	2
n-butane	2019	400-800	8	100-250	3	2
n-decane <sup><math>b</math></sup>	2015	300	8	200	4	2
2-methylpropane	2019	400	8	100-200	4	3
2,2-dimethylpropane	2015	500	8	60	4	2
2-methylpropene	2014	500	8	60	4	2
2-methyl-1,3-butadiene	2013	500	8	80	4	3
${ m naphthalene}$	2013	400	8	100	5	3
ethanol	2019	1000	8	80	3	2
2-butanol	2019	1000	8	100	5	2
ethanal	2018	800	8	100-150	4	3
pentanal	2019	400-800	16	120-280	5	4
acetone	2013	500	8	120	6	3
2-methoxy-2-methylpropane	2014	500	8	80	4	2
methyl acetate	2019	500-600	16	200	5	4
2-butanethiol	2019	500	8	100	4	2
dimethyl sulfide	2018	800	8	100-150	4	3
<i>n</i> -perfluoropentane	2019	400	8-16	100-200	4	4

<sup>&</sup>lt;sup>a</sup> The validation simulations for ethane were previously reported in: Shah, M. S.; Tsapatsis, M.; Siepmann, J. I. Transferable Potentials for Phase Equilibria. Improved United-atom Description of Ethane and Ethylene. *AIChE J.* **2017**, *63*, 5098–5110.

<sup>&</sup>lt;sup>b</sup> The validation simulations for *n*-decane were previously reported in: Dinpajooh, M.; Bai, P.; Allan, D. A.; Siepmann, J. I. Accurate and Precise Determination of Critical Properties from Gibbs Ensemble Monte Carlo Simulations. *J. Chem. Phys.* **2015**, *143*, 114113.

## **VLCC** Data for Validation Models

Table S2: Vapor-Liquid Coexistence Data for TraPPE Validation Compounds When available,  $Z_{\rm i}$  values computed from instantaneous z values including histogram analysis are also provided. Subscripts provide the uncertainties in the last digit(s), given as the standard error of the mean estimated from the set of independent simulations (i.e.,  $31.6_2$  stands for  $31.6 \pm 0.2$  and  $5679_{34}$  stands for  $5679 \pm 34$ )

molecule	T [K]	$\rho_{\mathrm{liq}} \; [\mathrm{g/ml}]$	$\rho_{\rm vap} \ [{\rm g/ml}]$	$P_{\text{vap}} [kPa]$	$Z_{ m i}$
oxygen	80	$1.1854_{1}$	$0.00154_1$	$31.6_{2}$	
	100	$1.0826_{1}$	$0.01117_7$	$272_{2}$	
	120	$0.9639_1$	$0.0423_4$	$1101_{9}$	
	139	$0.8147_{6}$	$0.1169_{5}$	$2835_{7}$	
	142	$0.7841_9$	$0.136_{2}$	$3210_{20}$	
	145	$0.7536_{6}$	$0.165_{2}$	$3690_{10}$	
	148	$0.712_{1}$	$0.192_2$	$4120_{10}$	
carbon dioxide	220	$1.1586_{4}$	$0.0161_2$	$616_{5}$	
	230	$1.1219_{5}$	$0.0238_{2}$	$922_{7}$	
	240	$1.0836_{4}$	$0.0341_1$	$1330_{5}$	
	250	$1.0432_{2}$	$0.0485_{4}$	$1874_{11}$	
	260	$0.999_{1}$	$0.0673_2$	$2557_{6}$	
	270	$0.951_{1}$	$0.095_{1}$	$3447_{14}$	
	275	$0.923_{1}$	$0.109_{1}$	$3870_{24}$	
	280	$0.896_{1}$	$0.128_{1}$	$4412_{24}$	
	285	$0.866_{1}$	$0.157_{2}$	$5050_{32}$	
	290	$0.834_{1}$	$0.196_{4}$	$5679_{34}$	
ethane	178	$0.5511_1$	$0.00233_1$	$111.2_{4}$	
	197	$0.52643_3$	$0.00541_1$	$276.3_{6}$	
	212	$0.50573_3$	$0.00942_1$	$500.0_{4}$	
	236	$0.46940_3$	$0.02019_3$	$1102_{2}$	
	256	$0.43442_5$	$0.0354_1$	$1901_{2}$	
	275	$0.39405_4$	$0.0599_{6}$	$2995_{15}$	
	280	$0.3814_1$	$0.0683_4$	$3320_{10}$	
	285	$0.3676_{1}$	$0.079_{1}$	$3680_{10}$	
	290	$0.3524_{3}$	$0.093_{1}$	$4080_{10}$	

Table S2: (continued)

molecule	T [K]	$\rho_{ m liq} \; [{ m g/ml}]$	$\rho_{\rm vap} \ [{\rm g/ml}]$	P <sub>vap</sub> [kPa]	$Z_{ m i}$
n-butane	204	$0.67206_{17}$	0.0001884 <sub>42</sub>	5.47 <sub>13</sub>	$0.99581_{10}$
	234	$0.64232_{15}$	$0.000938_{14}$	$30.90_{44}$	$0.98494_{38}$
	264	$0.61093_{16}$	$0.003050_{30}$	$110.9_{10}$	$0.96314_{39}$
	294	$0.57735_{20}$	$0.00774_{10}$	$300.3_{29}$	$0.92354_{61}$
	324	$0.54024_{40}$	$0.01668_{24}$	$668_{10}$	$0.8676_{13}$
	343	$0.51386_{54}$	$0.02577_{32}$	$1031_{10}$	$0.8189_{11}$
	354	$0.49690_{37}$	$0.03235_{41}$	$1287_{10}$	$0.7913_{22}$
	384	$0.44432_{28}$	$0.05768_{14}$	$2209_{10}$	$0.6998_{13}$
	392	$0.42652_{41}$	$0.0686_{10}$	$2544_{15}$	$0.6643_{35}$
	400	$0.40651_{37}$	$0.0814_{11}$	$2907_{19}$	$0.6284_{47}$
	408	$0.3841_{11}$	$0.1003_{10}$	$3318_{14}$	$0.5697_{25}$
n-decane	400	$0.65236_{23}$	$0.001610_{20}$	$36.6_{5}$	
	420	$0.63502_{24}$	$0.00281_{6}$	$66.3_{1}$	
	440	$0.6164_{3}$	$0.00459_{7}$	$111_{2}$	
	460	$0.5971_4$	$0.00717_{13}$	$177_{3}$	
	480	$0.5770_{3}$	$0.01090_{15}$	$273_{3}$	
	500	$0.5551_{3}$	$0.01605_{22}$	$402_{4}$	
	520	$0.5316_{4}$	$0.0230_{4}$	$571_{7}$	
	540	$0.5059_{6}$	$0.0329_{6}$	$798_{10}$	
	560	$0.4761_7$	$0.0462_{11}$	$1078_{19}$	
	580	$0.4411_7$	$0.0656_{11}$	$1451_{16}$	
	600	$0.3956_{12}$	$0.0946_{14}$	$1859_{18}$	
2-methylpropane	198	$0.65805_{17}$	$0.0002214_{41}$	$6.24_{11}$	$0.99558_{10}$
	228	$0.62736_5$	$0.001088_3$	$34.87_{10}$	$0.98328_{12}$
	258	$0.59519_3$	$0.0035549_{54}$	$125.60_{19}$	$0.95821_{40}$
	278	$0.57243_{8}$	$0.006767_{31}$	$250_{1}$	$0.93300_{55}$
	308	$0.53527_{10}$	$0.015166_{50}$	$584_{2}$	$0.87747_{64}$
	323	$0.51453_9$	$0.02148_{8}$	$832_{3}$	$0.84045_{65}$
	338	$0.49222_{10}$	$0.03005_{11}$	$1156_{3}$	$0.8001_{11}$
	343	$0.48495_{18}$	$0.03400_{15}$	$1298_{4}$	$0.7823_{10}$
	353	$0.46703_{25}$	$0.04154_{14}$	$1567_{4}$	$0.7519_{10}$
	368	$0.44129_{40}$	$0.05697_{37}$	$2077_{9}$	$0.6934_{16}$
	376	$0.42281_{47}$	$0.06599_{73}$	$2367_{16}$	$0.6689_{33}$
	384	$0.40401_{52}$	$0.0793_{10}$	$2721_{18}$	$0.6272_{40}$
	390	$0.38710_{50}$	$0.0933_{16}$	$3030_{21}$	$0.5864_{55}$

Table S2: (continued)

molecule	T [K]	$\rho_{\mathrm{liq}} \; [\mathrm{g/ml}]$	$\rho_{\rm vap} \ [{\rm g/ml}]$	$P_{\text{vap}}$ [kPa]	$Z_{ m i}$
2,2-dimethylpropane	270	$0.6135_{8}$	$0.00324_2$	$96.9_{4}$	
	300	$0.5804_1$	$0.00787_5$	$252_{2}$	
	330	$0.5444_7$	$0.01668_5$	$551_{1}$	
	360	$0.5025_{2}$	$0.0321_2$	$1055_{4}$	
	390	$0.4501_{4}$	$0.0585_{9}$	$1820_{16}$	
	400	$0.4283_5$	$0.0710_{7}$	$2131_{10}$	
	410	$0.4050_{8}$	$0.091_2$	$2550_{23}$	
	420	$0.373_{2}$	$0.114_{5}$	$2930_{30}$	
2-methylpropene	253	$0.64146_{8}$	$0.00236_2$	$86.0_{6}$	
	274	$0.61759_{8}$	$0.00490_3$	$188.3_{10}$	
	299	$0.58749_{14}$	$0.01014_{6}$	$408_{2}$	
	329	$0.5468_{3}$	$0.0213_2$	$877_{7}$	
	350	$0.5141_{3}$	$0.0336_{3}$	$1369_{8}$	
	375	$0.4678_{4}$	$0.0570_{8}$	$2197_{19}$	
	380	$0.4572_{4}$	$0.0625_{6}$	$2384_{16}$	
	385	$0.4454_{8}$	$0.0711_{8}$	$2621_{19}$	
	390	$0.4328_9$	$0.0774_{10}$	$2831_{18}$	
2-methyl-1,3-butadiene	275	$0.6962_1$	$0.00135_1$	$44.4_{2}$	
	300	$0.67044_7$	$0.00318_1$	$112.0_{4}$	
	325	$0.6431_2$	$0.00645_3$	$239.4_{9}$	
	400	$0.5456_{3}$	$0.0344_2$	$1321_{5}$	
	435	$0.4831_5$	$0.0665_{6}$	$2380_{10}$	
	445	$0.4602_{8}$	$0.0801_{8}$	$2750_{10}$	
	450	$0.4464_{8}$	$0.089_{1}$	$2980_{20}$	
	455	$0.433_1$	$0.101_{1}$	$3220_{20}$	
naphthalene	475	$0.8895_2$	$0.00297_3$	$88.6_{9}$	
	500	$0.8673_2$	$0.00495_3$	$153_{1}$	
	550	$0.8202_2$	$0.01216_5$	$393_{1}$	
	600	$0.7679_4$	$0.0257_{2}$	$841_{6}$	
	650	$0.7058_{6}$	$0.0504_{4}$	$1600_{9}$	
	680	$0.6630_4$	$0.0762_9$	$2280_{10}$	
	690	$0.6477_{6}$	$0.090_{1}$	$2560_{20}$	
	700	$0.627_{1}$	$0.100_{2}$	$2800_{30}$	
	710	$0.614_{1}$	$0.116_{3}$	$3120_{30}$	
	720	$0.593_{1}$	$0.134_{2}$	$3440_{10}$	

Table S2: (continued)

molecule	T [K]	$\rho_{\mathrm{liq}} \; [\mathrm{g/ml}]$	$\rho_{\rm vap} \ [{\rm g/ml}]$	$P_{\text{vap}}$ [kPa]	$Z_{ m i}$
ethanol	300	$0.781_2$	$0.000152_1$	$8.12_{4}$	
	325	$0.757_{2}$	$0.000546_3$	$30.8_{2}$	
	350	$0.732_{3}$	$0.00162_1$	$95.8_{4}$	
	375	$0.704_{2}$	$0.0041_1$	$245_{6}$	
	400	$0.672_{4}$	$0.0088_{1}$	$538_{6}$	
	425	$0.634_{3}$	$0.0178_{4}$	$1065_{22}$	
	450	$0.589_{5}$	$0.034_{1}$	$1934_{32}$	
	475	$0.527_{7}$	$0.061_2$	$3190_{71}$	
	485	$0.497_{9}$	$0.083_{3}$	$3906_{75}$	
	495	$0.454_{16}$	$0.108_{4}$	$4716_{89}$	
2-butanol	375	$0.72416_{36}$	$0.003142_{34}$	$124.9_{15}$	$0.9455_{2}$
	400	$0.69253_{38}$	$0.00724_{10}$	$294.2_{37}$	0.9070
	425	$0.65617_{55}$	$0.01489_{18}$	$605.0_{62}$	0.8537
	450	$0.61440_{75}$	$0.02837_{38}$	$1127_{12}$	0.7895
	460	$0.59458_{75}$	$0.03570_{48}$	$1396_{11}$	0.7600
	470	$0.57385_{69}$	$0.04446_{12}$	$1706_{31}$	0.7271
	480	$0.5506_{14}$	$0.0560_{18}$	$2080_{34}$	0.6855
	490	$0.5237_{16}$	$0.0690_{14}$	$2488_{24}$	$0.652_{1}$
	500	$0.4943_{28}$	$0.0915_{40}$	$3003_{45}$	$0.588_{1}$
	510	$0.4537_{43}$	$0.1154_{59}$	$3530_{45}$	$0.533_{1}$
ethanal	220	$0.8761_2$	$0.0000529_{19}$	$2.18_{8}$	0.9962
	240	$0.8523_{3}$	$0.000184_{6}$	$8.27_{25}$	0.9914
	260	$0.8275_{3}$	$0.000517_{8}$	$24.9_{4}$	0.9826
	280	$0.8023_{4}$	$0.001234_{19}$	$63.1_{9}$	0.9681
	300	$0.7760_{4}$	$0.00258_4$	$138.2_{22}$	0.9474
	320	$0.7486_{4}$	$0.00492_5$	$273.1_{25}$	0.9205
	340	$0.7197_{5}$	$0.00872_{10}$	$495_{5}$	0.8849
	360	$0.6880_{3}$	$0.01435_{10}$	$822_{5}$	0.8446
	380	$0.6537_{10}$	$0.0231_3$	$1310_{15}$	0.7932
	400	$0.6156_{5}$	$0.0360_{7}$	$1984_{27}$	0.7332
	420	$0.5721_{17}$	$0.0554_{13}$	$2900_{40}$	0.658
	425	$0.5585_{17}$	$0.0608_{20}$	$3160_{50}$	$0.645_{1}$
	430	$0.5459_{20}$	$0.0676_{15}$	$3430_{40}$	0.623
	435	$0.5307_{14}$	$0.0759_{23}$	$3740_{50}$	$0.600_{1}$

Table S2: (continued)

molecule	T [K]	$\rho_{\mathrm{liq}}$ [g/ml]	$\rho_{\mathrm{vap}} \; [\mathrm{g/ml}]$	$P_{\text{vap}}$ [kPa]	$Z_{ m i}$
pentanal	300	$0.80526_{8}$	$0.0002305_{14}$	$6.63_{4}$	$0.99407_{12}$
	330	$0.77562_7$	$0.000819_3$	$25.67_{11}$	$0.98444_{21}$
	360	$0.74507_{7}$	$0.002303_9$	$77.4_{3}$	$0.96691_{17}$
	390	$0.71208_{8}$	$0.00530_2$	$187.4_{5}$	$0.93955_{39}$
	420	$0.67664_{13}$	$0.01084_5$	$396_{2}$	$0.89967_{60}$
	450	$0.6377_{13}$	$0.02007_{11}$	$740_{3}$	$0.8473_{10}$
	480	$0.5929_{3}$	$0.0354_2$	$1283_{5}$	$0.7830_{13}$
	510	$0.5391_4$	$0.0610_5$	$2077_{10}$	$0.6934_{23}$
	520	$0.5172_{6}$	$0.0735_{5}$	$2403_{11}$	$0.6539_{20}$
	530	$0.4922_5$	$0.0890_{5}$	$2768_{7}$	$0.6103_{21}$
	540	$0.4635_{8}$	$0.1084_{13}$	$3188_{9}$	$0.557_{13}$
	545	$0.4433_9$	$0.120_{3}$	$3400_{20}$	$0.545_{10}$
acetone	300	$0.7753_2$	$0.00135_1$	$56.6_{4}$	
	340	$0.7308_{2}$	$0.00471_3$	$217_{1}$	
	380	$0.6820_2$	$0.01250_4$	$605_{2}$	
	420	$0.6264_2$	$0.0285_{1}$	$1385_{5}$	
	460	$0.5572_{6}$	$0.0602_2$	$2740_{20}$	
	470	$0.5358_{5}$	$0.0718_{6}$	$3180_{10}$	
	475	$0.5258_{7}$	$0.081_{1}$	$3450_{20}$	
	480	$0.5107_{9}$	$0.0853_{6}$	$3640_{10}$	
	485	$0.4985_{6}$	$0.097_{2}$	$3940_{30}$	
	490	$0.483_{2}$	$0.107_{3}$	$4210_{30}$	
	495	$0.464_{3}$	$0.114_2$	$4460_{30}$	
2-methoxy-2-methylpropane	300	$0.7464_1$	$0.00213_3$	58.8 <sub>7</sub>	
	325	$0.7180_2$	$0.00464_{7}$	$136_{2}$	
	350	$0.6877_1$	$0.00919_4$	$279_{1}$	
	400	$0.6187_{4}$	$0.0273_2$	$857_{5}$	
	450	$0.5263_{8}$	$0.072_{1}$	$2050_{20}$	
	460	$0.5014_{3}$	$0.0857_{6}$	$2380_{10}$	
	465	$0.487_{1}$	$0.094_{1}$	$2540_{20}$	
	470	$0.475_{2}$	$0.110_{3}$	$2800_{30}$	

Table S2: (continued)

molecule	T [K]	$\rho_{\mathrm{liq}} \; [\mathrm{g/ml}]$	$\rho_{\rm vap} \ [{\rm g/ml}]$	$P_{\text{vap}}$ [kPa]	$Z_{ m i}$
methyl acetate	260	$0.94896_{12}$	$0.000173_4$	$5.04_{11}$	$0.99657_{11}$
	295	$0.90907_{13}$	$0.000850_{12}$	$27.8_{4}$	$0.98817_{24}$
	330	$0.86706_{10}$	$0.00291_3$	$104.5_{9}$	$0.96932_{31}$
	365	$0.82244_{10}$	$0.00763_4$	$292.9_{14}$	$0.93642_{25}$
	400	$0.77326_{10}$	$0.01693_9$	$674_{3}$	$0.88648_{46}$
	435	$0.7177_{3}$	$0.03324_{14}$	$1334_{4}$	$0.8223_{10}$
	470	$0.6516_{4}$	$0.0630_{3}$	$2412_{9}$	$0.7279_{14}$
	480	$0.6297_{4}$	$0.0745_{4}$	$2794_{10}$	$0.6971_{11}$
	490	$0.6043_5$	$0.0888_{6}$	$3230_{11}$	$0.6629_{20}$
	500	$0.5769_{9}$	$0.1061_{7}$	$3701_{12}$	$0.6235_{20}$
	510	$0.5434_{7}$	$0.1290_{7}$	$4246_{13}$	$0.5788_{24}$
2-butanethiol	280	$0.84987_{11}$	$0.0002081_{20}$	$5.358_{51}$	$0.99616_{12}$
	300	$0.830242_{85}$	$0.000514_{10}$	$14.09_{27}$	$0.99211_{19}$
	320	$0.810012_{72}$	$0.0011012_{47}$	$32.00_{13}$	$0.98521_{22}$
	340	$0.789451_{69}$	$0.0021309_{77}$	$65.13_{24}$	$0.97534_{24}$
	360	$0.76835_{11}$	$0.003814_{16}$	$121.55_{48}$	$0.96079_{24}$
	380	$0.74624_{15}$	$0.006344_{47}$	$209.2_{14}$	$0.94266_{61}$
	400	$0.72309_{12}$	$0.010022_{64}$	$339.6_{20}$	$0.92042_{54}$
	420	$0.69859_{10}$	$0.015056_{60}$	$520.0_{20}$	$0.89382_{81}$
	440	$0.67308_{18}$	$0.022291_{89}$	$773.4_{25}$	$0.85808_{83}$
	460	$0.64455_{18}$	$0.03172_{16}$	$1094.0_{41}$	$0.8175_{11}$
	480	$0.61345_{23}$	$0.04457_{10}$	$1512.2_{25}$	$0.7723_{10}$
	500	$0.57837_{29}$	$0.06204_{37}$	$2030.3_{70}$	$0.7190_{21}$
	510	$0.55816_{58}$	$0.07331_{53}$	$2333_{11}$	$0.6912_{47}$
	520	$0.53510_{93}$	$0.08613_{69}$	$2662_{12}$	$0.6670_{28}$
	525	$0.52585_{51}$	$0.0981_{11}$	$2894_{12}$	$0.6373_{60}$
	530	$0.51110_{78}$	$0.1054_{10}$	$3055_{10}$	$0.6228_{42}$

Table S2: (continued)

molecule	T [K]	$\rho_{\mathrm{liq}} \; [\mathrm{g/ml}]$	$\rho_{\rm vap} \ [{\rm g/ml}]$	$P_{\text{vap}}$ [kPa]	$Z_{ m i}$
dimethyl sulfide	255	$0.8856_{4}$	$0.000385_{12}$	$13.1_{4}$	$0.99415_{30}$
	290	$0.84597_9$	$0.00163_2$	$62.0_{9}$	$0.98123_{62}$
	325	$0.8042_{3}$	$0.00486_{7}$	$202_{3}$	$0.9551_{13}$
	360	$0.75948_{14}$	$0.01175_9$	$517_{3}$	$0.9135_{16}$
	395	$0.7099_2$	$0.02427_{15}$	$1094_{7}$	$0.8544_{10}$
	430	$0.6524_{5}$	$0.0463_4$	$2052_{12}$	$0.7734_{31}$
	455	$0.603_{5}$	$0.0711_{7}$	$3050_{30}$	$0.7036_{58}$
	465	$0.5801_{7}$	$0.0837_{13}$	$3505_{26}$	$0.6712_{57}$
	475	$0.5538_{17}$	$0.1004_{23}$	$4030_{50}$	$0.633_{10}$
	485	$0.525_{3}$	$0.124_{6}$	$4640_{60}$	$0.581_{21}$
n-perfluoropentane	200	$1.9183_{7}$	$0.000419_{25}$	$2.41_{15}$	$0.9966_4$
	220	$1.8625_{9}$	$0.00134_3$	$8.42_{18}$	$0.9913_5$
	240	$1.8048_{6}$	$0.00347_3$	$23.62_{17}$	$0.9811_{5}$
	260	$1.7450_9$	$0.00764_{7}$	$55.3_{5}$	$0.9658_{9}$
	280	$1.6827_{12}$	$0.01483_{19}$	$112.8_{13}$	$0.9424_{17}$
	310	$1.5805_{13}$	$0.0341_5$	$273_{3}$	$0.896_{3}$
	340	$1.4645_{18}$	$0.0697_{8}$	$563_{5}$	$0.827_{3}$
	370	$1.3243_{13}$	$0.1324_{17}$	$1025_{11}$	$0.734_{4}$
	380	$1.272_{2}$	$0.1602_{16}$	$1236_{8}$	$0.700_{5}$
	385	$1.241_{2}$	$0.178_{4}$	$1349_{15}$	$0.687_{6}$
	390	$1.208_{4}$	$0.199_{4}$	$1475_{17}$	$0.660_{6}$
	395	$1.173_{6}$	$0.224_{6}$	$1600_{20}$	$0.618_{8}$

 $\begin{tabular}{ll} Table S3: {\bf Critical\ Properties\ and\ Normal\ Boiling\ Points\ for\ TraPPE\ Validation\ Compounds} \end{tabular}$ 

Subscripts provide the uncertainties in the last digit(s), given as the standard error of the mean estimated from the set of independent simulations (i.e.,  $302.8_4$  stands for  $302.8 \pm 0.4$  and  $0.2354_{11}$  stands for  $0.2354 \pm 0.0011$ )

Molecule	$T_{\rm crit}$ [K]	$\rho_{\rm crit} \ [{ m g/ml}]$	$P_{\rm crit}$ [MPa]	$Z_{ m crit}$	$T_{ m boil}$
oxygen	$153.5_{1}$	$0.440_{1}$	$5.06_{3}$	$0.288_{2}$	$89.73_{4}$
carbon dioxide	$303.7_{5}$	$0.507_{3}$	$7.8_{4}$	$0.268_{14}$	_
${ m ethane}^a$	$302.8_{4}$	$0.218_{1}$	$5.2_{1}$	$0.285_{6}$	$176.2_{1}$
n-butane	$423.0_{5}$	$0.2354_{11}$	$4.20_{10}$	$0.295_{7}$	$262.0_{2}$
n-decane <sup><math>b</math></sup>	$619.8_{7}$	$0.237_{2}$	$2.38_{3}$	$0.277_{5}$	$436.3_{1}$
2-methylpropane	$407.3_{6}$	$0.2313_{14}$	$3.93_{18}$	$0.292_{14}$	$252.5_{4}$
2,2-dimethylpropane	$431_{1}$	$0.238_{2}$	$3.47_{9}$	$0.293_{8}$	$271.2_{1}$
2-methylpropene	$417_{1}$	$0.243_{3}$	$4.3_{6}$	$0.286_{41}$	$256.7_{1}$
2-methyl-1,3-butadiene	$475.1_{8}$	$0.258_{2}$	$4.2_{2}$	$0.281_{14}$	$297.3_{7}$
naphthalene	$755_{1}$	$0.357_{2}$	$4.7_{2}$	$0.269_{12}$	$480.9_{3}$
ethanol	$509_{1}$	$0.275_{7}$	$6.0_{7}$	$0.238_{28}$	$346_{2}$
2-butanol	$523.4_{12}$	$0.2767_{32}$	$4.40_{16}$	$0.271_{10}$	$369.7_{3}$
ethanal	$466_{3}$	$0.281_{6}$	$6_2$	$0.243_{82}$	$291.8_{2}$
pentanal	$559.8_{4}$	$0.2761_{10}$	$4.12_{6}$	$0.276_{5}$	$369.0_{1}$
acetone	$512.3_{9}$	$0.283_{2}$	$5.6_{2}$	$0.270_{10}$	$316.1_{1}$
$2\hbox{-methoxy-}2\hbox{-methylpropane}$	$491_{1}$	$0.278_{3}$	$3.7_{2}$	$0.287_{16}$	$315.8_{3}$
methyl acetate	$530.6_{3}$	$0.3253_9$	$5.49_{7}$	$0.283_{4}$	$328.8_{2}$
2-butanethiol	$557_{2}$	$0.299_{4}$	$4.3_{6}$	$0.280_{40}$	$353.9_{2}$
dimethyl sulfide	$507_{2}$	$0.313_{5}$	$6.0_{4}$	$0.283_{19}$	$303.6_{3}$
<i>n</i> -perfluoropentane	$419_{2}$	$0.67_{1}$	$2.3_{4}$	$0.284_{50}$	$277.0_2$

## Description of GitHub Repositories

The software packages used to generate and analyze the data in this manuscript are publicly available online as GitHub repositories.

Monte Carlo for Complex Chemical Systems—Minnesota (MCCCS-MN) is a Fortran software package developed by the Siepmann research group. The source code and makefile for the specific version of MCCCS-MN used for the validation simulations of pentanal, as well as sample input files (fort.4, fort.77, and topmon.inp) and output files (run1a.dat and fort.12) for a short production run of pentanal at 510 K in the NVT-Gibbs ensemble, are available at https://github.com/SiepmannGroup/VLE-Validation.

VLE\_Outlier allows for the detection of outliers in VLE simulations using trends in the compressibility factor Z and Clausius-Clapeyron triads. To guard against typographical mistakes, VLE\_Outlier compares the  $Z_{\rm sim}$  value provided in the input file (for GEMC simulations,  $Z_{\rm sim}$  should be calculated using Eqn. 5 and, only for  $T_{\rm r} > 0.9$ , using histogram analysis) to that computed using Eqn. 4. Then,  $\ln(Z_{\rm sim}/Z_{\rm exd})$  (where  $Z_{\rm exd}$  is taken from Eqn. 7) is compared to the prescribed bounds for the specific  $T_{\rm r}$  range to determine whether  $Z_{\rm sim}$  is an outlier. Because the Z metric (particularly, when  $Z_{\rm i}$  from Eqn. 5 is used) can fail to detect inadequate sampling in GEMC simulations, VLE\_Outlier also checks for outliers based on Clausius-Clapeyron triads. This is done by applying Eqn. 8 within triads of data, identifying  $P_{\rm CC}$  and testing whether  $\ln(P_{\rm sim}/P_{\rm CC})$  falls within the prescribed bounds. VLE\_Outlier is available at https://github.com/SiepmannGroup/VLE-Validation.

GEMC\_Hist is an analysis package for utilizing histograms to calculate accurate vapor and liquid coexistence densities, saturated vapor pressure, and compressibility factor from a Gibbs ensemble Monte Carlo trajectory for unary vapor—liquid equilibria near the critical point. GEMC\_Hist is available at https://github.com/dejac001/GEMC\_histogram\_analysis with documentation available at https://dejac001.github.io/GEMC\_histogram\_analysis/. The exact version used of GEMC\_hist used for making Figures 2-3 and Table 3 can be downloaded at https://github.com/dejac001/GEMC\_histogram\_analysis/archive/master.zip.

## Outliers based on Compressibility Factor and CC Triads

Table S4: All  $\ln{(Z_{\rm sim}/Z_{\rm exd})}$  Outliers in the TraPPE Development Data

Outliers are defined as having  $\ln{(Z_{\rm sim}/Z_{\rm exd})}$  less than -0.03 or greater than 0.03 when  $T_{\rm r} \leq 0.70$ , less than -0.06 or greater than 0.05 when 0.70  $< T_{\rm r} \leq 0.85$ , and less than -0.09 or greater than 0.11 when  $T_{\rm r} > 0.85$ . Uncertainties (unc) are provided as the standard error of the mean. The nearest boundary that each outlier exceeds is also provided, for easy reference, in the table in column NB.

Molecule	T [K]	$T_{ m r}$	Z	unc	$\ln\left(Z_{\rm sim}/Z_{\rm exd}\right)$	unc	NB
n-octane (UA)	540	0.947	0.674	0.022	0.117	0.033	0.11
ethene (UA)	184	0.650	0.917	0.042	-0.037	0.046	-0.03
	225	0.795	0.730	0.031	-0.145	0.043	-0.06
propene (UA)	182	0.503	0.967		-0.032		-0.03
1,5-hexadiene (UA)	324	0.653	0.980		0.031		0.03
ethylbenzene (UA)	397	0.640	0.928		-0.030		-0.03
	447	0.721	1.085		0.179		0.05
	497	0.802	0.935		0.111		0.05
propylbenzene (UA)	450	0.696	0.866		-0.066		-0.03
isopropylbenzene (UA)	450	0.700	0.958		0.038		0.03
o-xylene (UA)	400	0.632	1.101		0.136		0.03
	450	0.711	0.967		0.055		0.05
	595	0.940	0.721		0.154		0.11
m-xylene (UA)	451	0.719	0.963		0.057		0.05
	547	0.872	0.683		-0.091		-0.09
p-xylene (UA)	397	0.643	0.816		-0.157		-0.03
methanol (UA)	425	0.847	0.678	0.039	-0.145	0.057	-0.06
	475	0.946	0.366	0.017	-0.499	0.046	-0.09
propan-1-ol (UA)	500	0.929	0.570	0.065	-0.122	0.114	-0.09
pentan-1-ol (UA)	400	0.691	0.965	0.057	0.039	0.059	0.03
	450	0.777	0.922	0.078	0.068	0.084	0.05

Table S4: (continued)

Molecule	T [K]	$T_{ m r}$	Z	unc	$\ln\left(Z_{\rm sim}/Z_{\rm exd}\right)$	unc	NB
octan-1-ol (UA)	300	0.477	1.160	0.136	0.149	0.117	0.03
	350	0.556	1.053	0.228	0.064	0.216	0.03
	450	0.715	0.963	0.073	0.055	0.076	0.05
	500	0.795	0.908	0.039	0.073	0.043	0.05
	600	0.954	0.680	0.043	0.157	0.064	0.11
propan-2-ol (UA)	300	0.598	0.688	0.099	-0.348	0.144	-0.03
	400	0.797	0.783	0.089	-0.072	0.113	-0.06
butan-2-ol (UA)	350	0.668	0.996	0.102	0.055	0.102	0.03
2-methylpropan-2-ol (UA)	350	0.694	0.959	0.093	0.035	0.097	0.03
	480	0.952	0.441	0.025	-0.284	0.057	-0.09
1,3-propanediol (UA)	450	0.620	1.001	0.078	0.036	0.078	0.03
, , ,	500	0.689	0.962	0.034	0.034	0.035	0.03
	550	0.758	0.924	0.076	0.051	0.082	0.05
pentane-1,5-diol (UA)	550	0.775	0.934	0.084	0.079	0.090	0.05
- , , , ,	600	0.845	0.854	0.043	0.083	0.051	0.05
dimethyl ether (UA)	329	0.827	0.755	0.021	-0.068	0.028	-0.06
ethanal (UA)	260	0.561	0.685		-0.364		-0.03
	300	0.647	0.893		-0.065		-0.03
	440	0.950	0.529		-0.114		-0.09
pentanal (UA)	380	0.672	0.983		0.044		0.03
octanal (UA)	600	0.957	0.511		-0.114		-0.09
acetone (UA)	300	0.591	0.895		-0.088		-0.03
	340	0.669	0.858		-0.093		-0.03
	380	0.748	0.830		-0.067		-0.06
2-octanone (UA)	360	0.562	0.575		-0.540		-0.03
	400	0.625	0.861		-0.113		-0.03
	520	0.812	0.883		0.068		0.05
acetonitrile (UA)	398	0.725	0.849	0.050	-0.064	0.059	-0.06
	448	0.816	0.730	0.031	-0.117	0.042	-0.06
	498	0.907	0.585	0.031	-0.163	0.053	-0.09

Table S4: (continued)

Molecule	T [K]	$T_{ m r}$	Z	unc	$\ln\left(Z_{\rm sim}/Z_{\rm exd}\right)$	unc	NB
propionitrile (UA)	448	0.806	0.776	0.030	-0.070	0.039	-0.06
	498	0.896	0.625	0.034	-0.128	0.055	-0.09
pyrimidine (UA)	298	0.489	0.771	0.016	-0.260	0.021	-0.03
10	365	0.598	1.075	0.051	0.098	0.048	0.03
	398			0.097	-0.072	0.109	-0.03
	480		0.588		-0.371	0.218	-0.06
nitrobenzene (UA)	298	0.399	0.022	0.108	-3.835	5.002	-0.03
	375	0.502	0.585	0.182	-0.534	0.311	-0.03
methanethiol (UA)	220	0.463	0.658		-0.419		-0.03
` ,	240	0.505	0.891		-0.113		-0.03
	260	0.547	0.931		-0.062		-0.03
ethanethiol (UA)	240	0.478	1.112		0.106		0.03
pentanethiol (UA)	300	0.498	3.214		1.169		0.03
	320	0.532	1.843		0.618		0.03
	340	0.565	1.395		0.347		0.03
	360	0.598	1.192		0.202		0.03
	380	0.631	1.099		0.135		0.03
	400	0.664	1.035		0.092		0.03
	420	0.698	0.998		0.077		0.03
	440	0.731	0.958		0.063		0.05
	460	0.764	0.921		0.054		0.05
octanethiol (UA)	360	0.537	0.869		-0.133		-0.03
	380	0.566	0.950		-0.037		-0.03
	460	0.686	0.961		0.031		0.03
2-butanethiol (UA)	260	0.467	0.521		-0.651		-0.03
,	280	0.503	0.704		-0.349		-0.03
	300	0.539	0.887		-0.112		-0.03
	320	0.575	0.951		-0.032		-0.03
2-methyl-1-propanethiol (UA)	300	0.539	0.443		-0.807		-0.03
/	320	0.575	0.729		-0.299		-0.03
	340		0.855		-0.126		-0.03
	360		0.897		-0.062		-0.03

Table S4: (continued)

Molecule	T [K]	$T_{ m r}$	Z	unc	$\ln\left(Z_{\rm sim}/Z_{\rm exd}\right)$	unc	NB
2-methyl-2-propanethiol (UA)	300	0.577	0.912		-0.074		-0.03
	320	0.615	0.920		-0.050		-0.03
	340		0.912		-0.041		-0.03
	360	0.692	0.897		-0.033		-0.03
dimethyl sulfide (UA)	240		0.934		-0.068		-0.03
	260	0.516	0.958		-0.039		-0.03
ethylmethyl sulfide (UA)	300	0.560	0.944		-0.044		-0.03
dimethyl disulfide (UA)	280	0.462	0.450		-0.799		-0.03
	300	0.495	0.657		-0.419		-0.03
	320		0.885		-0.116		-0.03
	340	0.561	0.929		-0.060		-0.03
diethyl disulfide (UA)	400	0.608	0.893		-0.084		-0.03
	420	0.638	0.919		-0.041		-0.03
thiophene (UA)	293	0.484	0.953		-0.048		-0.03
methyl acrylate (UA)	450	0.800	0.917	0.041	0.090	0.045	0.05
n-octyl acrylate (UA)	490	0.697	0.992	0.035	0.071	0.035	0.03
2-ethylhexyl acrylate (UA)	550	0.795	0.905	0.046	0.070	0.051	0.05
2-hydroxyethyl acrylate (UA)	470	0.693	0.958	0.024	0.033	0.025	0.03
n-butyl methacrylate (UA)	400	0.625	1.006	0.049	0.043	0.048	0.03
1,4-dioxane (UA)	555	0.944	0.539	0.035	-0.121	0.065	-0.09
SPC-pol3 (pol)	573	0.924	0.584	0.040	-0.115	0.068	-0.09
TIP4P-pol1 (pol)	373	0.643	1.005	0.126	0.051	0.125	0.03
	523	0.902	0.570	0.076	-0.205	0.134	-0.09
TIP4P-pol3 (pol)	523	0.902	0.614	0.036	-0.129	0.059	-0.09
n-octane (EH)	550	0.958	0.634	0.091	0.110	0.143	0.11
n-dodecane (EH)	450	0.675	0.996	0.084	0.060	0.085	0.03
	500	0.750	0.948	0.078	0.068	0.083	0.05
	550	0.825	0.902	0.054	0.106	0.060	0.05

Table S4: (continued)

Molecule	T [K]	$T_{ m r}$	Z	unc	$\ln\left(Z_{\rm sim}/Z_{\rm exd}\right)$	unc	NB
methylamine (EH)	298 350	0.695 0.816	1.008 0.696		$0.085 \\ -0.165$	0.119 0.017	$0.03 \\ -0.06$
dimethylamine (EH)	250 280 308	0.564 0.632 0.695	1.084 1.007 0.867	0.553 1.009 0.104	0.095 $0.047$ $-0.066$	0.510 1.002 0.120	0.03 $0.03$ $-0.03$
ethylamine (EH)	293	0.648	1.002	0.178	0.050	0.178	0.03
nitromethane (EH)	375 550	0.637 0.934	0.923 0.575	0.135 0.030	-0.038 $-0.097$	0.146 0.052	-0.03 $-0.09$
nitroethane (EH)	323	0.555	1.048	0.175	0.059	0.167	0.03
acetonitrile (EH)	298 398 448 498	0.545 0.728 0.819 0.910	0.954 0.843 0.745 0.529		-0.038 $-0.068$ $-0.094$ $-0.255$	0.092 0.025 0.032 0.062	-0.03 $-0.06$ $-0.06$ $-0.09$
propionitrile (EH)	498	0.897	0.631	0.036	-0.114	0.058	-0.09
benzene (EH)	315 465	0.560 0.826	1.023 0.722		$0.035 \\ -0.115$	0.408 0.168	$0.03 \\ -0.06$
pyridine (EH)	298	0.482	0.912	0.600	-0.092	0.659	-0.03
pyrimidine (EH)	298 575	0.472 0.910	0.969 0.615	1.616 0.061	-0.031 $-0.106$	1.667 0.099	-0.03 $-0.09$
pyrazine (EH)	348	0.565	1.107	0.313	0.116	0.283	0.03
pyridazine (EH)	298 348 398 468	$0.457 \\ 0.523$	1.616 0.791 0.864 1.003	0.357 $0.169$	0.480 $-0.235$ $-0.141$ $0.036$	0.640 0.452 0.195 0.179	0.03 $-0.03$ $-0.03$ $0.03$
thiophene (EH)	293 345		0.967 1.010		-0.032 $0.032$	0.214 0.158	-0.03 0.03
furan (EH)	250	0.506	1.048	0.182	0.049	0.173	0.03
pyrrole (EH)	300 370 520	0.568	0.690 0.945 0.776	0.321	-0.372 $-0.041$ $-0.079$		-0.03 $-0.03$ $-0.06$

Table S4: (continued)

Molecule	T [K]	$T_{ m r}$	Z	unc	$\ln\left(Z_{\rm sim}/Z_{\rm exd}\right)$	unc	NB
thiazole (EH)	350	0.550	1.024	0.194	0.034	0.190	0.03
	400	0.629	1.035	0.213	0.073	0.206	0.03
	450	0.708	0.980	0.116	0.066	0.118	0.05
oxazole (EH)	300	0.557	0.850	0.199	-0.150	0.234	-0.03
imidazole (EH)	400	0.489	1.159	0.192	0.148	0.166	0.03
	450	0.550	1.031	0.546	0.041	0.530	0.03
pyrazole (EH)	350	0.475	1.097	0.113	0.092	0.103	0.03
	400	0.543	0.955	0.259	-0.037	0.271	-0.03
chlorobenzene (EH)	575	0.909	0.599	0.117	-0.136	0.195	-0.09
1,2-dichlorobenzene (EH)	398	0.570	0.937	0.143	-0.049	0.153	-0.03
1,3-dichlorobenzene (EH)	650	0.938	0.562	0.059	-0.103	0.105	-0.09
1,2,3-trichlorobenzene (EH)	400	0.532	0.818	0.682	-0.194	0.833	-0.03
	700	0.931	0.582	0.124	-0.095	0.212	-0.09
	725	0.964	0.394	0.096	-0.331	0.243	-0.09
hexachlorobenzene (EH)	500	0.564	1.042	0.435	0.056	0.417	0.03
	575	0.648	0.894	0.372	-0.064	0.417	-0.03
1,2-dihydroxybenzene (EH)	500	0.619	1.059	0.276	0.092	0.260	0.03
	520	0.644	1.019	0.326	0.065	0.320	0.03
1,3-dihydroxybenzene (EH)	520	0.625	1.007	0.142	0.044	0.141	0.03
1,4-dihydroxybenzene (EH)	580	0.683	0.979	0.286	0.048	0.293	0.03
benzonitrile (EH)	298	0.435	1.189	0.180	0.173	0.151	0.03
	540	0.787	0.738	0.144	-0.143	0.195	-0.06
	640	0.933	0.554	0.086	-0.138	0.155	-0.09
p-benzoquinone (EH)	395	0.568	0.944	0.093	-0.043	0.098	-0.03
	430	0.618	1.002	0.073	0.035	0.073	0.03
	460	0.661	0.989	0.188	0.045	0.190	0.03
naphthalene (EH)	700	0.933	0.550	0.059	-0.142	0.107	-0.09

Table S4: (continued)

Molecule	T [K]	$T_{ m r}$	Z	unc	$\ln\left(Z_{\rm sim}/Z_{\rm exd}\right)$	unc	NB
anthracene (EH)	550	0.615	0.612	0.172	-0.458	0.281	-0.03
	600	0.670	0.590	0.119	-0.466	0.201	-0.03
	625	0.698	0.598	0.113	-0.435	0.188	-0.03
	650	0.726	0.587	0.078	-0.432	0.133	-0.06
	700	0.782	0.544	0.128	-0.453	0.236	-0.06
	750	0.838	0.485	0.080	-0.493	0.166	-0.06
	800	0.894	0.414	0.135	-0.544	0.325	-0.09
phenanthrene (EH)	550	0.613	0.607	0.040	-0.467	0.067	-0.03
	600	0.669	0.603	0.119	-0.445	0.197	-0.03
	625	0.697	0.564	0.066	-0.495	0.117	-0.03
	650	0.725	0.559	0.081	-0.481	0.144	-0.06
	700	0.780	0.549	0.094	-0.447	0.171	-0.06
	750	0.836	0.500	0.055	-0.466	0.110	-0.06
	800	0.892	0.433	0.074	-0.503	0.170	-0.09
	825	0.920	0.405	0.037	-0.496	0.091	-0.09
naphthalen-2-ol (EH)	500	0.588	0.650	0.173	-0.408	0.266	-0.03
	550	0.647	0.631	0.167	-0.413	0.265	-0.03
	575	0.676	0.635	0.207	-0.389	0.327	-0.03
	600	0.706	0.635	0.127	-0.369	0.200	-0.06
	650	0.765	0.576	0.045	-0.414	0.078	-0.06
	700	0.824	0.519	0.115	-0.448	0.221	-0.06
	750	0.882	0.468	0.100	-0.449	0.214	-0.09
	775	0.912	0.430	0.084	-0.458	0.195	-0.09
naphthalene-2-carbonitrile (EH)	450	0.534	0.682	0.089	-0.375	0.130	-0.03
	500	0.593	0.676	0.167	-0.369	0.247	-0.03
	525	0.623	0.643	0.217	-0.405	0.338	-0.03
	550	0.652	0.609	0.206	-0.445	0.338	-0.03
	580	0.688	0.665	0.107	-0.336	0.161	-0.03
	600	0.712	0.594	0.076	-0.431	0.128	-0.06
	650	0.771	0.582	0.078	-0.398	0.134	-0.06
	700	0.830	0.550	0.064	-0.380	0.116	-0.06
	750	0.890	0.441	0.101	-0.491	0.229	-0.09
quinoline (EH)	300	0.373	0.964	0.022	-0.037	0.022	-0.03

Table S4: (continued)

Molecule	T [K]	$T_{ m r}$	Z	unc	$\ln\left(Z_{\rm sim}/Z_{\rm exd}\right)$	unc	NB
indole (EH)	400	0.522	1.123	0.165	0.121	0.147	0.03
	450	0.587	1.060	0.184	0.079	0.174	0.03
	500	0.652	1.073	0.158	0.121	0.147	0.03
	550	0.717	1.032	0.193	0.125	0.187	0.05
	600	0.782	0.958	0.081	0.113	0.085	0.05
isoindole (EH)	400	0.485	0.896	0.150	-0.110	0.168	-0.03
	450	0.546	0.895	0.211	-0.102	0.236	-0.03
	500	0.607	0.916	0.208	-0.059	0.227	-0.03
	550	0.667	1.067	0.114	0.125	0.107	0.03
	600	0.728	0.842	0.187	-0.069	0.223	-0.06
	650	0.789	0.795	0.098	-0.067	0.123	-0.06
	700	0.850	0.707	0.062	-0.098	0.088	-0.06
	750	0.910	0.582	0.062	-0.161	0.107	-0.09
benzimidazole (EH)	500	0.531	1.089	0.952	0.092	0.874	0.03
	700	0.744	0.956	0.167	0.072	0.175	0.05
	850	0.903	0.635	0.122	-0.093	0.193	-0.09
indazole (EH)	500	0.579	1.089	0.492	0.105	0.451	0.03
	550	0.637	1.158	0.239	0.190	0.207	0.03
	800	0.927	0.582	0.090	-0.110	0.156	-0.09
purine (EH)	500	0.525	1.051	0.389	0.054	0.370	0.03
	550	0.578	1.103	0.574	0.117	0.521	0.03
	600	0.630	1.115	0.241	0.148	0.216	0.03
	875	0.919	0.607	0.070	-0.092	0.115	-0.09
benzo[c]thiophene (EH)	690	0.899	0.633	0.099	-0.107	0.156	-0.09
benzisoxazole (EH)	600	0.733	1.075	0.161	0.179	0.149	0.05
	750	0.917	0.573	0.138	-0.157	0.240	-0.09
benzothiazole (EH)	450	0.572	1.023	0.256	0.039	0.251	0.03
	550	0.699	1.079	0.130	0.156	0.120	0.03

Table S5: All  $\ln{(P_{\text{sim}}/P_{\text{CC}})}$  Outliers in the TraPPE Development Data

 $CC_{LOW}$  outliers are defined as having  $\ln{(P_{\rm sim}/P_{\rm CC})}$  greater than 0.06 or less than -0.09 when  $T_{\rm r} \leq 0.70$ , 0.05 and -0.06 when 0.70  $< T_{\rm r} \leq 0.85$ ,and 0.06 and -0.06 when  $T_{\rm r} > 0.85$ .  $CC_{\rm MID}$  outliers are defined as having  $\ln{(P_{\rm sim}/P_{\rm CC})}$  greater than 0.03 or less than -0.01 when  $T_{\rm r} \leq 0.70$ , 0.03 and -0.02 when 0.70  $< T_{\rm r} \leq 0.85$ ,and 0.03 and -0.03 when  $T_{\rm r} > 0.85$ .  $CC_{\rm HIGH}$  outliers are defined as having  $\ln{(P_{\rm sim}/P_{\rm CC})}$  greater than 0.05 or less than -0.09 when  $T_{\rm r} \leq 0.70$ , 0.03 and -0.05 when 0.70  $< T_{\rm r} \leq 0.85$ ,and 0.04 and -0.04 when  $T_{\rm r} > 0.85$ . The extrapolation range, ER, is provided for  $CC_{\rm LOW}$  and  $CC_{\rm HIGH}$  as the ratio of two differences, in 1000/K: the difference between the predicted temperature and its nearest temperature divided by the difference of the two temperatures used to make the prediction.  $CC_{\rm MID}$  involves and interpolation. The nearest boundary that each outlier exceeds is also provided, for easy reference, in the table in column NB.

Molecule	T [K]	$T_{ m r}$	$P_{\text{sim}}$ [kPa]	Test	$\ln\left(P_{\mathrm{sim}}/P_{\mathrm{CC}}\right)$	ER	NB
ethane (UA)	178	0.586	$105_{3}$	$CC_{LOW}$	-0.264	1.158	-0.09
	197	0.648	$286_{25}$	$\mathrm{CC}_{\mathrm{LOW}}$	0.248	1.261	0.06
				$\mathrm{CC}_{\mathrm{MID}}$	0.122	_	-0.01
	217	0.714	$541_{16}$	$\mathrm{CC}_{\mathrm{LOW}}$	-0.180	1.121	-0.06
				$\mathrm{CC}_{\mathrm{MID}}$	-0.110	_	-0.02
				$\mathrm{CC}_{\mathrm{HIGH}}$	-0.228	0.863	-0.05
	236	0.776	$1092_{75}$	$\mathrm{CC}_{\mathrm{LOW}}$	0.166	1.227	0.05
				$\mathrm{CC}_{\mathrm{MID}}$	0.085	_	-0.02
				$\mathrm{CC}_{\mathrm{HIGH}}$	0.197	0.793	-0.05
	256	0.842	$1740_{181}$	$\mathrm{CC}_{\mathrm{MID}}$	-0.075	_	-0.02
				$\mathrm{CC}_{\mathrm{HIGH}}$	-0.161	0.892	-0.05
	275	0.905	$2913_{254}$	$CC_{HIGH}$	0.135	0.815	0.04
propane (UA)	217	0.590	79 <sub>6</sub>	$CC_{LOW}$	0.124	1.295	0.06
Posposit (SEE)	249	0.677	_	$CC_{LOW}$	-0.229		-0.09
			- 11	$CC_{MID}$	-0.054	_	-0.01
	281	0.764	$798_{42}$	$CC_{LOW}$	0.133	1.186	0.05
			42	$CC_{MID}$	0.100	_	-0.02
				$CC_{HIGH}$		0.772	-0.05
	312	0.848	$1519_{78}$	$CC_{MID}$	-0.061	_	-0.02
			.5	$CC_{HIGH}$		0.773	-0.05
	344	0.935	$2925_{100}$	$CC_{HIGH}$			0.04

Table S5: (continued)

Molecule	T [K]	$T_{ m r}$	$P_{\text{sim}}$ [kPa]	Test	$\ln{(P_{\rm sim}/P_{\rm CC})}$	ER	NB
n-butane (UA)	262	0.619	$109_{21}$	$CC_{LOW}$	0.291	1.287	0.06
	295	0.697	$285_{28}$	$\mathrm{CC}_{\mathrm{LOW}}$	-0.176	1.183	-0.09
				$\mathrm{CC}_{\mathrm{MID}}$	-0.127	_	-0.01
	327	0.773	$754_{101}$	$CC_{MID}$	0.081	_	0.03
				$CC_{HIGH}$	0.226	0.777	-0.05
	360	0.851	$1478_{177}$	$\mathrm{CC}_{\mathrm{HIGH}}$	-0.149	0.845	-0.04
n-pentane (UA)	298	0.634	$105_{4}$	$CC_{LOW}$	-0.208	1.318	-0.09
	336	0.715	$338_{15}$	$\mathrm{CC}_{\mathrm{LOW}}$	0.271	1.436	0.05
				$\mathrm{CC}_{\mathrm{MID}}$	0.090	_	-0.02
	372	0.791	$701_{38}$	$\mathrm{CC}_{\mathrm{LOW}}$	-0.224	0.957	-0.06
				$CC_{MID}$	-0.111	_	-0.02
				$\mathrm{CC}_{\mathrm{HIGH}}$	-0.158	0.759	-0.05
	402	0.855	$1407_{35}$	$CC_{MID}$	0.114	_	0.03
				$CC_{HIGH}$		0.697	-0.04
	439	0.934	$2306_{58}$	$CC_{HIGH}$	-0.234	1.045	-0.04
n-octane (UA)	440	0.772	$353_{7}$	$CC_{LOW}$	-0.160	1.227	-0.06
<b>,</b> ,	490	0.860	9087	$CC_{MID}$	0.072	_	0.03
	540	0.947	$1721_{21}$	$CC_{HIGH}$	-0.130	0.815	-0.04
(774)			4.0		0.010		
n-dodecane (UA)	450	0.675	467	$CC_{LOW}$	-0.212		-0.09
	500	0.750	$169_{13}$	$CC_{LOW}$	0.132	1.671	
	550	0.005	410	$CC_{MID}$	0.095	1 107	-0.02
	550	0.825	$412_{20}$	$CC_{LOW}$	-0.108		-0.06
				$CC_{MID}$	-0.050 $-0.174$		-0.02 $-0.05$
	525	0.877	$760_{34}$	$CC_{HIGH}$ $CC_{MID}$	-0.174 $0.051$	0.818	-0.03
	909	0.011	10034	$CC_{MID}$			-0.04
	620	0.930	1189 <sub>46</sub>	$CC_{HIGH}$			-0.04 $-0.04$
				-11011			

Table S5: (continued)

Molecule	T [K]	$T_{ m r}$	$P_{\rm sim}$ [kPa]	Test	$\ln\left(P_{\mathrm{sim}}/P_{\mathrm{CC}}\right)$	ER	NB
2-methylpropane (UA)	232	0.567	$45_{1}$	$CC_{LOW}$	0.372	1.549	0.06
	271	0.663	$176_{4}$	$\mathrm{CC}_{\mathrm{LOW}}$	-0.110	1.546	-0.09
				$\mathrm{CC}_{\mathrm{MID}}$	-0.146	_	-0.01
	304	0.743	$540_{22}$	$\mathrm{CC}_{\mathrm{MID}}$	0.043	_	0.03
				$\mathrm{CC}_{\mathrm{HIGH}}$	0.240	0.646	-0.05
	330	0.807	$1039_{29}$	$CC_{HIGH}$	-0.071	0.647	-0.05
2,2-dimethylpropane (UA)	281	0.650	$138_{2}$	$\mathrm{CC}_{\mathrm{LOW}}$	-0.150	0.613	-0.09
	309	0.715	$341_{7}$	$\mathrm{CC}_{\mathrm{LOW}}$	0.206	2.753	0.05
				$\mathrm{CC}_{\mathrm{MID}}$	0.093	_	-0.02
	369	0.854	$1169_{30}$	$\mathrm{CC}_{\mathrm{MID}}$	-0.055	_	-0.03
				$\mathrm{CC}_{\mathrm{HIGH}}$	-0.244	1.632	-0.04
	397	0.918	$1971_{38}$	$CC_{HIGH}$	0.075	0.363	0.04
2,3-dimethylbutane (UA)	330	0.656	$134_{3}$	$CC_{LOW}$	0.322	1.592	0.06
	384	0.763	$487_{32}$	$CC_{LOW}$	-0.434	1.229	-0.06
				$\mathrm{CC}_{\mathrm{MID}}$	-0.124	_	-0.02
	428	0.851	$1341_{40}$	$\mathrm{CC}_{\mathrm{MID}}$	0.195	_	0.03
				$\mathrm{CC}_{\mathrm{HIGH}}$	0.202	0.628	-0.04
	472	0.938	$2148_{119}$	$CC_{HIGH}$	-0.353	0.814	-0.04
2,2-dimethylhexane (UA)	354	0.642	$64_{1}$	$CC_{LOW}$	-0.230	1.467	-0.09
	403	0.731	$256_{8}$	$\mathrm{CC}_{\mathrm{LOW}}$	0.077	1.051	0.05
				$\mathrm{CC}_{\mathrm{MID}}$	0.093	_	-0.02
	445	0.808	$563_{17}$	$\mathrm{CC}_{\mathrm{MID}}$	-0.037	_	-0.02
				$\mathrm{CC}_{\mathrm{HIGH}}$	-0.157	0.682	-0.05
	494	0.897	$1282_{47}$	$CC_{HIGH}$	0.073	0.952	0.04
2,5-dimethylhexane (UA)	349	0.624	$47.1_{7}$	$CC_{LOW}$	-0.127	4.085	-0.09
	440	0.787	$469_{16}$	$CC_{LOW}$	-0.063	1.136	-0.06
	470	0.841	$798_{18}$	$\mathrm{CC}_{\mathrm{LOW}}$	0.070	1.451	0.05
	500	0.894	$1205_{65}$	$\mathrm{CC}_{\mathrm{HIGH}}$	-0.056	0.880	-0.04
	523	0.936	$1680_{60}$	$\mathrm{CC}_{\mathrm{HIGH}}$	0.048	0.689	0.04

Table S5: (continued)

Molecule	T [K]	$T_{ m r}$	$P_{\rm sim}$ [kPa]	Test	$\ln{(P_{\rm sim}/P_{\rm CC})}$	ER	NB
3,4-dimethylhexane (UA)	352	0.603	$41.7_{9}$	$CC_{LOW}$	-0.560	3.917	-0.09
	440	0.753	$409_{24}$	$\mathrm{CC}_{\mathrm{MID}}$	0.114	_	0.03
	470	0.805	$635_{27}$	$\mathrm{CC}_{\mathrm{LOW}}$	0.150	1.061	0.05
				$\mathrm{CC}_{\mathrm{MID}}$	-0.021	_	-0.02
				$\mathrm{CC}_{\mathrm{HIGH}}$	-0.143	0.255	-0.05
	500	0.856	$973_{17}$	$\mathrm{CC}_{\mathrm{MID}}$	-0.073	_	-0.03
	532	0.911	$1675_{72}$	$CC_{HIGH}$	0.141	0.942	0.04
ethene (UA)	144	0.509	$27_{1}$	$\mathrm{CC}_{\mathrm{LOW}}$	0.123	1.278	0.06
	164	0.580	$95_{3}$	$\mathrm{CC}_{\mathrm{MID}}$	-0.054	_	-0.01
	184	0.650	$280_{8}$	$\mathrm{CC}_{\mathrm{LOW}}$	-0.109	1.284	-0.09
				$\mathrm{CC}_{\mathrm{HIGH}}$	0.096	0.783	-0.09
	205	0.724	$690_{21}$	$\mathrm{CC}_{\mathrm{LOW}}$	0.128	1.195	0.05
				$CC_{MID}$	0.048	_	-0.02
	225	0.795	$1280_{38}$	$CC_{MID}$	-0.058	_	-0.02
				$\mathrm{CC}_{\mathrm{HIGH}}$	-0.085	0.779	-0.05
	245	0.866	$2390_{71}$	$CC_{HIGH}$	0.107	0.837	0.04
propene (UA)	245	0.677	310	$\mathrm{CC}_{\mathrm{LOW}}$	0.200	1.218	0.06
	276	0.762	760	$CC_{MID}$	-0.090	_	-0.02
	308	0.851	1870	$CC_{HIGH}$	0.164	0.821	0.04
1-butene (UA)	245	0.592	$64_{2}$	$\mathrm{CC}_{\mathrm{LOW}}$	-0.153	1.256	-0.09
	271	0.655	$190_{6}$	$CC_{MID}$	0.068	_	0.03
	296	0.715	$400_{12}$	$\mathrm{CC}_{\mathrm{HIGH}}$	-0.122	0.796	-0.05
	322	0.778	$770_{23}$	$\mathrm{CC}_{\mathrm{LOW}}$	0.079	1.114	0.05
	347	0.838	$1320_{40}$	$CC_{MID}$	-0.038	_	-0.02
	373	0.901	$2300_{69}$	$CC_{HIGH}$	0.071	0.898	0.04
cis-2-butene (UA)	245	0.563	47	$\mathrm{CC}_{\mathrm{LOW}}$	-0.218	2.434	-0.09
	295	0.678	290	$\mathrm{CC}_{\mathrm{LOW}}$	0.138	0.669	0.06
				$\mathrm{CC}_{\mathrm{MID}}$	0.064	_	-0.01
	322	0.740	560	$\mathrm{CC}_{\mathrm{MID}}$	-0.083	_	-0.02
				$\mathrm{CC}_{\mathrm{HIGH}}$	-0.090	0.411	-0.05
	373	0.857	1840	$CC_{HIGH}$	0.207	1.494	0.04

Table S5: (continued)

Molecule	T [K]	$T_{ m r}$	$P_{\rm sim}$ [kPa]	Test	$\ln\left(P_{\mathrm{sim}}/P_{\mathrm{CC}}\right)$	ER	NB
trans-2-butene (UA)	247	0.580	58	$CC_{LOW}$	0.065	0.641	0.06
	272	0.638	145	$\mathrm{CC}_{\mathrm{MID}}$	-0.040	_	-0.01
	323	0.758	670	$CC_{HIGH}$	0.101	1.560	0.03
2-methylpropene (UA)	274	0.656	190	$CC_{MID}$	0.045	_	0.03
	299	0.715	410	$\mathrm{CC}_{\mathrm{LOW}}$	0.153	1.672	0.05
				$\mathrm{CC}_{\mathrm{MID}}$	0.038	_	-0.02
				$\mathrm{CC}_{\mathrm{HIGH}}$	-0.090	1.007	-0.05
	329	0.787	820	$\mathrm{CC}_{\mathrm{MID}}$	-0.057	_	-0.02
				$\mathrm{CC}_{\mathrm{HIGH}}$	-0.076	0.999	-0.05
	350	0.837	1360	$CC_{HIGH}$	0.091	0.598	0.03
1-octene (UA)	393	0.693	130	$CC_{LOW}$	0.102	1.138	0.06
	441	0.778	390	$CC_{MID}$	-0.048	_	-0.02
	494	0.871	1120	$CC_{HIGH}$	0.090	0.878	0.04
1,5-hexadiene (UA)	289	0.583	21	$CC_{LOW}$	-0.325	1.630	-0.09
	324	0.653	90	$\mathrm{CC}_{\mathrm{LOW}}$	0.141	0.642	0.06
				$\mathrm{CC}_{\mathrm{MID}}$	0.124	_	-0.01
	350	0.706	180	$\mathrm{CC}_{\mathrm{LOW}}$	0.050	1.286	0.05
				$\mathrm{CC}_{\mathrm{MID}}$	-0.086	_	-0.02
				$\mathrm{CC}_{\mathrm{HIGH}}$	-0.200	0.613	-0.05
	400	0.806	660	$\mathrm{CC}_{\mathrm{MID}}$	-0.022	_	-0.02
				$CC_{HIGH}$	0.220	1.558	-0.05
benzene 6-site (UA)	300	0.531	25	$CC_{LOW}$	0.093	1.333	0.06
	350	0.619	130	$CC_{LOW}$	-0.205	1.286	-0.09
				$\mathrm{CC}_{\mathrm{MID}}$	-0.040	_	-0.01
	400	0.708	480	$\mathrm{CC}_{\mathrm{LOW}}$	0.085	1.250	0.05
				$\mathrm{CC}_{\mathrm{MID}}$	0.090	_	-0.02
				$\mathrm{CC}_{\mathrm{HIGH}}$	0.070	0.750	-0.05
	450	0.796	1130	$\mathrm{CC}_{\mathrm{MID}}$	-0.038	_	-0.02
				$\mathrm{CC}_{\mathrm{HIGH}}$	-0.160	0.778	-0.05
	500	0.885	2400	$\mathrm{CC}_{\mathrm{HIGH}}$	0.068	0.800	0.04

Table S5: (continued)

Molecule	T [K]	$T_{ m r}$	$P_{\rm sim}$ [kPa]	Test	$\ln\left(P_{\mathrm{sim}}/P_{\mathrm{CC}}\right)$	ER	NB
toluene 7-site (UA)	400	0.673	220	$\mathrm{CC}_{\mathrm{LOW}}$	0.108	1.250	0.06
	450	0.758	600	$\mathrm{CC}_{\mathrm{LOW}}$	-0.148	1.963	-0.06
				$\mathrm{CC}_{\mathrm{MID}}$	-0.048	_	-0.02
	500	0.842	1460	$\mathrm{CC}_{\mathrm{MID}}$	0.050	_	0.03
				$\mathrm{CC}_{\mathrm{HIGH}}$	0.087	0.800	-0.05
	530	0.892	2130	$CC_{HIGH}$	-0.075	0.509	-0.04
ethylbenzene (UA)	397	0.640	101	$\mathrm{CC}_{\mathrm{LOW}}$	-0.288	1.252	-0.09
	447	0.721	380	$\mathrm{CC}_{\mathrm{MID}}$	0.128	_	0.03
	497	0.802	870	$\mathrm{CC}_{\mathrm{HIGH}}$	-0.230	0.799	-0.05
propylbenzene (UA)	350	0.541	10	$CC_{LOW}$	0.072	1.286	0.06
	400	0.618	53	$\mathrm{CC}_{\mathrm{LOW}}$	-0.142	1.250	-0.09
				$\mathrm{CC}_{\mathrm{MID}}$	-0.031	_	-0.01
	450	0.696	205	$\mathrm{CC}_{\mathrm{MID}}$	0.063	_	0.03
				$\mathrm{CC}_{\mathrm{HIGH}}$	0.056	0.778	-0.09
	500	0.773	540	$CC_{HIGH}$	-0.114	0.800	-0.05
isopropylbenzene (UA)	400	0.622	59	$\mathrm{CC}_{\mathrm{LOW}}$	0.444	1.250	0.06
	450	0.700	164	$\mathrm{CC}_{\mathrm{LOW}}$	-0.132	1.222	-0.09
				$\mathrm{CC}_{\mathrm{MID}}$	-0.197	_	-0.01
	500	0.778	530	$\mathrm{CC}_{\mathrm{MID}}$	0.059	_	0.03
				$\mathrm{CC}_{\mathrm{HIGH}}$	0.355	0.800	-0.05
	550	0.855	1242	$CC_{HIGH}$	-0.108	0.818	-0.04
o-xylene (UA)	450	0.711	310	$CC_{LOW}$	0.065	1.222	0.05
	500	0.790	740	$\mathrm{CC}_{\mathrm{MID}}$	-0.029	_	-0.02
	550	0.869	1590	$\mathrm{CC}_{\mathrm{HIGH}}$	0.053	0.818	0.04

Table S5: (continued)

Molecule	T [K]	$T_{ m r}$	$P_{\rm sim}$ [kPa]	Test	$\ln\left(P_{\mathrm{sim}}/P_{\mathrm{CC}}\right)$	ER	NB
m-xylene (UA)	451	0.719	340	$\mathrm{CC}_{\mathrm{LOW}}$	-0.149	1.433	-0.06
				$\mathrm{CC}_{\mathrm{MID}}$	0.033	_	-0.02
	503	0.802	900	$\mathrm{CC}_{\mathrm{LOW}}$	0.091	1.455	0.05
				$\mathrm{CC}_{\mathrm{MID}}$	0.061	_	-0.02
				$\mathrm{CC}_{\mathrm{HIGH}}$	-0.058	0.776	-0.05
	547	0.872	1600	$CC_{MID}$	-0.037	_	-0.03
				$\mathrm{CC}_{\mathrm{HIGH}}$	-0.104	0.698	-0.04
	582	0.928	2530	$CC_{HIGH}$	0.063	0.687	0.04
p-xylene (UA)	397	0.643	104	$\mathrm{CC}_{\mathrm{LOW}}$	-0.135	1.471	-0.09
	452	0.733	370	$\mathrm{CC}_{\mathrm{LOW}}$	0.062	1.065	0.05
				$CC_{MID}$	0.055	_	-0.02
	499	0.809	800	$CC_{MID}$	-0.030	_	-0.02
				$CC_{HIGH}$			-0.05
	553	0.896	1750	$CC_{HIGH}$	0.059	0.939	0.04
naphthalene (UA)	550	0.733	440	$\mathrm{CC}_{\mathrm{LOW}}$	-0.091	1.182	-0.06
	600	0.800	920	$CC_{MID}$	0.042	_	0.03
	650	0.867	1590	$CC_{HIGH}$	-0.077	0.846	-0.04
methanol (UA)	275	0.548	$3.8_{2}$	$\mathrm{CC}_{\mathrm{LOW}}$	-0.177	1.182	-0.09
	300	0.598	$17_{1}$	$\mathrm{CC}_{\mathrm{LOW}}$	0.081	0.625	0.06
				$CC_{MID}$	0.081	_	-0.01
	325	0.647	$52_{2}$	$CC_{MID}$	-0.050		-0.01
				$CC_{HIGH}$		0.846	-0.09
	375	0.747	$354_{7}$	$CC_{HIGH}$	0.129	1.600	0.03
ethanol (UA)	275	0.535	$1.4_{2}$	$\mathrm{CC}_{\mathrm{LOW}}$	-0.208	1.182	-0.09
	300	0.584	$8.1_{5}$	$\mathrm{CC}_{\mathrm{MID}}$	0.095	_	0.03
	325	0.632	$30_{3}$	$\mathrm{CC}_{\mathrm{HIGH}}$	-0.176	0.846	-0.09
	375	0.730	$234_{10}$	$\mathrm{CC}_{\mathrm{LOW}}$	-0.216	1.267	-0.06
	425	0.827	$1110_{50}$	$CC_{MID}$	0.095	_	0.03
	475	0.924	$3200_{200}$	$\mathrm{CC}_{\mathrm{HIGH}}$	-0.170	0.789	-0.04

Table S5: (continued)

Molecule	T [K]	$T_{ m r}$	$P_{\rm sim}$ [kPa]	Test	$\ln{(P_{\rm sim}/P_{\rm CC})}$	ER	NB
propan-1-ol (UA)	300	0.558	$4.5_{2}$	$CC_{LOW}$	0.627	1.333	0.06
	350	0.651	$43_{1}$	$\mathrm{CC}_{\mathrm{LOW}}$	-0.653	1.286	-0.09
				$\mathrm{CC}_{\mathrm{MID}}$	-0.269	_	-0.01
	400	0.743	$374_{15}$	$\mathrm{CC}_{\mathrm{LOW}}$	0.114	1.250	0.05
				$CC_{MID}$	0.286	_	-0.02
				$\mathrm{CC}_{\mathrm{HIGH}}$	0.470	0.750	-0.05
	450	0.836	$1210_{30}$	$\mathrm{CC}_{\mathrm{LOW}}$	-0.545	3.815	-0.06
				$CC_{MID}$	-0.051	_	-0.02
				$\mathrm{CC}_{\mathrm{HIGH}}$	-0.508	0.778	-0.05
	500	0.929	$3390_{150}$	$CC_{MID}$	0.113	_	0.03
				$\mathrm{CC}_{\mathrm{HIGH}}$		0.800	-0.04
	515	0.957	$3850_{190}$	$\mathrm{CC}_{\mathrm{HIGH}}$	-0.143	0.262	-0.04
pentan-1-ol (UA)	300	0.518	$0.46_{4}$	$\mathrm{CC}_{\mathrm{LOW}}$	-0.204	1.333	-0.09
	350	0.604	$10.3_{4}$	$\mathrm{CC}_{\mathrm{LOW}}$	-0.253	1.286	-0.09
				$\mathrm{CC}_{\mathrm{MID}}$	0.087	_	-0.01
	400	0.691	$91_{4}$	$\mathrm{CC}_{\mathrm{LOW}}$	-0.105	1.250	-0.09
				$\mathrm{CC}_{\mathrm{MID}}$	0.111	_	-0.01
				$\mathrm{CC}_{\mathrm{HIGH}}$	-0.153	0.750	-0.09
	450	0.777	$407_{25}$	$\mathrm{CC}_{\mathrm{MID}}$	0.047	_	0.03
				$\mathrm{CC}_{\mathrm{HIGH}}$	-0.197	0.778	-0.05
	500	0.864	$1240_{30}$	$\mathrm{CC}_{\mathrm{LOW}}$	-0.185	3.767	-0.06
				$\mathrm{CC}_{\mathrm{HIGH}}$	-0.084	0.800	-0.04
	550	0.950	$2940_{140}$	$\mathrm{CC}_{\mathrm{MID}}$	0.039	_	0.03
				$\mathrm{CC}_{\mathrm{HIGH}}$	-0.048	0.818	-0.04
	565	0.976	$3520_{100}$	$\mathrm{CC}_{\mathrm{HIGH}}$	-0.049	0.265	-0.04

Table S5: (continued)

Molecule	T [K]	$T_{ m r}$	$P_{\rm sim}$ [kPa]	Test	$\ln{(P_{\rm sim}/P_{\rm CC})}$	ER	NB
octan-1-ol (UA)	300	0.477	$0.018_{2}$	$\mathrm{CC}_{\mathrm{LOW}}$	-0.184	1.333	-0.09
	350	0.556	$0.8_{1}$	$\mathrm{CC}_{\mathrm{LOW}}$	-0.222	1.286	-0.09
				$\mathrm{CC}_{\mathrm{MID}}$	0.079	_	-0.01
	400	0.636	$12_{1}$	$\mathrm{CC}_{\mathrm{LOW}}$	-0.287	1.250	-0.09
				$CC_{MID}$	0.097	_	-0.01
				$CC_{HIGH}$	-0.138	0.750	-0.09
	450	0.715	$83_{3}$	$CC_{LOW}$	-0.144	1.222	-0.06
				$CC_{MID}$	0.127	_	-0.02
				$CC_{HIGH}$			-0.05
	500	0.795	$310_{10}$	$CC_{LOW}$	-0.114		-0.06
				$CC_{MID}$	0.065	_	-0.02
				$CC_{HIGH}$		0.800	-0.05
	550	0.874	$810_{40}$	$CC_{MID}$	0.052	_	0.03
				$CC_{HIGH}$			-0.04
	600	0.954	$1640_{70}$	$CC_{HIGH}$	-0.095	0.833	-0.04
propan-2-ol (UA)	300	0.598	$4.0_{5}$	$CC_{LOW}$	-0.974	1.333	-0.09
	350	0.697	$98_{9}$	$\mathrm{CC}_{\mathrm{LOW}}$	-0.094	1.286	-0.09
				$\mathrm{CC}_{\mathrm{MID}}$	0.417	_	-0.01
	400	0.797	$520_{40}$	$\mathrm{CC}_{\mathrm{LOW}}$	-0.096	1.531	-0.06
				$\mathrm{CC}_{\mathrm{MID}}$	0.041	_	-0.02
				$\mathrm{CC}_{\mathrm{HIGH}}$	-0.730	0.750	-0.05
	450	0.896	$1770_{60}$	$CC_{MID}$	0.038	_	0.03
				$CC_{HIGH}$	-0.073	0.778	-0.04
	490	0.976	$3700_{500}$	$CC_{HIGH}$	-0.063	0.653	-0.04
butan-2-ol (UA)	300	0.573	$3.4_{1}$	$\mathrm{CC}_{\mathrm{LOW}}$	0.139	1.333	0.06
	350	0.668	$43_{2}$	$\mathrm{CC}_{\mathrm{LOW}}$	-0.408	1.286	-0.09
				$CC_{MID}$	-0.059	_	-0.01
	400	0.763	$320_{20}$	$\mathrm{CC}_{\mathrm{LOW}}$	0.080	1.250	0.05
				$\mathrm{CC}_{\mathrm{MID}}$	0.178	_	-0.02
				$\mathrm{CC}_{\mathrm{HIGH}}$	0.104	0.750	-0.05
	450	0.859	$1110_{50}$	$\mathrm{CC}_{\mathrm{MID}}$	-0.035	_	-0.03
				$\mathrm{CC}_{\mathrm{HIGH}}$		0.778	-0.04
	500	0.954	$3200_{100}$	$CC_{HIGH}$	0.064	0.800	0.04

Table S5: (continued)

Molecule	T[K]	$T_{ m r}$	$P_{\rm sim}$ [kPa]	Test	$\ln\left(P_{\mathrm{sim}}/P_{\mathrm{CC}}\right)$	ER	NB
2-methylpropan-2-ol (UA)	300	0.595	$6.3_{3}$	$CC_{LOW}$	-0.532	1.333	-0.09
	350	0.694	$113_{8}$	$\mathrm{CC}_{\mathrm{LOW}}$	-0.537	1.286	-0.09
				$\mathrm{CC}_{\mathrm{MID}}$	0.228	_	-0.01
	400	0.794	$661_{23}$	$\mathrm{CC}_{\mathrm{LOW}}$	0.576	2.000	0.05
				$\mathrm{CC}_{\mathrm{MID}}$	0.235	_	-0.02
				$\mathrm{CC}_{\mathrm{HIGH}}$	-0.399	0.750	-0.05
	450	0.893	$1720_{15}$	$CC_{MID}$	-0.192	_	-0.03
				$\mathrm{CC}_{\mathrm{HIGH}}$	-0.418	0.778	-0.04
	480	0.952	$3700_{200}$	$CC_{HIGH}$	0.288	0.500	0.04
1,2-ethanediol (UA)	450	0.627	$55_{3}$	$CC_{LOW}$	-0.515	1.222	-0.09
	500	0.696	$272_{11}$	$\mathrm{CC}_{\mathrm{LOW}}$	0.382	1.200	0.06
				$\mathrm{CC}_{\mathrm{MID}}$	0.232	_	-0.01
	550	0.766	$660_{40}$	$\mathrm{CC}_{\mathrm{LOW}}$	-0.207	1.182	-0.06
				$\mathrm{CC}_{\mathrm{MID}}$	-0.174	_	-0.02
				$\mathrm{CC}_{\mathrm{HIGH}}$	-0.421	0.818	-0.05
	600	0.836	$1900_{30}$	$\mathrm{CC}_{\mathrm{MID}}$	0.095	_	0.03
				$\mathrm{CC}_{\mathrm{HIGH}}$	0.319	0.833	-0.05
	650	0.905	$3900_{200}$	$CC_{HIGH}$	-0.176	0.846	-0.04
1,3-propanediol (UA)	450	0.620	$25.1_{13}$	$\mathrm{CC}_{\mathrm{LOW}}$	-0.541	1.222	-0.09
	500	0.689	$166_{4}$	$\mathrm{CC}_{\mathrm{MID}}$	0.244	_	0.03
	550	0.758	$500_{30}$	$\mathrm{CC}_{\mathrm{MID}}$	-0.024	_	-0.02
				$\mathrm{CC}_{\mathrm{HIGH}}$	-0.443	0.818	-0.05
	600	0.826	$1310_{80}$	$CC_{HIGH}$	0.044	0.833	0.03
pentane-1,5-diol (UA)	500	0.704	$77_{5}$	$CC_{LOW}$	-0.184	1.200	-0.06
<u>-</u>	550	0.775	$320_{20}$	$\mathrm{CC}_{\mathrm{MID}}$	0.083	_	0.03
	600	0.845	$900_{20}$	$CC_{HIGH}$	-0.153	0.833	-0.05
dimethyl ether (UA)	273	0.687	$308_{3}$	$CC_{LOW}$	-0.176	1.363	-0.09
v ( )	303	0.761	839 <sub>39</sub>	$CC_{MID}$	0.075	_	0.03
	329	0.827	$1538_{24}$	$CC_{HIGH}$		0.734	-0.05
		- · ·	3 24	111011	5 <b>-</b> -5		2.00

Table S5: (continued)

Molecule	T [K]	$T_{ m r}$	$P_{\text{sim}}$ [kPa]	Test	$\ln\left(P_{\mathrm{sim}}/P_{\mathrm{CC}}\right)$	ER	NB
ethyl methyl ether (UA)	273	0.628	$105_{2}$	$\mathrm{CC}_{\mathrm{LOW}}$	-0.199	2.273	-0.09
	323	0.743	$543_{24}$	$\mathrm{CC}_{\mathrm{LOW}}$	0.161	1.987	0.05
				$\mathrm{CC}_{\mathrm{MID}}$	0.061	_	-0.02
	351	0.808	$1025_{30}$	$\mathrm{CC}_{\mathrm{MID}}$	-0.054	_	-0.02
				$\mathrm{CC}_{\mathrm{HIGH}}$	-0.087	0.440	-0.05
	367	0.845	$1530_{56}$	$\mathrm{CC}_{\mathrm{LOW}}$	-0.103	2.542	-0.06
				$\mathrm{CC}_{\mathrm{HIGH}}$	0.081	0.503	-0.05
	392	0.902	$2472_{46}$	$\mathrm{CC}_{\mathrm{HIGH}}$	-0.069	1.371	-0.04
	403	0.927	$2867_{50}$	$CC_{HIGH}$	-0.041	0.393	-0.04
diethyl ether (UA)	343	0.736	$401_{27}$	$\mathrm{CC}_{\mathrm{LOW}}$	0.082	2.055	0.05
	393	0.844	$1202_{23}$	$CC_{MID}$	-0.027	_	-0.02
dipropyl ether (UA)	325	0.617	$40.6_{26}$	$\mathrm{CC}_{\mathrm{LOW}}$	-0.219	1.308	-0.09
	375	0.712	$209_{4}$	$\mathrm{CC}_{\mathrm{LOW}}$	0.186	1.267	0.05
				$CC_{MID}$	0.095	_	-0.02
	425	0.806	$619_{18}$	$CC_{MID}$	-0.082	_	-0.02
				$\mathrm{CC}_{\mathrm{HIGH}}$	-0.167		-0.05
	475	0.901	$1690_{36}$	$CC_{HIGH}$	0.147	0.789	0.04
diisopropyl ether (UA)	350	0.706	$184_{8}$	$\mathrm{CC}_{\mathrm{LOW}}$	0.097	2.429	0.05
	400	0.806	$622_{19}$	$\mathrm{CC}_{\mathrm{MID}}$	-0.028	_	-0.02
	425	0.857	$1069_{52}$	$\mathrm{CC}_{\mathrm{HIGH}}$	0.040	0.412	0.04
methyl t-butyl ether (UA)	323	0.652	$119_{2}$	$\mathrm{CC}_{\mathrm{LOW}}$	-0.213	0.980	-0.09
				$CC_{MID}$	-0.015	_	-0.01
	373	0.752	$511_{11}$	$CC_{MID}$	0.108	_	0.03
				$\mathrm{CC}_{\mathrm{HIGH}}$	0.039	1.598	-0.05
	443	0.893	$1820_{36}$	$\mathrm{CC}_{\mathrm{HIGH}}$	-0.217	1.021	-0.04
1,2-dimethoxyethane (UA)	325	0.600	$28.4_{7}$	$\mathrm{CC}_{\mathrm{LOW}}$	-0.235	1.308	-0.09
	375	0.692	$185_{4}$	$\mathrm{CC}_{\mathrm{MID}}$	0.102	_	0.03
	425	0.784	$648_{25}$	$CC_{MID}$	0.038	_	0.03
				$\mathrm{CC}_{\mathrm{HIGH}}$	-0.179	0.765	-0.05
	475	0.876	$1629_{44}$	$CC_{HIGH}$	-0.068	0.789	-0.04

Table S5: (continued)

Molecule	T [K]	$T_{ m r}$	$P_{\text{sim}}$ [kPa]	Test	$\ln\left(P_{\mathrm{sim}}/P_{\mathrm{CC}}\right)$	ER	NB
2-methoxyethan-1-ol (UA)	347	0.589	$18.5_{6}$	$CC_{LOW}$	-0.474	1.237	-0.09
	397	0.674	$150_{3}$	$\mathrm{CC}_{\mathrm{MID}}$	0.212	_	0.03
	450	0.763	$555_{20}$	$CC_{HIGH}$	-0.383	0.808	-0.05
ethanal (UA)	260	0.561	18.5	$\mathrm{CC}_{\mathrm{LOW}}$	-0.288	1.308	-0.09
	300	0.647	135	$\mathrm{CC}_{\mathrm{MID}}$	0.125	_	0.03
	340	0.734	495	$CC_{HIGH}$	-0.221	0.765	-0.05
pentanal (UA)	300	0.530	6.07	$CC_{LOW}$	-0.106	1.267	-0.09
	340	0.601	35.7	$\mathrm{CC}_{\mathrm{MID}}$	0.047	_	0.03
	380	0.672	133	$\mathrm{CC}_{\mathrm{MID}}$	0.032	_	0.03
	420	0.742	364	$CC_{HIGH}$	-0.058	0.810	-0.05
2-pentanone (UA)	340	0.606	39.7	$\mathrm{CC}_{\mathrm{MID}}$	0.034	_	0.03
2-octanone (UA)	360	0.562	4.43	$\mathrm{CC}_{\mathrm{LOW}}$	-0.383	1.222	-0.09
	400	0.625	29.7	$\mathrm{CC}_{\mathrm{LOW}}$	-0.105	1.200	-0.09
				$\mathrm{CC}_{\mathrm{MID}}$	0.172	_	-0.01
	440	0.688	103	$\mathrm{CC}_{\mathrm{MID}}$	0.048	_	0.03
				$\mathrm{CC}_{\mathrm{HIGH}}$	-0.313	0.818	-0.09
	480	0.750	266	$CC_{MID}$	0.032	_	0.03
				$\mathrm{CC}_{\mathrm{HIGH}}$	-0.088	0.833	-0.05
	520	0.812	560	$CC_{HIGH}$	-0.058	0.846	-0.05
acetonitrile (UA)	298	0.543	$13_{1}$	$\mathrm{CC}_{\mathrm{LOW}}$	0.094	1.336	0.06
	348	0.634	$81_{1}$	$CC_{MID}$	-0.040	_	-0.01
	398	0.725	$342_{15}$	$\mathrm{CC}_{\mathrm{LOW}}$	-0.068	1.251	-0.06
				$\mathrm{CC}_{\mathrm{HIGH}}$	0.071	0.749	-0.05
	448	0.816	$1060_{30}$	$\mathrm{CC}_{\mathrm{MID}}$	0.030	_	0.03
	498	0.907	$2480_{60}$	$CC_{HIGH}$	-0.054	0.799	-0.04
propionitrile (UA)	298	0.536	$8.7_{2}$	$\mathrm{CC}_{\mathrm{LOW}}$	-0.183	0.752	-0.09
	348	0.626	$69_{2}$	$\mathrm{CC}_{\mathrm{MID}}$	0.105	_	0.03
	448	0.806	$850_{20}$	$\mathrm{CC}_{\mathrm{HIGH}}$	-0.244	1.330	-0.05

Table S5: (continued)

Molecule	T [K]	$T_{ m r}$	$P_{\text{sim}}$ [kPa]	Test	$\ln\left(P_{\mathrm{sim}}/P_{\mathrm{CC}}\right)$	ER	NB
pyridine (UA)	298	0.482	$1.2_{1}$	$CC_{LOW}$	-0.466	1.336	-0.09
	348	0.563	$22_{2}$	$\mathrm{CC}_{\mathrm{LOW}}$	-0.206	0.961	-0.09
				$\mathrm{CC}_{\mathrm{MID}}$	0.200	_	-0.01
	398	0.644	$137_{5}$	$\mathrm{CC}_{\mathrm{LOW}}$	-0.121	1.672	-0.09
				$\mathrm{CC}_{\mathrm{MID}}$	0.105	_	-0.01
				$\mathrm{CC}_{\mathrm{HIGH}}$	-0.349	0.749	-0.09
	468	0.757	$742_{21}$	$CC_{MID}$	0.045	_	0.03
				$\mathrm{CC}_{\mathrm{HIGH}}$	-0.215	1.041	-0.05
	523	0.846	$1895_{21}$	$\mathrm{CC}_{\mathrm{HIGH}}$	-0.072	0.598	-0.05
pyrimidine (UA)	298	0.489	$1.86_{3}$	$CC_{LOW}$	0.288	2.712	0.06
	365	0.598	$33_{1}$	$\mathrm{CC}_{\mathrm{MID}}$	-0.078	_	-0.01
	398	0.652	$106_{9}$	$\mathrm{CC}_{\mathrm{LOW}}$	-0.155	1.266	-0.09
				$\mathrm{CC}_{\mathrm{HIGH}}$	0.106	0.369	-0.09
	440	0.721	$356_{21}$	$CC_{MID}$	0.068	_	0.03
	480	0.787	$820_{32}$	$CC_{HIGH}$	-0.122	0.790	-0.05
nitrobenzene (UA)	298	0.399	$0.1_{5}$	$\mathrm{CC}_{\mathrm{LOW}}$	0.060	1.147	0.06
	375	0.502	$4_1$	$\mathrm{CC}_{\mathrm{LOW}}$	0.142	2.422	0.06
				$CC_{MID}$	-0.028	_	-0.01
	484	0.648	$105_{6}$	$CC_{MID}$	-0.041	_	-0.01
				$\mathrm{CC}_{\mathrm{HIGH}}$	0.053	0.872	-0.09
	550	0.736	$429_{32}$	$CC_{LOW}$	-0.128		-0.06
				$\mathrm{CC}_{\mathrm{HIGH}}$	0.058	0.413	-0.05
	625	0.837	$1409_{46}$	$CC_{MID}$	0.056	_	0.03
	700	0.937	$3244_{68}$	$CC_{HIGH}$	-0.100	0.786	-0.04
methanethiol (UA)	220	0.463	4	$\mathrm{CC}_{\mathrm{LOW}}$	-0.271	1.182	-0.09
	240	0.505	17	$\mathrm{CC}_{\mathrm{MID}}$	0.124	_	0.03
	260	0.547	46	$\mathrm{CC}_{\mathrm{HIGH}}$	-0.229	0.846	-0.09
ethanethiol (UA)	240	0.478	5	$\mathrm{CC}_{\mathrm{LOW}}$	0.072	1.167	0.06
	260	0.518	14	$\mathrm{CC}_{\mathrm{MID}}$	-0.033	_	-0.01
	280	0.558	36	$\mathrm{CC}_{\mathrm{HIGH}}$	0.062	0.857	0.05

Table S5: (continued)

Molecule	T [K]	$T_{ m r}$	$P_{\rm sim}$ [kPa]	Test	$\ln{(P_{\rm sim}/P_{\rm CC})}$	ER	NB
pentanethiol (UA)	300	0.498	10	$CC_{LOW}$	0.164	1.133	0.06
	320	0.532	16	$\mathrm{CC}_{\mathrm{LOW}}$	0.093	1.125	0.06
				$\mathrm{CC}_{\mathrm{MID}}$	-0.077	_	-0.01
	340	0.565	28	$\mathrm{CC}_{\mathrm{MID}}$	-0.044	_	-0.01
				$\mathrm{CC}_{\mathrm{HIGH}}$	0.145	0.882	-0.09
	360	0.598	50	$\mathrm{CC}_{\mathrm{MID}}$	-0.019	_	-0.01
				$CC_{HIGH}$	0.082	0.889	-0.09
octanethiol (UA)	380	0.566	8	$\mathrm{CC}_{\mathrm{MID}}$	0.037	_	0.03
2-butanethiol (UA)	280	0.503	4	$\mathrm{CC}_{\mathrm{LOW}}$	-0.149	1.143	-0.09
	300	0.539	13	$CC_{MID}$	0.070	_	0.03
	320	0.575	32	$\mathrm{CC}_{\mathrm{MID}}$	0.038	_	0.03
				$CC_{HIGH}$	-0.131	0.875	-0.09
2-methyl-1-propanethiol (UA)	300	0.539	6	$\mathrm{CC}_{\mathrm{LOW}}$	-0.335	1.133	-0.09
	320	0.575	23	$\mathrm{CC}_{\mathrm{LOW}}$	-0.120	1.125	-0.09
				$CC_{MID}$	0.157	_	-0.01
	340	0.610	56	$CC_{MID}$	0.057	_	0.03
				$\mathrm{CC}_{\mathrm{HIGH}}$		0.882	-0.09
	360	0.646	111	$CC_{HIGH}$	-0.107	0.889	-0.09
dimethyl disulfide (UA)	300	0.495	4	$\mathrm{CC}_{\mathrm{LOW}}$	-0.269	1.133	-0.09
	320	0.528	13	$CC_{MID}$	0.126	_	0.03
	340	0.561	29	$CC_{HIGH}$	-0.238	0.882	-0.09
thiophene (UA)	293	0.484	8	$\mathrm{CC}_{\mathrm{LOW}}$	-0.474	1.341	-0.09
	343	0.567	74	$CC_{MID}$	0.202	_	0.03
	393	0.650	273	$\mathrm{CC}_{\mathrm{HIGH}}$	-0.353	0.746	-0.09
	443	0.732	755	$\mathrm{CC}_{\mathrm{LOW}}$	0.199	1.617	0.05
	493	0.815	1632	$CC_{LOW}$	-0.210	1.666	-0.06
				$\mathrm{CC}_{\mathrm{MID}}$	-0.076	_	-0.02
	530	0.876	2973	$CC_{MID}$	0.079	_	0.03
				$CC_{HIGH}$			-0.04
	555	0.917	3757	$CC_{HIGH}$	-0.126	0.600	-0.04

Table S5: (continued)

Molecule	T [K]	$T_{ m r}$	$P_{\text{sim}}$ [kPa]	Test	$\ln\left(P_{\mathrm{sim}}/P_{\mathrm{CC}}\right)$	ER	NB
1,3-butadiene (UA)	275	0.644	$170_{2}$	$\mathrm{CC}_{\mathrm{MID}}$	-0.017	_	-0.01
	300	0.703	$386_{4}$	$\mathrm{CC}_{\mathrm{MID}}$	0.037	_	0.03
				$\mathrm{CC}_{\mathrm{HIGH}}$	0.032	0.833	-0.05
	325	0.761	$722_{7}$	$CC_{HIGH}$	-0.068	0.846	-0.05
methyl acrylate (UA)	298	0.530	$11.2_{5}$	$CC_{LOW}$	0.168	4.933	0.06
	340	0.605	$61_{1}$	$\mathrm{CC}_{\mathrm{MID}}$	-0.028	_	-0.01
	350	0.622	$89_{1}$	$\mathrm{CC}_{\mathrm{MID}}$	0.038	_	0.03
	360	0.640	$118_{2}$	$\mathrm{CC}_{\mathrm{MID}}$	-0.016	_	-0.01
	400	0.711	$341_{3}$	$CC_{HIGH}$	0.074	3.500	0.03
ethyl acrylate (UA)	298	0.516	$4.9_{2}$	$CC_{LOW}$	-0.253	7.698	-0.09
,	380	0.657		$CC_{LOW}$	-0.224	1.842	-0.09
				$\mathrm{CC}_{\mathrm{MID}}$	-0.029	_	-0.01
	450	0.779	$652_{15}$	$CC_{LOW}$	0.119	2.333	0.05
				$\mathrm{CC}_{\mathrm{MID}}$	0.079	_	-0.02
				$\mathrm{CC}_{\mathrm{HIGH}}$	0.195	5.756	-0.05
	500	0.865	$1481_{32}$	$\mathrm{CC}_{\mathrm{MID}}$	-0.036	_	-0.03
				$\mathrm{CC}_{\mathrm{HIGH}}$	-0.121	0.543	-0.04
	525	0.908	$2215_{53}$	$CC_{HIGH}$	0.051	0.429	0.04
n-butyl acrylate (UA)	450	0.721	$196_{2}$	$CC_{LOW}$	-0.159	1.222	-0.06
				$\mathrm{CC}_{\mathrm{MID}}$	-0.026	_	-0.02
	500	0.801	$570_{12}$	$\mathrm{CC}_{\mathrm{LOW}}$	0.183	2.300	0.05
				$\mathrm{CC}_{\mathrm{MID}}$	0.071	_	-0.02
				$\mathrm{CC}_{\mathrm{HIGH}}$	0.070	1.700	-0.05
	550	0.881	$1199_{29}$	$\mathrm{CC}_{\mathrm{MID}}$	-0.056	_	-0.03
				$\mathrm{CC}_{\mathrm{HIGH}}$	-0.130	0.818	-0.04
	575	0.921	$1794_{14}$	$CC_{HIGH}$	0.080	0.435	0.04
n-octyl acrylate (UA)	450	0.640	$23.7_{8}$	$CC_{LOW}$	0.092	4.444	0.06
	490	0.697	$68_{1}$	$\mathrm{CC}_{\mathrm{MID}}$	-0.017	_	-0.01
	550	0.783	$261_{4}$	$\mathrm{CC}_{\mathrm{HIGH}}$	-0.113	3.636	-0.05

Table S5: (continued)

Molecule	T [K]	$T_{ m r}$	$P_{\text{sim}}$ [kPa]	Test	$\ln\left(P_{\mathrm{sim}}/P_{\mathrm{CC}}\right)$	ER	NB
2-ethylhexyl acrylate (UA)	450	0.650	$32.6_{9}$	$CC_{LOW}$	-0.130	3.267	-0.09
	480	0.694	$75_{2}$	$\mathrm{CC}_{\mathrm{MID}}$	0.031	_	0.03
	490	0.708	$93_{2}$	$\mathrm{CC}_{\mathrm{MID}}$	-0.020	_	-0.02
	500	0.723	$119_{5}$	$\mathrm{CC}_{\mathrm{LOW}}$	-0.113	1.200	-0.06
				$\mathrm{CC}_{\mathrm{HIGH}}$	0.040	0.960	-0.05
	550	0.795	$328_{6}$	$\mathrm{CC}_{\mathrm{LOW}}$	0.150	1.182	0.05
				$\mathrm{CC}_{\mathrm{MID}}$	0.051	_	-0.02
				$\mathrm{CC}_{\mathrm{HIGH}}$	-0.084	4.455	-0.05
	600	0.867	$695_{32}$	$\mathrm{CC}_{\mathrm{MID}}$	-0.069	_	-0.03
				$\mathrm{CC}_{\mathrm{HIGH}}$	-0.094	0.833	-0.04
	650	0.939	$1490_{21}$	$CC_{HIGH}$	0.127	0.846	0.04
2-hydroxyethyl acrylate (UA)	470	0.693	$128_{2}$	$CC_{MID}$	-0.014	_	-0.01
	500	0.737	$273_{5}$	$CC_{HIGH}$		1.880	-0.05
	600	0.885	$1709_{25}$	$CC_{HIGH}$		0.833	-0.04
methyl methacrylate (UA)	298	0.508	$4.7_{2}$	$CC_{LOW}$	0.210	7.698	0.06
	360	0.614	$57_1$	$CC_{MID}$	-0.024	_	-0.01
ethyl methacrylate (UA)	360	0.602	$35_{1}$	$CC_{LOW}$	0.131	2.167	0.06
, , , , , , , , , , , , , , , , , , , ,	380	0.636	$63.1_9$	$CC_{MID}$	-0.041	_	-0.01
	390	0.652	884	$CC_{HIGH}$		0.462	0.05
n-butyl methacrylate (UA)	375	0.586	$14.2_{5}$	$\mathrm{CC}_{\mathrm{LOW}}$	0.068	1 400	0.06
ii buoyi incomaciyiaac (C11)	400	0.625	$32_1$	$CC_{MID}$	-0.028	_	-0.01
	420	0.657	$60_2$	$CC_{MID}$	-0.014	_	-0.01
	440	0.688	$111_{2}$	$CC_{MID}$	0.049	_	0.03
	500	0.782	$392_{8}$	CC <sub>HIGH</sub>		5.160	-0.05
	600	0.938	$1818_{31}$	CC <sub>HIGH</sub>			-0.04

Table S5: (continued)

Molecule	T [K]	$T_{ m r}$	$P_{\rm sim}$ [kPa]	Test	$\ln{(P_{\rm sim}/P_{\rm CC})}$	ER	NB
cyclopentane (UA)	272	0.528	$23.0_{7}$	$CC_{LOW}$	0.170	1.213	0.06
	301	0.584	$66_{2}$	$\mathrm{CC}_{\mathrm{LOW}}$	-0.172	1.193	-0.09
				$\mathrm{CC}_{\mathrm{MID}}$	-0.077	_	-0.01
	330	0.641	$181_{4}$	$\mathrm{CC}_{\mathrm{LOW}}$	0.136	1.590	0.06
				$\mathrm{CC}_{\mathrm{MID}}$	0.079	_	-0.01
				$\mathrm{CC}_{\mathrm{HIGH}}$	0.140	0.824	-0.09
	359	0.697	$365_{7}$	$\mathrm{CC}_{\mathrm{LOW}}$	-0.092	1.069	-0.09
				$CC_{MID}$	-0.052	_	-0.01
				$CC_{HIGH}$			-0.09
	380	0.738	$618_{4}$	$CC_{LOW}$	0.053	1.609	
				$CC_{MID}$	0.044		-0.02
				$CC_{HIGH}$			-0.05
	402	0.781	$928_{13}$	$CC_{MID}$	-0.020		-0.02
				$CC_{HIGH}$			-0.05
	417	0.810	$1235_{20}$	$CC_{HIGH}$		0.621	
	482	0.936	$3260_{30}$	$CC_{HIGH}$	0.041	1.007	0.04
cyclohexane (UA)	323	0.583	$52.9_{10}$	$\mathrm{CC}_{\mathrm{MID}}$	-0.026	_	-0.01
tetrahydrofuran (UA)	330	0.607	$99_{2}$	$\mathrm{CC}_{\mathrm{LOW}}$	0.065	1.121	0.06
				$\mathrm{CC}_{\mathrm{MID}}$	0.041	_	-0.01
	350	0.643	$171_{2}$	$\mathrm{CC}_{\mathrm{MID}}$	-0.031	_	-0.01
	370	0.680	$295_{2}$	$CC_{MID}$	-0.012	_	-0.01
				$CC_{HIGH}$	0.058	0.892	-0.09
1,3-dioxolane (UA)	290	0.513	$11.0_{2}$	$CC_{LOW}$	0.135	1.138	0.06
	310	0.549	$25.7_{14}$	$\mathrm{CC}_{\mathrm{MID}}$	-0.063	_	-0.01
	330	0.584	$61_{2}$	$\mathrm{CC}_{\mathrm{LOW}}$	-0.107	1.121	-0.09
				$\mathrm{CC}_{\mathrm{MID}}$	0.034	_	-0.01
				$\mathrm{CC}_{\mathrm{HIGH}}$	0.119	0.879	-0.09
	350	0.619	$123_{2}$	$\mathrm{CC}_{\mathrm{LOW}}$	0.070	1.114	0.06
				$\mathrm{CC}_{\mathrm{MID}}$	0.050	_	-0.01
	370	0.655	$209_{3}$	$\mathrm{CC}_{\mathrm{MID}}$	-0.033	_	-0.01
				$CC_{HIGH}$		0.892	-0.09
	390	0.690	$358_{4}$	$CC_{HIGH}$	0.062	0.897	0.05

Table S5: (continued)

Molecule	T [K]	$T_{ m r}$	$P_{\rm sim}$ [kPa]	Test	$\ln{(P_{\rm sim}/P_{\rm CC})}$	ER	NB
oxane (UA)	340	0.582	$54.1_{13}$	$\mathrm{CC}_{\mathrm{MID}}$	0.034	_	0.03
	360	0.616	$98_{2}$	$\mathrm{CC}_{\mathrm{MID}}$	-0.016	_	-0.01
	400	0.685	$276_{3}$	$\mathrm{CC}_{\mathrm{MID}}$	-0.015	_	-0.01
	440	0.753	$634_{4}$	$CC_{MID}$	-0.022	_	-0.02
	460	0.788	$930_{7}$	$CC_{HIGH}$	0.041	0.913	0.03
1,3-dioxane (UA)	335	0.552	$25.5_{6}$	$\mathrm{CC}_{\mathrm{MID}}$	-0.012	_	-0.01
1,5 dioxane (CH)	355	0.585	$52.5_{12}$	$CC_{MID}$	-0.012	_	-0.01
	375	0.618	$103_2$	$CC_{MID}$	0.040	_	0.03
1,4-dioxane (UA)	355	0.604	$85_{2}$	$CC_{MID}$	-0.010	_	-0.01
	555	0.944	$4040_{60}$	$\mathrm{CC}_{\mathrm{HIGH}}$	0.049	0.928	0.04
1,3,5-trioxane (UA)	510	0.839	$1930_{20}$	$\mathrm{CC}_{\mathrm{LOW}}$	0.051	1.078	0.05
	550	0.905	$3460_{30}$	$CC_{HIGH}$	0.047	0.927	0.04
	570	0.938	$4370_{30}$	$CC_{HIGH}$	-0.050	0.930	-0.04
	272	0.000	1 5 5	aa	0.10	1 200	0.00
SPC-pol3 (pol)	373	0.602	$155_{6}$	$CC_{LOW}$	0.195		0.06
	423	0.682	$638_{27}$	$CC_{LOW}$	-0.114	1.236	-0.09
	479	0.700	0070	$CC_{MID}$	-0.086	_	-0.01
	473	0.763	$2270_{90}$	$CC_{MID}$	0.051	_ 0.780	0.03
	523	0.844	5780 <sub>160</sub>	$CC_{HIGH}$			-0.05 $-0.05$
	929	0.044	3700160	$CC_{HIGH}$	-0.092	0.003	-0.03
TIP4P-pol1 (pol)	373	0.643	$173_{13}$	$CC_{LOW}$	0.073	1.268	0.06
	423	0.729	$734_{37}$	$\mathrm{CC}_{\mathrm{LOW}}$	0.064	1.236	0.05
				$\mathrm{CC}_{\mathrm{MID}}$	-0.032	_	-0.02
	473	0.816	$2430_{70}$	$\mathrm{CC}_{\mathrm{MID}}$	-0.029	_	-0.02
				$\mathrm{CC}_{\mathrm{HIGH}}$	0.057	0.789	-0.05
	523	0.902	$6740_{370}$	$CC_{HIGH}$	0.052	0.809	0.04

Table S5: (continued)

Molecule	T [K]	$T_{ m r}$	$P_{\text{sim}}$ [kPa]	Test	$\ln\left(P_{\rm sim}/P_{\rm CC}\right)$	ER	NB
TIP4P-pol3 (pol)	373	0.643	$275_{13}$	$\mathrm{CC}_{\mathrm{LOW}}$	0.086	1.268	0.06
	423	0.729	$1122_{48}$	$\mathrm{CC}_{\mathrm{LOW}}$	-0.092	1.236	-0.06
				$\mathrm{CC}_{\mathrm{MID}}$	-0.038	_	-0.02
	473	0.816	$3640_{100}$	$\mathrm{CC}_{\mathrm{MID}}$	0.041	_	0.03
				$CC_{HIGH}$		0.789	-0.05
	523	0.902	$8750_{260}$	$CC_{HIGH}$	-0.075	0.809	-0.04
methane (EH)	120	0.633	2067	$\mathrm{CC}_{\mathrm{LOW}}$	0.162	1.250	0.06
	135	0.712	$501_{15}$	$\mathrm{CC}_{\mathrm{LOW}}$	-0.152	1.222	-0.06
				$\mathrm{CC}_{\mathrm{MID}}$	-0.072	_	-0.02
	150	0.791	$1161_{38}$	$\mathrm{CC}_{\mathrm{MID}}$	0.068	_	0.03
				$CC_{HIGH}$		0.800	-0.05
	165	0.870	$2040_{60}$	$CC_{HIGH}$	-0.124	0.818	-0.04
ethane (EH)	185	0.601	$101_{3}$	$CC_{LOW}$	-0.415	2.486	-0.09
	215	0.698	$447_{13}$	$\mathrm{CC}_{\mathrm{LOW}}$	0.144	1.140	0.06
				$\mathrm{CC}_{\mathrm{MID}}$	0.119	_	-0.01
	230	0.747	$688_{31}$	$\mathrm{CC}_{\mathrm{MID}}$	-0.067	_	-0.02
				$CC_{HIGH}$		0.402	-0.05
	245	0.795	$1140_{60}$	$CC_{HIGH}$	0.127	0.878	0.03
propane (EH)	260	0.699	$302_{11}$	$CC_{MID}$	-0.018	_	-0.01
	280	0.753	$582_{23}$	$\mathrm{CC}_{\mathrm{LOW}}$	0.083	1.143	0.05
				$\mathrm{CC}_{\mathrm{HIGH}}$	0.033	0.857	-0.05
	300	0.806	$973_{43}$	$\mathrm{CC}_{\mathrm{MID}}$	-0.039	_	-0.02
				$CC_{HIGH}$	-0.055	0.867	-0.05
	320	0.860	$1641_{55}$	$CC_{HIGH}$	0.073	0.875	0.04
n-pentane (EH)	360	0.761	$461_{36}$	$CC_{LOW}$	0.065	1.167	0.05
	390	0.825	$864_{46}$	$\mathrm{CC}_{\mathrm{MID}}$	-0.030	_	-0.02
	420	0.888	$1565_{87}$	$\mathrm{CC}_{\mathrm{LOW}}$	0.231	2.143	0.06
				$\mathrm{CC}_{\mathrm{HIGH}}$	0.056	0.857	-0.04
	440	0.930	$2230_{130}$	$\mathrm{CC}_{\mathrm{MID}}$	-0.073	_	-0.03
	450	0.951	$2930_{80}$	$\mathrm{CC}_{\mathrm{HIGH}}$	0.108	0.467	0.04

Table S5: (continued)

Molecule	T [K]	$T_{ m r}$	$P_{\rm sim}$ [kPa]	Test	$\ln\left(P_{\mathrm{sim}}/P_{\mathrm{CC}}\right)$	ER	NB
n-octane (EH)	400	0.697	$105_{8}$	$CC_{LOW}$	-0.236	1.567	-0.09
	440	0.767	$306_{12}$	$\mathrm{CC}_{\mathrm{LOW}}$	0.100	1.136	0.05
				$\mathrm{CC}_{\mathrm{MID}}$	0.092	_	-0.02
	470	0.819	$521_{22}$	$\mathrm{CC}_{\mathrm{MID}}$	-0.047	_	-0.02
				$\mathrm{CC}_{\mathrm{HIGH}}$	-0.151	0.638	-0.05
	500	0.871	$909_{38}$	$\mathrm{CC}_{\mathrm{HIGH}}$		0.880	0.04
	530	0.923	$1424_{32}$	$CC_{HIGH}$	-0.045	0.887	-0.04
n-dodecane (EH)	450	0.675	$35_{2}$	$CC_{LOW}$	0.101	1.222	0.06
	500	0.750	$111_{6}$	$\mathrm{CC}_{\mathrm{LOW}}$	0.156	1.671	0.05
				$CC_{MID}$	-0.045	_	-0.02
	550	0.825	$310_{14}$	$\mathrm{CC}_{\mathrm{MID}}$	-0.058	_	-0.02
				$\mathrm{CC}_{\mathrm{HIGH}}$	0.083	0.818	-0.05
	585	0.877	$629_{30}$	$\mathrm{CC}_{\mathrm{HIGH}}$	0.093	0.598	0.04
methylamine (EH)	267	0.622	$99_{2}$	$CC_{LOW}$	-0.139	0.781	-0.09
	200	0.005	2.02	$CC_{MID}$	-0.036	_	-0.01
	298	0.695	$362_{15}$	$CC_{MID}$	0.078	- 1 500	0.03
	350	0.816	$1592_{24}$	$CC_{HIGH}$ $CC_{HIGH}$			-0.09 $-0.05$
dimethylamine (EH)	250	0.564	$20_{2}$	$CC_{LOW}$	-0.165	1.320	-0.09
,	280	0.632	=	$CC_{LOW}$	-0.093		-0.09
				$CC_{MID}$	0.071		-0.01
	308	0.695	$320_{17}$	$CC_{MID}$	0.051	_	0.03
				$CC_{HIGH}$		0.758	-0.09
	350	0.790	$1102_{78}$	$\mathrm{CC}_{\mathrm{MID}}$	0.040	_	0.03
				$\mathrm{CC}_{\mathrm{HIGH}}$	-0.112	1.200	-0.05
	400	0.903	$3173_{99}$	$\mathrm{CC}_{\mathrm{HIGH}}$	-0.076	0.917	-0.04

Table S5: (continued)

Molecule	T [K]	$T_{ m r}$	$P_{\text{sim}}$ [kPa]	Test	$\ln\left(P_{\rm sim}/P_{\rm CC}\right)$	ER	NB
trimethylamine (EH)	240	0.554	$25_{1}$	$CC_{LOW}$	0.876	2.374	0.06
	275	0.635	$98_{2}$	$\mathrm{CC}_{\mathrm{LOW}}$	-0.397	0.402	-0.09
				$\mathrm{CC}_{\mathrm{MID}}$	-0.260	_	-0.01
	293	0.677	$252_{28}$	$\mathrm{CC}_{\mathrm{MID}}$	0.283	_	0.03
				$\mathrm{CC}_{\mathrm{HIGH}}$	0.369	0.421	-0.09
	350	0.808	$985_{55}$	$\mathrm{CC}_{\mathrm{MID}}$	-0.022	_	-0.02
				$CC_{HIGH}$	-0.987	2.488	-0.05
ethylamine (EH)	270	0.597	$46_{2}$	$CC_{LOW}$	0.479	0.523	0.06
	293	0.648	$92_{2}$	$\mathrm{CC}_{\mathrm{LOW}}$	-0.639	1.556	-0.09
				$\mathrm{CC}_{\mathrm{MID}}$	-0.315	_	-0.01
	350	0.774	$865_{46}$	$CC_{MID}$	0.250	_	0.03
				$\mathrm{CC}_{\mathrm{HIGH}}$	0.916	1.912	-0.05
	400	0.885	$2422_{145}$	$CC_{HIGH}$	-0.410	0.643	-0.04
diethylamine (EH)	293	0.584	$40_{3}$	$CC_{LOW}$	0.435	1.002	0.06
diethylamme (E11)	329	0.655	$98_{6}$	$CC_{LOW}$	0.100	1.188	
	020	0.000	<i>3</i> 0 <sub>6</sub>	$CC_{MID}$	-0.217	_	-0.01
	375	0.747	$370_{23}$	$CC_{LOW}$	-0.193		-0.06
	3.3	01111	31023	$CC_{MID}$	-0.046	_	-0.02
				$CC_{HIGH}$			-0.05
	425	0.847	$1231_{63}$	$CC_{MID}$	0.085	_	0.03
				$CC_{HIGH}$		0.841	-0.05
	475	0.946	$2731_{104}$	$\mathrm{CC}_{\mathrm{HIGH}}$		0.789	-0.04
	202	0 5 4 4	10.0	a a	0.014	1 400	0.00
triethylamine (EH)	293	0.544	_	$CC_{LOW}$	0.316		0.06
	363	0.673	$132_{1}$	$CC_{LOW}$	-0.209	1.139	-0.09
	105	0.700	coo	$CC_{MID}$	-0.120	_	-0.01
	425	0.788	$633_{5}$	$CC_{MID}$	0.098	_ 0.611	0.03
	500	0.000	2000	$CC_{HIGH}$			-0.05
	500	0.928	$2088_{23}$	$CC_{HIGH}$	-0.183	0.878	-0.04

Table S5: (continued)

Molecule	T[K]	$T_{ m r}$	$P_{\rm sim}$ [kPa]	Test	$\ln\left(P_{\mathrm{sim}}/P_{\mathrm{CC}}\right)$	ER	NB
nitromethane (EH)	293	0.497	$2.2_{2}$	$\mathrm{CC}_{\mathrm{LOW}}$	-0.422	1.679	-0.09
	375	0.637	$99_{3}$	$\mathrm{CC}_{\mathrm{LOW}}$	-0.316	2.000	-0.09
				$\mathrm{CC}_{\mathrm{MID}}$	0.158	_	-0.01
	450	0.764	$743_{17}$	$\mathrm{CC}_{\mathrm{LOW}}$	0.235	1.222	0.05
				$CC_{MID}$	0.105	_	-0.02
				$CC_{HIGH}$	-0.251	0.596	-0.05
	500	0.849	$1738_{45}$	$CC_{LOW}$	-0.227	2.300	-0.06
				$CC_{MID}$	-0.106	_	-0.02
				$CC_{HIGH}$		0.500	-0.05
	550	0.934	$4221_{48}$	$CC_{MID}$	0.069	_	0.03
				$CC_{HIGH}$	0.192		-0.04
	575	0.976	$5624_{190}$	$CC_{HIGH}$	-0.099	0.435	-0.04
nitroethane (EH)	323	0.555	$9_{1}$	$CC_{LOW}$	-0.094	1.461	-0.09
	388	0.667	$108_{6}$	$CC_{MID}$	0.038	_	0.03
	450	0.773	$555_{15}$	$CC_{LOW}$	0.056	1.222	
				$CC_{HIGH}$			-0.05
	550	0.945	$3568_{160}$	$CC_{HIGH}$	0.046	0.818	0.04
acetonitrile (EH)	348	0.636	$81_{1}$	$CC_{LOW}$	-0.153		-0.09
	398	0.728	$367_{6}$	$CC_{LOW}$	0.157	1.251	
				$CC_{MID}$	0.067	_	-0.02
	448	0.819	$1054_{20}$	$CC_{MID}$	-0.070	_	-0.02
				$CC_{HIGH}$			-0.05
	498	0.910	$2776_{62}$	$CC_{HIGH}$	0.125	0.799	0.04
propionitrile (EH)	348	0.627	$56_{1}$	$CC_{LOW}$	-0.125	1.287	-0.09
	398	0.717	$266_{5}$	$CC_{MID}$	0.054	_	0.03
	448	0.807	$810_{20}$	$CC_{HIGH}$	-0.097	0.777	-0.05
acetamide (EH)	400	0.535	$3.4_{1}$	$CC_{LOW}$	-0.218	1.250	-0.09
	450	0.602	$27_{1}$	$CC_{MID}$	0.097	_	0.03
	500	0.669	$119_{3}$	$CC_{MID}$	-0.016	_	-0.01
				$CC_{HIGH}$	-0.174	0.800	-0.09

Table S5: (continued)

Molecule	T [K]	$T_{ m r}$	$P_{\text{sim}}$ [kPa]	Test	$\ln\left(P_{\mathrm{sim}}/P_{\mathrm{CC}}\right)$	ER	NB
propanamide (EH)	400	0.542	$3.4_{2}$	$\mathrm{CC}_{\mathrm{LOW}}$	-0.109	1.250	-0.09
	450	0.610	$25_{1}$	$CC_{MID}$	0.049	_	0.03
butanamide (EH)	400	0.535	$1.6_{1}$	$\mathrm{CC}_{\mathrm{LOW}}$	-0.115	1.250	-0.09
	450	0.602	$15_{1}$	$\mathrm{CC}_{\mathrm{MID}}$	0.051	_	0.03
	500	0.668	$82_{3}$	$\mathrm{CC}_{\mathrm{MID}}$	0.035	_	0.03
				$\mathrm{CC}_{\mathrm{HIGH}}$	-0.092	0.800	-0.09
	550	0.735	$309_{9}$	$\mathrm{CC}_{\mathrm{HIGH}}$	-0.063	0.818	-0.05
benzene (EH)	415	0.737	$470_{60}$	$CC_{LOW}$	0.060	1.139	0.05
	465	0.826	$1250_{110}$	$CC_{MID}$	-0.028	_	-0.02
	520	0.924	$3110_{150}$	$\mathrm{CC}_{\mathrm{HIGH}}$	0.053	0.878	0.04
pyridine (EH)	298	0.482	$2_1$	$CC_{LOW}$	-0.317	1.335	-0.09
	348	0.562	$26_{1}$	$CC_{LOW}$	-0.180	0.961	-0.09
				$CC_{MID}$	0.136	_	-0.01
	398	0.643	$140_{20}$	$\mathrm{CC}_{\mathrm{LOW}}$	0.078	1.672	0.06
				$CC_{MID}$	0.092	_	-0.01
				$\mathrm{CC}_{\mathrm{HIGH}}$	-0.237	0.749	-0.09
	468	0.756	$670_{50}$	$\mathrm{CC}_{\mathrm{LOW}}$	-0.111	1.299	-0.06
				$\mathrm{CC}_{\mathrm{MID}}$	-0.029	_	-0.02
				$\mathrm{CC}_{\mathrm{HIGH}}$	-0.187	1.041	-0.05
	523	0.845	$1790_{130}$	$\mathrm{CC}_{\mathrm{MID}}$	0.048	_	0.03
				$\mathrm{CC}_{\mathrm{HIGH}}$	0.047	0.598	-0.05
	575	0.929	$3500_{200}$	$\mathrm{CC}_{\mathrm{HIGH}}$	-0.086	0.770	-0.04
pyrimidine (EH)	298	0.472	$0.3_{4}$	$\mathrm{CC}_{\mathrm{LOW}}$	-1.528	1.335	-0.09
	348	0.551	$18_{5}$	$\mathrm{CC}_{\mathrm{LOW}}$	-0.452	0.961	-0.09
				$\mathrm{CC}_{\mathrm{MID}}$	0.654	_	-0.01
	398	0.630	$123_{16}$	$\mathrm{CC}_{\mathrm{LOW}}$	0.233	1.672	0.06
				$CC_{MID}$	0.231	_	-0.01
				$\mathrm{CC}_{\mathrm{HIGH}}$	-1.144	0.749	-0.09
	468	0.741	$568_{12}$	$\mathrm{CC}_{\mathrm{MID}}$	-0.087	_	-0.02
				$\mathrm{CC}_{\mathrm{HIGH}}$	-0.471	1.041	-0.05
	523	0.828	$1630_{80}$	$\mathrm{CC}_{\mathrm{HIGH}}$	0.139	0.598	0.03

Table S5: (continued)

Molecule	T [K]	$T_{ m r}$	$P_{\rm sim}$ [kPa]	Test	$\ln\left(P_{\mathrm{sim}}/P_{\mathrm{CC}}\right)$	ER	NB
pyrazine (EH)	348	0.565	$20_{4}$	$CC_{LOW}$	-0.407	0.961	-0.09
	398	0.646	$150_{24}$	$CC_{MID}$	0.208	_	0.03
	468	0.760	$800_{50}$	$\mathrm{CC}_{\mathrm{LOW}}$	0.054	1.581	0.05
				$\mathrm{CC}_{\mathrm{HIGH}}$	-0.424	1.041	-0.05
	523	0.849	$2100_{300}$	$\mathrm{CC}_{\mathrm{MID}}$	-0.021	_	-0.02
pyridazine (EH)	298	0.392	$0.10_{4}$	$CC_{LOW}$	2.382	1.335	0.06
		0.457	$0.20_{7}$	$CC_{LOW}$	0.551	0.961	
			•	$CC_{MID}$	-1.020	_	-0.01
	398	0.523	$2.0_{3}$	$CC_{LOW}$	-0.489	1.672	-0.09
				$\mathrm{CC}_{\mathrm{MID}}$	-0.281	_	-0.01
				$CC_{HIGH}$	1.784	0.749	-0.09
	468	0.615	$39_{5}$	$\mathrm{CC}_{\mathrm{LOW}}$	-0.177	0.751	-0.09
				$\mathrm{CC}_{\mathrm{MID}}$	0.183	_	-0.01
				$\mathrm{CC}_{\mathrm{HIGH}}$	0.573	1.041	-0.09
	523	0.687	$172_{11}$	$\mathrm{CC}_{\mathrm{LOW}}$	0.073	2.490	0.06
				$CC_{MID}$	0.101	_	-0.01
				$\mathrm{CC}_{\mathrm{HIGH}}$	-0.292	0.598	-0.09
	620	0.815	$980_{90}$	$CC_{MID}$	-0.021	_	-0.02
				$CC_{HIGH}$	-0.236	1.331	-0.05
furan (EH)	250	0.506	81	$CC_{LOW}$	-0.413	1.400	-0.09
	300	0.607	$98_{7}$	$\mathrm{CC}_{\mathrm{LOW}}$	0.122	1.333	0.06
				$\mathrm{CC}_{\mathrm{MID}}$	0.172	_	-0.01
	350	0.709	$437_{11}$	$\mathrm{CC}_{\mathrm{LOW}}$	-0.092	1.571	-0.06
				$\mathrm{CC}_{\mathrm{MID}}$	-0.052	_	-0.02
				$\mathrm{CC}_{\mathrm{HIGH}}$	-0.295	0.714	-0.05
	400	0.810	$1470_{70}$	$CC_{MID}$	0.036	_	0.03
				$\mathrm{CC}_{\mathrm{HIGH}}$	0.092	0.750	-0.05
	440	0.891	$3000_{200}$	$\mathrm{CC}_{\mathrm{HIGH}}$	-0.059	0.636	-0.04

Table S5: (continued)

Molecule	T [K]	$T_{ m r}$	$P_{\text{sim}}$ [kPa]	Test	$\ln\left(P_{\mathrm{sim}}/P_{\mathrm{CC}}\right)$	ER	NB
thiophene (EH)	393	0.670	$274_{19}$	$CC_{LOW}$	-0.189	1.289	-0.09
				$\mathrm{CC}_{\mathrm{MID}}$	0.036	_	-0.01
	460	0.784	$1200_{100}$	$\mathrm{CC}_{\mathrm{MID}}$	0.083	_	0.03
				$\mathrm{CC}_{\mathrm{HIGH}}$	-0.073	1.043	-0.05
	530	0.903	$3260_{160}$	$CC_{HIGH}$	-0.147	0.776	-0.04
pyrrole (EH)	300	0.461	$1.0_{2}$	$\mathrm{CC}_{\mathrm{LOW}}$	-0.783	1.467	-0.09
	370	0.568	$39_{10}$	$\mathrm{CC}_{\mathrm{LOW}}$	0.109	1.230	0.06
				$CC_{MID}$	0.317	_	-0.01
	440	0.676	$278_{22}$	$CC_{LOW}$	-0.232	1.758	-0.09
				$CC_{MID}$	-0.049	_	-0.01
				$CC_{HIGH}$			-0.09
	520	0.799	$1500_{100}$	$CC_{MID}$	0.084	_	0.03
				$CC_{HIGH}$	0.088		-0.05
	580	0.891	$3430_{80}$	$CC_{HIGH}$	-0.132	0.569	-0.04
thiazole (EH)	300	0.472	$9.0_{4}$	$\mathrm{CC}_{\mathrm{LOW}}$	1.418	1.333	0.06
	350	0.550	$28_{4}$	$CC_{LOW}$	-0.525	1.286	-0.09
				$CC_{MID}$	-0.608	_	-0.01
	400	0.629	$190_{27}$	$CC_{MID}$	0.230	_	0.03
			~	$CC_{HIGH}$			-0.09
	450	0.708	$560_{50}$	$CC_{LOW}$	0.075		0.05
	<b>5</b> 00	0.700	1220	$CC_{HIGH}$			-0.05
		0.786	$1330_{60}$	$CC_{MID}$	-0.034	_ 0.010	-0.02
	550	0.865	$2870_{170}$	$CC_{HIGH}$	0.061	0.818	0.04
oxazole (EH)	300	0.557	$43_{4}$	$\mathrm{CC}_{\mathrm{LOW}}$	0.319	1.333	0.06
	350	0.649	$195_{13}$	$\mathrm{CC}_{\mathrm{LOW}}$	-0.114	1.286	-0.09
				$\mathrm{CC}_{\mathrm{MID}}$	-0.137	_	-0.01
	400	0.742	$770_{30}$	$\mathrm{CC}_{\mathrm{MID}}$	0.050	_	0.03
				$\mathrm{CC}_{\mathrm{HIGH}}$	0.240	0.750	-0.05
	450	0.835	$2050_{150}$	$\mathrm{CC}_{\mathrm{HIGH}}$	-0.089	0.778	-0.05

Table S5: (continued)

Molecule	T [K]	$T_{ m r}$	$P_{\text{sim}}$ [kPa]	Test	$\ln\left(P_{\mathrm{sim}}/P_{\mathrm{CC}}\right)$	ER	NB
isoxazole (EH)	400	0.677	$272_{17}$	$\mathrm{CC}_{\mathrm{MID}}$	0.038	_	0.03
	450	0.761	$835_{24}$	$\mathrm{CC}_{\mathrm{HIGH}}$	-0.067	0.778	-0.05
	475	0.804	$1340_{90}$	$\mathrm{CC}_{\mathrm{MID}}$	-0.030	_	-0.02
	540	0.914	$4100_{300}$	$CC_{HIGH}$	0.093	2.167	0.04
imidazole (EH)	400	0.489	$3.0_{3}$	$\mathrm{CC}_{\mathrm{LOW}}$	0.121	1.250	0.06
	450	0.550	$17_{7}$	$CC_{MID}$	-0.054	_	-0.01
	500	0.611	$75_{4}$	$CC_{MID}$	0.035	_	0.03
				$CC_{HIGH}$	0.097	0.800	-0.09
pyrazole (EH)	350	0.475	$3.0_{2}$	$\mathrm{CC}_{\mathrm{LOW}}$	-0.522	1.286	-0.09
	400	0.543	$28_{6}$	$\mathrm{CC}_{\mathrm{LOW}}$	0.265	1.250	0.06
				$CC_{MID}$	0.228	_	-0.01
	450	0.611	$106_{6}$	$CC_{LOW}$	-0.157	1.222	-0.09
				$CC_{MID}$	-0.118	_	-0.01
				$CC_{HIGH}$		0.778	-0.09
	500	0.678	$380_{30}$	$CC_{MID}$	0.071	_	0.03
				$CC_{HIGH}$	0.212		-0.09
	550	0.746	$950_{60}$	$CC_{HIGH}$	-0.128	0.818	-0.05
fluorobenzene (EH)	300	0.531	$9.6_{8}$	$\mathrm{CC}_{\mathrm{LOW}}$	-0.317	1.331	-0.09
	350	0.619	$80_{4}$	$\mathrm{CC}_{\mathrm{MID}}$	0.136	_	0.03
	400	0.708	$310_{30}$	$\mathrm{CC}_{\mathrm{HIGH}}$	-0.238	0.751	-0.05
chlorobenzene (EH)	298	0.471	$5.7_{2}$	$\mathrm{CC}_{\mathrm{LOW}}$	1.138	1.335	0.06
	348	0.550	$17.6_{10}$	$\mathrm{CC}_{\mathrm{LOW}}$	-0.213	0.961	-0.09
				$CC_{MID}$	-0.487		-0.01
	398	0.629	$96_{8}$	$CC_{LOW}$	0.229	1.672	
				$CC_{MID}$	0.108		-0.01
				$CC_{HIGH}$			-0.09
	468	0.739	$450_{30}$	$CC_{LOW}$	-0.064		-0.06
				$CC_{MID}$	-0.086		-0.02
	<b>F</b> 0 0	0.005	1000	$CC_{HIGH}$			-0.05
		0.826	$1300_{70}$	$CC_{HIGH}$			0.03
	575	0.909	$2800_{200}$	$CC_{HIGH}$	-0.049	0.770	-0.04

Table S5: (continued)

Molecule	T [K]	$T_{ m r}$	$P_{\text{sim}}$ [kPa]	Test	$\ln\left(P_{\mathrm{sim}}/P_{\mathrm{CC}}\right)$	ER	NB
bromobenzene (EH)	300	0.447	$3.6_{1}$	$CC_{LOW}$	2.151	1.400	0.06
	360	0.537	$8.9_{2}$	$\mathrm{CC}_{\mathrm{LOW}}$	-0.316	1.335	-0.09
				$\mathrm{CC}_{\mathrm{MID}}$	-0.896	_	-0.01
	420	0.626	$79_{14}$	$\mathrm{CC}_{\mathrm{MID}}$	0.135	_	0.03
				$CC_{HIGH}$	1.537	0.714	-0.09
	480	0.715	$320_{30}$	$CC_{HIGH}$	-0.236	0.749	-0.05
1,2-dichlorobenzene (EH)	348	0.498	$9_{2}$	$CC_{LOW}$	1.236	2.050	0.06
	398	0.570	$19_{2}$	$\mathrm{CC}_{\mathrm{MID}}$	-0.405	_	-0.01
	428	0.613	$50_{2}$	$\mathrm{CC}_{\mathrm{LOW}}$	-0.244	0.889	-0.09
				$\mathrm{CC}_{\mathrm{MID}}$	-0.031	_	-0.01
				$\mathrm{CC}_{\mathrm{HIGH}}$	0.603	0.488	-0.09
	468	0.670	$160_{20}$	$CC_{LOW}$	0.174	1.299	0.06
				$\mathrm{CC}_{\mathrm{MID}}$	0.129	_	-0.01
				$CC_{HIGH}$	0.066	1.134	-0.09
	523	0.748	$450_{40}$	$CC_{LOW}$	-0.068	0.862	-0.06
				$CC_{MID}$	-0.076	_	-0.02
				$CC_{HIGH}$	-0.275	1.125	-0.05
	575	0.823	$1140_{50}$	$CC_{MID}$	0.036	_	0.03
				$CC_{HIGH}$			-0.05
	650	0.930	$3100_{200}$	$CC_{HIGH}$	-0.078	1.161	-0.04
1,3-dichlorobenzene (EH)	398	0.575	$27_{3}$	$\mathrm{CC}_{\mathrm{LOW}}$	0.404	0.882	0.06
	428	0.618	$53_{5}$	$\mathrm{CC}_{\mathrm{LOW}}$	-0.230	0.889	-0.09
				$\mathrm{CC}_{\mathrm{MID}}$	-0.215	_	-0.01
	468	0.676	$180_{20}$	$CC_{LOW}$	-0.125	1.299	-0.09
				$CC_{MID}$	0.122	_	-0.01
				$CC_{HIGH}$	0.458	1.134	-0.09
	523	0.755	$550_{30}$	$CC_{LOW}$	0.069	0.862	0.05
				$CC_{MID}$	0.054	_	-0.02
				$CC_{HIGH}$			-0.05
	575	0.830	$1180_{80}$	$CC_{MID}$	-0.037		-0.02
				$CC_{HIGH}$			-0.05
	650	0.938	$3100_{100}$	$CC_{HIGH}$	0.080	1.161	0.04

Table S5: (continued)

Molecule	T [K]	$T_{ m r}$	$P_{\rm sim}$ [kPa]	Test	$\ln\left(P_{\mathrm{sim}}/P_{\mathrm{CC}}\right)$	ER	NB
1,4-dichlorobenzene (EH)	348	0.503	$3.9_{7}$	$\mathrm{CC}_{\mathrm{LOW}}$	-0.174	2.050	-0.09
	398	0.575	$22_{4}$	$\mathrm{CC}_{\mathrm{LOW}}$	0.228	0.882	0.06
				$\mathrm{CC}_{\mathrm{MID}}$	0.057	_	-0.01
	428	0.619	$47_{6}$	$\mathrm{CC}_{\mathrm{MID}}$	-0.121	_	-0.01
	468	0.677	$144_{5}$	$CC_{MID}$	0.036	_	0.03
				$\mathrm{CC}_{\mathrm{HIGH}}$	0.259	1.134	-0.09
	523	0.756	$470_{30}$	$\mathrm{CC}_{\mathrm{LOW}}$	-0.132	0.862	-0.06
				$\mathrm{CC}_{\mathrm{HIGH}}$	-0.077	1.125	-0.05
	575	0.831	$1190_{90}$	$\mathrm{CC}_{\mathrm{MID}}$	0.071	_	0.03
	650	0.940	$3000_{80}$	$CC_{HIGH}$	-0.153	1.161	-0.04
1,2,3-trichlorobenzene (EH)	400	0.532	$6_4$	$CC_{LOW}$	-0.535	2 375	-0.09
1,2,3 (1101110100011110110 (211)	450	0.598	$38_{6}$	$CC_{MID}$	0.158	_	0.03
	475	0.632	$66_{9}$	$CC_{LOW}$	0.185	1.105	0.06
	-, -	0.00-		$CC_{MID}$	-0.012	_	-0.01
				$CC_{HIGH}$		0.421	-0.09
	500	0.665	111 <sub>11</sub>	$CC_{MID}$	-0.088	_	-0.01
	525	0.698	$210_{14}$	$\mathrm{CC}_{\mathrm{LOW}}$	-0.168	0.571	-0.09
				$CC_{HIGH}$	0.167	0.905	-0.09
	550	0.731	$380_{30}$	$\mathrm{CC}_{\mathrm{LOW}}$	0.214	1.182	0.05
				$\mathrm{CC}_{\mathrm{MID}}$	0.107	_	-0.02
	600	0.798	$800_{80}$	$\mathrm{CC}_{\mathrm{LOW}}$	-0.295	1.167	-0.06
				$\mathrm{CC}_{\mathrm{MID}}$	-0.098	_	-0.02
				$\mathrm{CC}_{\mathrm{HIGH}}$	-0.293	1.750	-0.05
	650	0.864	$1800_{200}$	$\mathrm{CC}_{\mathrm{LOW}}$	0.239	2.231	0.06
				$\mathrm{CC}_{\mathrm{MID}}$	0.136	_	-0.03
				$\mathrm{CC}_{\mathrm{HIGH}}$	0.181	0.846	-0.04
	700	0.931	$2800_{200}$	$CC_{MID}$	-0.074	_	-0.03
				$\mathrm{CC}_{\mathrm{HIGH}}$	-0.253	0.857	-0.04
	725	0.964	$3800_{100}$	$\mathrm{CC}_{\mathrm{HIGH}}$	0.107	0.448	0.04

Table S5: (continued)

Molecule	T [K]	$T_{ m r}$	$P_{\rm sim}$ [kPa]	Test	$\ln{(P_{\rm sim}/P_{\rm CC})}$	ER	NB
1,3,5-trichlorobenzene (EH)	400	0.546	$9_2$	$CC_{LOW}$	0.505	2.375	0.06
	450	0.614	$37_{7}$	$\mathrm{CC}_{\mathrm{LOW}}$	-0.227	1.111	-0.09
				$\mathrm{CC}_{\mathrm{MID}}$	-0.150	_	-0.01
	475	0.648	$83_{13}$	$\mathrm{CC}_{\mathrm{LOW}}$	0.073	1.105	0.06
				$\mathrm{CC}_{\mathrm{MID}}$	0.108	_	-0.01
				$\mathrm{CC}_{\mathrm{HIGH}}$	0.213	0.421	-0.09
	500	0.682	$140_{20}$	$CC_{MID}$	-0.035	_	-0.01
				$CC_{HIGH}$		0.900	-0.09
	525	0.716	$240_{30}$	$CC_{LOW}$	0.052	0.571	0.05
				$CC_{HIGH}$	0.066	0.905	-0.05
	550	0.750	$380_{30}$	$CC_{LOW}$	-0.115	1.182	-0.06
				$CC_{MID}$	-0.033	_	-0.02
	600	0.819	$930_{80}$	$CC_{MID}$	0.053	_	0.03
				$CC_{HIGH}$			-0.05
	650	0.887	$1800_{200}$	$CC_{HIGH}$	-0.097	0.846	-0.04
hexachlorobenzene (EH)	575	0.648	$60_{20}$	$\mathrm{CC}_{\mathrm{LOW}}$	-0.273	1.087	-0.09
				$\mathrm{CC}_{\mathrm{MID}}$	-0.019	_	-0.01
	600	0.676	$114_{11}$	$\mathrm{CC}_{\mathrm{MID}}$	0.131	_	0.03
	625	0.705	$160_{30}$	$\mathrm{CC}_{\mathrm{LOW}}$	0.094	0.560	0.05
				$\mathrm{CC}_{\mathrm{MID}}$	-0.026	_	-0.02
				$\mathrm{CC}_{\mathrm{HIGH}}$	-0.252	0.920	-0.05
	650	0.733	$230_{20}$	$\mathrm{CC}_{\mathrm{LOW}}$	-0.108	1.154	-0.06
				$CC_{MID}$	-0.060	_	-0.02
				$\mathrm{CC}_{\mathrm{HIGH}}$	0.050	0.923	-0.05
	700	0.789	$520_{60}$	$\mathrm{CC}_{\mathrm{LOW}}$	0.080	1.143	0.05
				$\mathrm{CC}_{\mathrm{MID}}$	0.050	_	-0.02
				$\mathrm{CC}_{\mathrm{HIGH}}$	0.168	1.786	-0.05
	750	0.846	$960_{70}$	$CC_{LOW}$	-0.115		-0.06
				$CC_{MID}$	-0.037	_	-0.02
				$\mathrm{CC}_{\mathrm{HIGH}}$	-0.094	0.867	-0.05
	800	0.902	$1760_{150}$	$CC_{MID}$	0.036	_	0.03
				$\mathrm{CC}_{\mathrm{HIGH}}$		0.875	-0.04
	825	0.930	$2200_{300}$	$CC_{HIGH}$	-0.052	0.455	-0.04

Table S5: (continued)

Molecule	T [K]	$T_{ m r}$	$P_{\rm sim}$ [kPa]	Test	$\ln\left(P_{\mathrm{sim}}/P_{\mathrm{CC}}\right)$	ER	NB
2-chlorofuran (EH)	300	0.525	$9_{3}$	$\mathrm{CC}_{\mathrm{LOW}}$	-0.346	1.167	-0.09
	325	0.569	$34_{4}$	$\mathrm{CC}_{\mathrm{LOW}}$	0.107	1.154	0.06
				$\mathrm{CC}_{\mathrm{MID}}$	0.159	_	-0.01
	350	0.613	$79_{5}$	$\mathrm{CC}_{\mathrm{MID}}$	-0.050	_	-0.01
				$\mathrm{CC}_{\mathrm{HIGH}}$	-0.296	0.857	-0.09
	375	0.657	$180_{10}$	$\mathrm{CC}_{\mathrm{HIGH}}$	0.093	0.867	0.05
	400	0.701	$350_{40}$	$\mathrm{CC}_{\mathrm{LOW}}$	0.060	1.250	0.05
				$CC_{MID}$	0.033	_	-0.02
				$\mathrm{CC}_{\mathrm{HIGH}}$	-0.056	0.875	-0.05
	450	0.788	$970_{40}$	$CC_{LOW}$	-0.155	1.963	-0.06
				$CC_{MID}$	-0.027	_	-0.02
				$\mathrm{CC}_{\mathrm{HIGH}}$		1.667	-0.05
	500	0.876	$2300_{200}$	$CC_{MID}$	0.052	_	0.03
				$\mathrm{CC}_{\mathrm{HIGH}}$			-0.04
	530	0.928	$3300_{200}$	$CC_{HIGH}$	-0.079	0.509	-0.04
2-chlorothiophene (EH)	300	0.459	$1.3_{3}$	$\mathrm{CC}_{\mathrm{LOW}}$	-0.327	2.500	-0.09
	350	0.536	$15_{5}$	$\mathrm{CC}_{\mathrm{LOW}}$	0.112	1.143	0.06
				$CC_{MID}$	0.094	_	-0.01
	375	0.574	$35_{2}$	$CC_{MID}$	-0.052	_	-0.01
				$\mathrm{CC}_{\mathrm{HIGH}}$	-0.131	0.400	-0.09
	400	0.613	$81_{5}$	$CC_{MID}$	0.032	_	0.03
				$\mathrm{CC}_{\mathrm{HIGH}}$	0.098	0.875	-0.09
	450	0.689	$290_{30}$	$CC_{LOW}$	-0.148	1.222	-0.09
				$CC_{MID}$	-0.011		-0.01
	500	0.766	$820_{40}$	$CC_{LOW}$	0.067	1.200	0.05
				$CC_{MID}$	0.067	_	-0.02
	550	0.842	$1700_{100}$	$CC_{MID}$	-0.030	_	-0.02
				$CC_{HIGH}$			-0.05
	600	0.919	$3300_{300}$	$CC_{HIGH}$	0.056	0.833	0.04

Table S5: (continued)

Molecule	T [K]	$T_{ m r}$	$P_{\rm sim}$ [kPa]	Test	$\ln\left(P_{\mathrm{sim}}/P_{\mathrm{CC}}\right)$	ER	NB
phenol (EH)	360	0.519	$3.6_{4}$	$CC_{LOW}$	-0.136	3.667	-0.09
	440	0.634	$65_{5}$	$\mathrm{CC}_{\mathrm{MID}}$	-0.027	_	-0.01
	480	0.692	$197_{14}$	$\mathrm{CC}_{\mathrm{MID}}$	0.033	_	0.03
				$CC_{HIGH}$	0.075	1.750	-0.09
	540	0.778	$710_{110}$	$\mathrm{CC}_{\mathrm{LOW}}$	0.056	1.444	0.05
				$\mathrm{CC}_{\mathrm{MID}}$	0.032	_	-0.02
				$\mathrm{CC}_{\mathrm{HIGH}}$	-0.073	1.222	-0.05
	600	0.865	$1870_{150}$	$\mathrm{CC}_{\mathrm{HIGH}}$	-0.057	0.800	-0.04
1,2-dihydroxybenzene (EH)	480	0.594	$24.1_{14}$	$CC_{LOW}$	-0.600	1.083	-0.09
	500	0.619	$60_{10}$	$CC_{LOW}$	0.307	0.733	0.06
				$CC_{MID}$	0.288	_	-0.01
	520	0.644	$80_{20}$	$\mathrm{CC}_{\mathrm{MID}}$	-0.177	_	-0.01
				$CC_{HIGH}$	-0.554	0.923	-0.09
	550	0.681	$180_{20}$	$\mathrm{CC}_{\mathrm{LOW}}$	-0.147	0.582	-0.09
				$CC_{HIGH}$	0.419	1.364	-0.09
	580	0.718	$360_{30}$	$\mathrm{CC}_{\mathrm{MID}}$	0.093	_	0.03
	640	0.792	$920_{50}$	$\mathrm{CC}_{\mathrm{LOW}}$	0.092	1.734	0.05
				$\mathrm{CC}_{\mathrm{HIGH}}$	-0.253	1.719	-0.05
	700	0.866	$2000_{150}$	$\mathrm{CC}_{\mathrm{MID}}$	-0.034	_	-0.03
	740	0.916	$3300_{130}$	$\mathrm{CC}_{\mathrm{HIGH}}$	0.053	0.577	0.04
1,3-dihydroxybenzene (EH)	480	0.577	$16.0_{11}$	$CC_{LOW}$	0.063	1.528	0.06
	520	0.625	$53_{5}$	$\mathrm{CC}_{\mathrm{MID}}$	-0.025	_	-0.01
	580	0.697	$240_{50}$	$\mathrm{CC}_{\mathrm{MID}}$	0.039	_	0.03
	640	0.769	$700_{40}$	$\mathrm{CC}_{\mathrm{LOW}}$	-0.200	1.188	-0.06
				$\mathrm{CC}_{\mathrm{HIGH}}$	-0.107	1.719	-0.05
	700	0.841	$1690_{90}$	$\mathrm{CC}_{\mathrm{MID}}$	0.091	_	0.03
	760	0.913	$3000_{150}$	$\mathrm{CC}_{\mathrm{HIGH}}$	-0.168	0.842	-0.04

Table S5: (continued)

Molecule	T [K]	$T_{ m r}$	$P_{\rm sim}$ [kPa]	Test	$\ln\left(P_{\mathrm{sim}}/P_{\mathrm{CC}}\right)$	ER	NB
1,4-dihydroxybenzene (EH)	480	0.565	$7_3$	$CC_{LOW}$	-0.766	1.528	-0.09
	520	0.612	$41_{5}$	$\mathrm{CC}_{\mathrm{LOW}}$	0.263	1.115	0.06
				$\mathrm{CC}_{\mathrm{MID}}$	0.303	_	-0.01
	550	0.648	$79_{6}$	$\mathrm{CC}_{\mathrm{LOW}}$	-0.174	0.582	-0.09
				$\mathrm{CC}_{\mathrm{MID}}$	-0.124	_	-0.01
				$\mathrm{CC}_{\mathrm{HIGH}}$	-0.501	0.655	-0.09
	580	0.683	$180_{40}$	$\mathrm{CC}_{\mathrm{LOW}}$	0.061	1.207	0.06
				$CC_{MID}$	0.110	_	-0.01
				$\mathrm{CC}_{\mathrm{HIGH}}$	0.235	0.897	-0.09
	640	0.754	$550_{30}$	$\mathrm{CC}_{\mathrm{LOW}}$	-0.161	1.188	-0.06
				$CC_{MID}$	-0.028	_	-0.02
				$\mathrm{CC}_{\mathrm{HIGH}}$	-0.298	1.719	-0.05
	700	0.824	$1460_{120}$	$CC_{MID}$	0.074	_	0.03
				$\mathrm{CC}_{\mathrm{HIGH}}$	0.051	0.829	-0.05
	760	0.895	$2900_{200}$	$CC_{HIGH}$	-0.136	0.842	-0.04
benzonitrile (EH)	298	0.435	$0.20_{1}$	$CC_{LOW}$	1.694	1.458	0.06
	360	0.525	$2.0_{1}$	$\mathrm{CC}_{\mathrm{LOW}}$	-0.557	1.331	-0.09
				$\mathrm{CC}_{\mathrm{MID}}$	-0.689	_	-0.01
	420	0.612	$31_{1}$	$\mathrm{CC}_{\mathrm{LOW}}$	-0.312	1.286	-0.09
				$\mathrm{CC}_{\mathrm{MID}}$	0.239	_	-0.01
				$\mathrm{CC}_{\mathrm{HIGH}}$	1.162	0.686	-0.09
	480	0.700	$160_{10}$	$\mathrm{CC}_{\mathrm{LOW}}$	0.282	1.250	0.06
				$\mathrm{CC}_{\mathrm{MID}}$	0.136	_	-0.01
				$\mathrm{CC}_{\mathrm{HIGH}}$	-0.418	0.751	-0.09
	540	0.787	$450_{60}$	$\mathrm{CC}_{\mathrm{LOW}}$	-0.104	1.778	-0.06
				$\mathrm{CC}_{\mathrm{MID}}$	-0.125	_	-0.02
				$\mathrm{CC}_{\mathrm{HIGH}}$	-0.242	0.778	-0.05
	600	0.875	$1290_{120}$	$\mathrm{CC}_{\mathrm{MID}}$	0.037	_	0.03
				$\mathrm{CC}_{\mathrm{HIGH}}$	0.226	0.800	-0.04
	640	0.933	$2200_{130}$	$\mathrm{CC}_{\mathrm{HIGH}}$	-0.059	0.563	-0.04

Table S5: (continued)

Molecule	T[K]	$T_{ m r}$	$P_{\text{sim}}$ [kPa]	Test	$\ln\left(P_{\rm sim}/P_{\rm CC}\right)$	ER	NB
p-benzoquinone (EH)	395	0.568	$17.2_{9}$	$CC_{LOW}$	0.194	1.359	0.06
	430	0.618	$53_{2}$	$\mathrm{CC}_{\mathrm{LOW}}$	-0.224	0.872	-0.09
				$\mathrm{CC}_{\mathrm{MID}}$	-0.082	_	-0.01
	460	0.661	$140_{20}$	$CC_{MID}$	0.119	_	0.03
				$\mathrm{CC}_{\mathrm{HIGH}}$	0.143	0.736	-0.09
	500	0.718	$330_{30}$	$CC_{LOW}$	0.093	1.200	0.05
				$CC_{HIGH}$	-0.256	1.147	-0.05
	550	0.790	$810_{60}$	$CC_{MID}$	-0.042	_	-0.02
	600	0.862	$1850_{70}$	$CC_{HIGH}$	0.078	0.833	0.04
naphthalene (EH)	423	0.564	$18.0_{4}$	$CC_{LOW}$	0.136	1.236	0.06
()	473	0.631	$65_{2}$	$CC_{MID}$	-0.061	_	-0.01
	523	0.697	$205_{12}$	$CC_{HIGH}$		0.809	
	575	0.767	$550_{20}$	$CC_{MID}$	0.033	_	0.03
	630	0.840	$1230_{120}$	$CC_{MID}$	-0.025	_	-0.02
				$CC_{HIGH}$	-0.062	0.878	-0.05
	700	0.933	$3000_{200}$	$CC_{HIGH}$		1.045	0.04
anthracene (EH)	550	0.615	$22_{4}$	$CC_{LOW}$	-0.164	2 273	-0.09
	600	0.670	$76_{10}$	$CC_{LOW}$	0.115	1.083	
			- 10	$CC_{MID}$	0.050	_	-0.01
	625	0.698	$122_{15}$	$CC_{MID}$	-0.055	_	-0.01
	650	0.726	$210_{20}$	$CC_{LOW}$	-0.101	1.154	-0.06
				$\mathrm{CC}_{\mathrm{MID}}$	0.051	_	-0.02
				$CC_{HIGH}$	0.106	0.923	-0.05
	700	0.782	$480_{70}$	$\mathrm{CC}_{\mathrm{LOW}}$	0.098	1.143	0.05
				$\mathrm{CC}_{\mathrm{MID}}$	0.047	_	-0.02
				$\mathrm{CC}_{\mathrm{HIGH}}$	-0.143	1.786	-0.05
	750	0.838	$900_{90}$	$\mathrm{CC}_{\mathrm{MID}}$	-0.046	_	-0.02
				$\mathrm{CC}_{\mathrm{HIGH}}$	-0.088	0.867	-0.05
	800	0.894	$1700_{300}$	$\mathrm{CC}_{\mathrm{HIGH}}$	0.086	0.875	0.04

Table S5: (continued)

Molecule	T [K]	$T_{ m r}$	$P_{\rm sim}$ [kPa]	Test	$\ln\left(P_{\mathrm{sim}}/P_{\mathrm{CC}}\right)$	ER	NB
phenanthrene (EH)	550	0.613	$24_{1}$	$CC_{LOW}$	-0.115	2.273	-0.09
	600	0.669	$76_{11}$	$\mathrm{CC}_{\mathrm{MID}}$	0.035	_	0.03
	625	0.697	$120_{10}$	$\mathrm{CC}_{\mathrm{MID}}$	-0.020	_	-0.01
	650	0.725	$190_{20}$	$\mathrm{CC}_{\mathrm{HIGH}}$	0.038	0.923	0.03
	750	0.836	$840_{60}$	$\mathrm{CC}_{\mathrm{LOW}}$	-0.102	2.200	-0.06
	800	0.892	$1520_{150}$	$\mathrm{CC}_{\mathrm{MID}}$	0.032	_	0.03
	825	0.920	$1900_{100}$	$CC_{HIGH}$	-0.046	0.455	-0.04
naphthalen-2-ol (EH)	500	0.588	$15_{3}$	$CC_{LOW}$	-0.394	2.300	-0.09
	550	0.647	$72_{13}$	$\mathrm{CC}_{\mathrm{MID}}$	0.119	_	0.03
	575	0.676	$120_{30}$	$\mathrm{CC}_{\mathrm{MID}}$	-0.022	_	-0.01
				$\mathrm{CC}_{\mathrm{HIGH}}$	-0.171	0.435	-0.09
	600	0.706	$200_{30}$	$\mathrm{CC}_{\mathrm{HIGH}}$	0.043	0.917	0.03
	650	0.765	$510_{30}$	$\mathrm{CC}_{\mathrm{LOW}}$	-0.181	1.154	-0.06
				$\mathrm{CC}_{\mathrm{HIGH}}$	0.032	1.769	-0.05
	700	0.824	$1090_{150}$	$\mathrm{CC}_{\mathrm{LOW}}$	0.226	2.214	0.05
				$\mathrm{CC}_{\mathrm{MID}}$	0.084	_	-0.02
	750	0.882	$1800_{300}$	$CC_{MID}$	-0.070	_	-0.03
				$CC_{HIGH}$		0.867	-0.04
	775	0.912	$2500_{300}$	$CC_{HIGH}$	0.102	0.452	0.04
naphthalene-2-carbonitrile (EH)	525	0.623	$22_{5}$	$\mathrm{CC}_{\mathrm{LOW}}$	0.149	0.921	0.06
	550	0.652	$40_{10}$	$\mathrm{CC}_{\mathrm{LOW}}$	-0.340	1.636	-0.09
				$CC_{MID}$	-0.077	_	-0.01
	580	0.688	$90_{10}$	$\mathrm{CC}_{\mathrm{LOW}}$	0.138	0.448	0.06
				$CC_{MID}$	0.129	_	-0.01
				$CC_{HIGH}$	0.162	1.086	-0.09
	600	0.712	$120_{10}$	$CC_{MID}$	-0.095		-0.02
				$CC_{HIGH}$			-0.05
	650	0.771	$310_{30}$	$CC_{HIGH}$	0.307	2.231	0.03

Table S5: (continued)

Molecule	T [K]	$T_{ m r}$	$P_{\rm sim}$ [kPa]	Test	$\ln\left(P_{\mathrm{sim}}/P_{\mathrm{CC}}\right)$	ER	NB
quinoline (EH)	300	0.373	$5.1_{1}$	$CC_{LOW}$	2.988	3.000	0.06
	400	0.497	$4.3_{2}$	$CC_{LOW}$	0.794	1.250	0.06
				$\mathrm{CC}_{\mathrm{MID}}$	-0.747	_	-0.01
	450	0.559	$11_{1}$	$\mathrm{CC}_{\mathrm{LOW}}$	0.113	1.222	0.06
				$\mathrm{CC}_{\mathrm{MID}}$	-0.353	_	-0.01
				$\mathrm{CC}_{\mathrm{HIGH}}$	0.996	0.333	-0.09
	500	0.621	$44_{6}$	$CC_{MID}$	-0.051	_	-0.01
				$\mathrm{CC}_{\mathrm{HIGH}}$	0.635	0.800	-0.09
	550	0.683	$150_{40}$	$CC_{MID}$	0.036	_	0.03
				$\mathrm{CC}_{\mathrm{HIGH}}$	0.092	0.818	-0.09
	600	0.745	$390_{30}$	$CC_{LOW}$	-0.118	1.167	-0.06
				$CC_{MID}$	-0.021		-0.02
				$CC_{HIGH}$		0.833	
	650	0.807	$910_{50}$	$CC_{LOW}$	0.085	1.423	
				$\mathrm{CC}_{\mathrm{MID}}$	0.055		-0.02
				$CC_{HIGH}$		0.846	
	700	0.870	$1700_{200}$	$\mathrm{CC}_{\mathrm{MID}}$	-0.035		-0.03
				$CC_{HIGH}$		0.857	
	740	0.919	$2800_{300}$	$CC_{HIGH}$	0.060	0.703	0.04
indole (EH)	400	0.522	$2.2_{2}$	$\mathrm{CC}_{\mathrm{LOW}}$	-0.422	1.250	-0.09
	450	0.587	$22_{3}$	$\mathrm{CC}_{\mathrm{LOW}}$	-0.225	1.222	-0.09
				$\mathrm{CC}_{\mathrm{MID}}$	0.188	_	-0.01
	500	0.652	$99_{9}$	$\mathrm{CC}_{\mathrm{LOW}}$	0.061	1.200	0.06
				$\mathrm{CC}_{\mathrm{MID}}$	0.101	_	-0.01
				$\mathrm{CC}_{\mathrm{HIGH}}$	-0.338	0.800	-0.09
	550	0.717	$282_{5}$	$\mathrm{CC}_{\mathrm{LOW}}$	0.052	1.182	0.05
				$CC_{MID}$	-0.028	_	-0.02
				$CC_{HIGH}$	-0.184	0.818	
	600	0.782	$710_{40}$	$CC_{LOW}$	-0.229	1.167	
				$CC_{MID}$	-0.024		-0.02
				$CC_{HIGH}$		0.833	
	650	0.847	$1620_{90}$	$CC_{MID}$	0.106	_	0.03
				$CC_{HIGH}$		0.846	
	700	0.913	$2700_{200}$	$CC_{HIGH}$	-0.196	0.857	-0.04

Table S5: (continued)

Molecule	T [K]	$T_{ m r}$	$P_{\rm sim}$ [kPa]	Test	$\ln\left(P_{\mathrm{sim}}/P_{\mathrm{CC}}\right)$	ER	NB
isoindole (EH)	400	0.485	$1.5_{2}$	$CC_{LOW}$	-1.253	1.250	-0.09
	450	0.546	$16_{3}$	$\mathrm{CC}_{\mathrm{LOW}}$	0.755	1.222	0.06
				$\mathrm{CC}_{\mathrm{MID}}$	0.557	_	-0.01
	500	0.607	$39_{6}$	$\mathrm{CC}_{\mathrm{LOW}}$	-0.401	1.200	-0.09
				$CC_{MID}$	-0.340	_	-0.01
				$\mathrm{CC}_{\mathrm{HIGH}}$	-1.003	0.800	-0.09
	550	0.667	$150_{10}$	$CC_{LOW}$	0.213	1.182	0.06
				$CC_{MID}$	0.182	_	-0.01
				$CC_{HIGH}$		0.818	-0.09
	600	0.728	$330_{50}$	$CC_{LOW}$	-0.117	1.167	-0.06
				$CC_{MID}$	-0.098	_	-0.02
				$CC_{HIGH}$		0.833	-0.05
	650	0.789	$770_{60}$	$CC_{MID}$	0.054	_	0.03
				$CC_{HIGH}$			-0.05
	700	0.850	$1440_{70}$	$CC_{HIGH}$	-0.100	0.857	-0.05
benzimidazole (EH)	500	0.531	$2.3_{13}$	$CC_{LOW}$	-1.391	1.200	-0.09
	550	0.584	$31_{3}$	$CC_{LOW}$	0.060	1.182	0.06
				$CC_{MID}$	0.632	_	-0.01
	600	0.638	$85_{9}$	$CC_{LOW}$	0.084	1.167	0.06
				$CC_{MID}$	-0.028	_	-0.01
				$CC_{HIGH}$			-0.09
	650	0.691	$210_{30}$	$CC_{LOW}$	-0.146	1.154	-0.09
				$CC_{MID}$	-0.039	_	-0.01
				$CC_{HIGH}$			-0.09
	700	0.744	$490_{60}$	$CC_{LOW}$	0.246		0.05
				$CC_{MID}$	0.068	_	-0.02
	==0	0.707	000	$CC_{HIGH}$			-0.05
	750	0.797	$900_{90}$	$CC_{LOW}$	-0.230		-0.06
				$CC_{MID}$	-0.115		-0.02
	000	0.050	1000	$CC_{HIGH}$			-0.05
	800	0.850	$1900_{200}$	$CC_{MID}$	0.108	_ 0.075	0.03
	050	0.000	2000	$CC_{HIGH}$			-0.04
	850	0.903	$3000_{300}$	$CC_{HIGH}$	-0.203	0.882	-0.04

Table S5: (continued)

Molecule	T [K]	$T_{ m r}$	$P_{\rm sim}$ [kPa]	Test	$\ln\left(P_{\mathrm{sim}}/P_{\mathrm{CC}}\right)$	ER	NB
indazole (EH)	450	0.521	$4.9_{6}$	$CC_{LOW}$	0.571	1.222	0.06
	500	0.579	$23_{7}$	$\mathrm{CC}_{\mathrm{LOW}}$	-0.900	1.200	-0.09
				$\mathrm{CC}_{\mathrm{MID}}$	-0.257	_	-0.01
	550	0.637	$130_{20}$	$\mathrm{CC}_{\mathrm{LOW}}$	0.315	1.182	0.06
				$CC_{MID}$	0.409	_	-0.01
				$\mathrm{CC}_{\mathrm{HIGH}}$	0.467	0.818	-0.09
	600	0.695	$260_{30}$	$\mathrm{CC}_{\mathrm{LOW}}$	-0.093	1.167	-0.09
				$CC_{MID}$	-0.144	_	-0.01
				$\mathrm{CC}_{\mathrm{HIGH}}$	-0.750	0.833	-0.09
	650	0.753	$610_{70}$	$CC_{MID}$	0.043	_	0.03
				$CC_{HIGH}$	0.266	0.846	-0.05
	700	0.811	$1170_{110}$	$CC_{LOW}$	0.062	1.143	0.05
				$CC_{HIGH}$			-0.05
	800	0.927	$3700_{300}$	$CC_{HIGH}$	0.055	0.875	0.04
purine (EH)	500	0.525	$4_1$	$CC_{LOW}$	0.061	1.200	
	550	0.578	$21_{7}$	$CC_{LOW}$	-0.463		-0.09
				$CC_{MID}$	-0.028		-0.01
	600	0.630	$88_{13}$	$CC_{LOW}$	0.248	1.167	
				$CC_{MID}$	0.212		-0.01
				$CC_{HIGH}$			-0.09
	650	0.683	$200_{30}$	$CC_{MID}$	-0.114		-0.01
				$CC_{HIGH}$			-0.09
	700	0.735	$500_{50}$	$CC_{LOW}$	-0.147		-0.06
				$CC_{HIGH}$			-0.05
	750	0.788	$1070_{50}$	$CC_{LOW}$	0.052	0.778	
				$CC_{MID}$	0.069		-0.02
	800	0.840	$1830_{90}$	$CC_{MID}$	-0.029		-0.02
				$CC_{HIGH}$			-0.05
	875	0.919	$3900_{300}$	$CC_{HIGH}$	0.067	1.286	0.04

Table S5: (continued)

Molecule	T [K]	$T_{ m r}$	$P_{\rm sim}$ [kPa]	Test	$\ln\left(P_{\mathrm{sim}}/P_{\mathrm{CC}}\right)$	ER	NB
benzo[b]thiophene (EH)	348	0.452	$14.4_{1}$	$\mathrm{CC}_{\mathrm{LOW}}$	1.606	0.960	0.06
	398	0.516	$10.6_{13}$	$\mathrm{CC}_{\mathrm{LOW}}$	1.121	1.672	0.06
				$\mathrm{CC}_{\mathrm{MID}}$	-0.819	_	-0.01
	468	0.607	$41_{4}$	$\mathrm{CC}_{\mathrm{LOW}}$	-0.178	1.299	-0.09
				$\mathrm{CC}_{\mathrm{MID}}$	-0.420	_	-0.01
				$\mathrm{CC}_{\mathrm{HIGH}}$	1.672	1.041	-0.09
	523	0.679	$180_{20}$	$\mathrm{CC}_{\mathrm{MID}}$	0.077	_	0.03
				$\mathrm{CC}_{\mathrm{HIGH}}$	0.670	0.598	-0.09
	575	0.746	$490_{40}$	$\mathrm{CC}_{\mathrm{LOW}}$	0.071	2.250	0.05
				$\mathrm{CC}_{\mathrm{MID}}$	0.039	_	-0.02
				$\mathrm{CC}_{\mathrm{HIGH}}$	-0.137	0.770	-0.05
	650	0.843	$1440_{110}$	$\mathrm{CC}_{\mathrm{MID}}$	-0.022	_	-0.02
				$\mathrm{CC}_{\mathrm{HIGH}}$	-0.084	1.161	-0.05
benzo[c]thiophene (EH)	348	0.453	11.1 <sub>1</sub>	$CC_{LOW}$	2.437	0.960	0.06
	398	0.518	$7.2_{7}$	$\mathrm{CC}_{\mathrm{LOW}}$	0.065	1.672	0.06
				$\mathrm{CC}_{\mathrm{MID}}$	-1.243	_	-0.01
	468	0.610	$58_{15}$	$CC_{MID}$	-0.024	_	-0.01
				$\mathrm{CC}_{\mathrm{HIGH}}$	2.537	1.041	-0.09
benzoxazole (EH)	400	0.541	$8.7_{3}$	$\mathrm{CC}_{\mathrm{LOW}}$	0.192	1.250	0.06
	450	0.608	$43_7$	$CC_{MID}$	-0.085	_	-0.01
	500	0.676	$180_{10}$	$CC_{LOW}$	-0.181		-0.09
			- 10	$CC_{HIGH}$	0.153		-0.09
	550	0.743	$550_{30}$	$CC_{MID}$	0.082	_	0.03
			- 50	$CC_{HIGH}$	-0.054		-0.05
	600	0.811	$1200_{100}$	$CC_{HIGH}$	-0.151		-0.05

Table S5: (continued)

Molecule	T [K]	$T_{ m r}$	$P_{\rm sim}$ [kPa]	Test	$\ln\left(P_{\mathrm{sim}}/P_{\mathrm{CC}}\right)$	ER	NB
benzisoxazole (EH)	400	0.489	$1.1_{1}$	$CC_{LOW}$	-0.598	1.250	-0.09
	450	0.550	$11_{3}$	$\mathrm{CC}_{\mathrm{MID}}$	0.266	_	0.03
	500	0.611	$43_{6}$	$\mathrm{CC}_{\mathrm{LOW}}$	0.384	1.200	0.06
				$\mathrm{CC}_{\mathrm{HIGH}}$	-0.479	0.800	-0.09
	550	0.672	$130_{20}$	$\mathrm{CC}_{\mathrm{LOW}}$	-0.518	1.182	-0.09
				$\mathrm{CC}_{\mathrm{MID}}$	-0.174	_	-0.01
	600	0.733	$450_{50}$	$\mathrm{CC}_{\mathrm{LOW}}$	0.210	1.167	0.05
				$\mathrm{CC}_{\mathrm{MID}}$	0.238	_	-0.02
				$\mathrm{CC}_{\mathrm{HIGH}}$	0.320	0.833	-0.05
	650	0.795	$830_{50}$	$\mathrm{CC}_{\mathrm{MID}}$	-0.097	_	-0.02
				$\mathrm{CC}_{\mathrm{HIGH}}$		0.846	-0.05
	700	0.856	$1680_{50}$	$\mathrm{CC}_{\mathrm{HIGH}}$	0.180	0.857	0.04
benzothiazole (EH)	400	0.508	$2.8_{3}$	$\mathrm{CC}_{\mathrm{LOW}}$	0.211	1.250	0.06
	450	0.572	$15_{3}$	$\mathrm{CC}_{\mathrm{LOW}}$	0.174	1.222	0.06
				$\mathrm{CC}_{\mathrm{MID}}$	-0.094	_	-0.01
	500	0.635	$68_{5}$	$\mathrm{CC}_{\mathrm{LOW}}$	-0.461	1.200	-0.09
				$\mathrm{CC}_{\mathrm{MID}}$	-0.078	_	-0.01
				$\mathrm{CC}_{\mathrm{HIGH}}$	0.169	0.800	-0.09
	550	0.699	$270_{20}$	$\mathrm{CC}_{\mathrm{LOW}}$	0.065	1.182	0.06
				$\mathrm{CC}_{\mathrm{MID}}$	0.210	_	-0.01
				$\mathrm{CC}_{\mathrm{HIGH}}$	0.142	0.818	-0.09
	600	0.762	$580_{20}$	$\mathrm{CC}_{\mathrm{LOW}}$	0.087	1.167	0.05
				$CC_{MID}$	-0.030	_	-0.02
				$\mathrm{CC}_{\mathrm{HIGH}}$		0.833	-0.05
	650	0.826	$1170_{40}$	$CC_{MID}$	-0.040	_	-0.02
				$CC_{HIGH}$	0.055	0.846	-0.05
	700	0.889	$2300_{200}$	$CC_{HIGH}$	0.074	0.857	0.04

Table S6: All combined  $\ln{(Z_{\rm sim}/Z_{\rm exd})}$  and  $\ln{(P_{\rm sim}/P_{\rm CC})}$  Outliers in the TraPPE Development Data.

Molecule	T [K]	$T_{ m r}$	$\ln\left(Z_{\rm sim}/Z_{\rm exd}\right)$	$\ln\left(P_{\mathrm{sim}}/P_{\mathrm{CC}}\right)$
ethene (UA)	184	0.650	-0.037	-0.109
1,5-hexadiene (UA)	324	0.653	0.031	0.141
pentan-1-ol (UA)	400	0.691	0.039	-0.105
octan-1-ol (UA)	300	0.477	0.149	-0.184
	350	0.556	0.064	-0.222
	450	0.715	0.055	-0.144
	500	0.795	0.073	-0.114
propan-2-ol (UA)	300	0.598	-0.348	-0.974
	400	0.797	-0.072	-0.096
butan-2-ol (UA)	350	0.668	0.055	-0.408
2-methylpropan-2-ol (UA)	350	0.694	0.035	-0.537
1,3-propanediol (UA)	450	0.620	0.036	-0.541
ethanal (UA)	260	0.561	-0.364	-0.288
2-octanone (UA)	360	0.562	-0.540	-0.383
	400	0.625	-0.113	-0.105
ethylbenzene (UA)	397	0.640	-0.030	-0.288
isopropylbenzene (UA)	450	0.700	0.038	-0.132
o-xylene (UA)	450	0.711	0.055	0.065
m-xylene (UA)	451	0.719	0.057	-0.149
p-xylene (UA)	397	0.643	-0.157	-0.135
acetonitrile (UA)	398	0.725	-0.064	-0.068
nitrobenzene (UA)	298	0.399	-3.835	0.060
, ,	375	0.502	-0.534	0.142
methanethiol (UA)	220	0.463	-0.419	-0.271
ethanethiol (UA)	240	0.478	0.106	0.072

Table S6: (continued)

Molecule	T [K]	$T_{ m r}$	$\ln\left(Z_{\rm sim}/Z_{\rm exd}\right)$	$\ln\left(P_{\rm sim}/P_{\rm CC}\right)$
pentanethiol (UA)	300	0.498	1.169	0.164
	320	0.532	0.618	0.093
2-butanethiol (UA)	280	0.503	-0.349	-0.149
2-methyl-1-propanethiol (UA)	300	0.539		-0.335
	320	0.575	-0.299	-0.120
dimethyl disulfide (UA)	300	0.495	-0.419	-0.269
thiophene (UA)	293	0.484	-0.048	-0.474
pyrimidine (UA)	298	0.489		0.288
	398	0.652	-0.072	-0.155
2-ethylhexyl acrylate (UA)	550	0.795	0.070	0.150
TIP4P-pol1 (pol)	373	0.643	0.051	0.073
n-dodecane (EH)	450	0.675	0.060	0.101
	500	0.750	0.068	0.156
dimethylamine (EH)	250	0.564		-0.165
	280	0.632		-0.093
ethylamine (EH)	293	0.648	0.050	-0.639
acetonitrile (EH)	398	0.728	-0.068	0.157
nitromethane (EH)	375	0.637	-0.038	-0.316
nitroethane (EH)	323	0.555	0.059	-0.094
pyridine (EH)	298	0.482	-0.092	-0.317
pyrimidine (EH)	298	0.472	-0.031	-1.528
pyrazine (EH)	348	0.565	0.116	-0.407
pyridazine (EH)	298	0.392	0.480	2.382
	348	0.457		0.551
	398 468	0.523 $0.615$		-0.489 $-0.177$
furor (FU)		0.506		
furan (EH)	250	0.500	0.049	-0.413

Table S6: (continued)

Molecule	T [K]	$T_{ m r}$	$\ln\left(Z_{\rm sim}/Z_{\rm exd}\right)$	$\ln\left(P_{\rm sim}/P_{\rm CC}\right)$
pyrrole (EH)	300	0.461	-0.372	-0.783
	370	0.568	-0.041	0.109
thiazole (EH)	350	0.550	0.034	-0.525
	450	0.708	0.066	0.075
oxazole (EH)	300	0.557	-0.150	0.319
imidazole (EH)	400	0.489	0.148	0.121
pyrazole (EH)	350	0.475	0.092	-0.522
	400	0.543	-0.037	0.265
1,2,3-trichlorobenzene (EH)	400	0.532	-0.194	-0.535
hexachlorobenzene (EH)	575	0.648	-0.064	-0.273
1,2-dihydroxybenzene (EH)	500	0.619	0.092	0.307
1,4-dihydroxybenzene (EH)	580	0.683	0.048	0.061
benzonitrile (EH)	298	0.435	0.173	1.694
	540	0.787	-0.143	-0.104
p-benzoquinone (EH)	395	0.568	-0.043	0.194
	430	0.618	0.035	-0.224
anthracene (EH)	550	0.615	-0.458	-0.164
	600	0.670		0.115
	650 700	0.726 0.782	-0.432 $-0.453$	-0.101 $0.098$
l /DII)				
phenanthrene (EH)	550 750	0.613 0.836	-0.467 $-0.466$	-0.115 $-0.102$
naphthalen-2-ol (EH)	500	0.588	-0.408	-0.394
naphthalen-2-of (Eff)	650	0.765	-0.408 $-0.414$	-0.394 $-0.181$
	700	0.824	-0.448	0.226
naphthalene-2-carbonitrile (EH)	525	0.623	-0.405	0.149
	550	0.652	-0.445	-0.340
	580	0.688	-0.336	0.138

Table S6: (continued)

Molecule	T [K]	$T_{ m r}$	$\ln\left(Z_{\rm sim}/Z_{\rm exd}\right)$	$\ln\left(P_{\rm sim}/P_{\rm CC}\right)$
quinoline (EH)	300	0.373	-0.037	2.988
indole (EH)	400	0.522	0.121	-0.422
	450	0.587	0.079	-0.225
	500	0.652	0.121	0.061
	550	0.717	0.125	0.052
	600	0.782	0.113	-0.229
isoindole (EH)	400	0.485	-0.110	-1.253
	450	0.546	-0.102	0.755
	500	0.607	-0.059	-0.401
	550	0.667	0.125	0.213
	600	0.728	-0.069	-0.117
benzimidazole (EH)	500	0.531	0.092	-1.391
	700	0.744	0.072	0.246
indazole (EH)	500	0.579	0.105	-0.900
	550	0.637	0.190	0.315
purine (EH)	500	0.525	0.054	0.061
	550	0.578	0.117	-0.463
	600	0.630	0.148	0.248
benzisoxazole (EH)	600	0.733	0.179	0.210
benzothiazole (EH)	450	0.572	0.039	0.174
	550	0.699	0.156	0.065